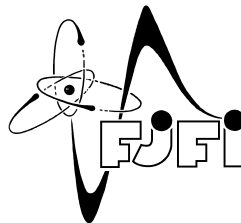


CZECH TECHNICAL UNIVERSITY IN PRAGUE
FACULTY OF NUCLEAR SCIENCES AND PHYSICAL
ENGINEERING

Department of Physics



Quantum walks with point
spectrum

DISSERTATION

Author: Ing. Iva Bezděková
Supervisor: prof. Ing. Igor Jex, DrSc.
Consultant: Ing. Martin Štefaňák, PhD.
Academic Year: 2016/17

Bibliografický záznam:

Autor: Ing. Iva Bezděková
České vysoké učení technické v Praze
Fakulta jaderná a fyzikálně inženýrská
Katedra fyziky

Název práce: Název práce

Studijní program: Matematické inženýrství

Studijní obor: Matematická fyzika

Školitel: prof. Ing. Igor Jex, DrSc.
České vysoké učení technické v Praze
Fakulta jaderná a fyzikálně inženýrská
Katedra fyziky

Konzultant: Ing. Martin Štefaňák, PhD.
České vysoké učení technické v Praze
Fakulta jaderná a fyzikálně inženýrská
Katedra fyziky

Akademický rok: 2016/2017

Počet stran: 126

Klíčová slova: Kvantová procházka, Grover, Wigner, mince, bodové spektrum, efekt záchyty, stacionrn stav, klasifikace, limitní rozdělení.

Bibliographic Entry:

Author: Ing. Iva Bezděková
Czech Technical University in Prague
Faculty of Nuclear Sciences and Physical Engineering
Department of Physics

Title of Dissertation: Quantum walks with point spectrum

Degree Programme: Mathematical Engineering

Field of Study: Mathematical Physics

Supervisor: prof. Ing. Igor Jex, DrSc.
Czech Technical University in Prague
Faculty of Nuclear Sciences and Physical Engineering
Department of Physics

Consultant: Ing. Martin Štefaňák, PhD.
Czech Technical University in Prague
Faculty of Nuclear Sciences and Physical Engineering
Department of Physics

Academic Year: 2016/2017

Number of Pages: 126

Keywords: Quantum walk, Grover, Wigner, coin, point spectrum, trapping, stationary state, classification, limiting distribution.

Acknowledgement

I would like to thank...tak to bude na dyl...:)

Abstrakt: [Abstrakt cesky](#)

Abstract:

Quantum walks have been introduced as a generalization of a classical random walk to a unitary evolution of a quantum particle. Their promising applications have been found. For instance we mention existence of speeding-up quantum walk based algorithms or applications to quantum transport. Discrete-time quantum walks are driven by an evolution operator consisting of a coin and a step operator. Spectrum of this evolution operator determines basic properties of the walk. We focus on the walks with non-empty point spectrum. Existence of a constant eigenvalue leads to an additional peak in a position probability distribution. This phenomena is called trapping. The new peak is located at the origin of the walk. After infinitely many steps, there is still a large amount of probability trapped in this additional peak, whereas the remaining probability peaks becomes less significant. Besides deep introduction into the problem, we analyse how is trapping affected by a choice of the coin operator and the choice of the initial state. This work summarizes results extending knowledge of the trapping walks, with focus on a full classification of the coins providing trapping walks on certain types of lattices. Significant effort is also dedicated to the analysis of the trapping walks and its spreading in the limit of infinitely many steps and to the control of the peaks in the position probability distribution. Special choices of the initial states affect the distribution and especially the trapping peak in a very non-intuitive way.

Prohlášení

Prohlašuji, že jsem tuto disertační práci vypracovala samostatně a výhradně s použitím uvedené literatury.

Nemám závažný důvod proti použití tohoto školního díla ve smyslu §60 Zákona č.121/2000 Sb., o právu autorském, o právech souvisejících s právem autorským a o změně některých zákonů (autorský zákon).

V Praze dne

.....

Ing. Iva Bezděková

Contents

Introduction	2
1 Discrete-time quantum walks with non-empty point spectrum	6
1.1 Quantum walks on a line	7
1.1.1 Three-state Grover walk on a line	10
Fourier analysis	11
Calculation of the peak velocities and trapping	13
1.1.2 Wigner walks	15
1.2 Quantum walks on a two-dimensional lattice	17
1.2.1 Four-state Grover walk on a two-dimensional lattice	18
1.2.2 Strong trapping	19
2 Continuous deformations of the Grover walk	23
2.1 Eigenvalue family of coins	23
2.1.1 Eigenvalue deformation of the three-state Grover walk on a line	24
2.1.2 Eigenvalue deformation of the four-state Grover walk on a two-dimensional lattice	25
2.1.3 Eigenvalue families for other types of higher-dimensional quantum walks	27
2.2 Eigenvector family of coins	28
2.2.1 Eigenvector deformation of the three-state Grover walk on a line	30
3 Classification of trapping coins for three-state quantum walk on a line	33
3.1 Conditions on a non-empty point spectrum	33
3.2 Unitarity	35
3.3 Spreading of a general three-state trapping quantum walk	37
4 Classification of trapping coins for four-state quantum walks on a two-dimensional lattice	44
4.1 Support of stationary states	45
4.2 Conditions on the trapping coins	48
4.3 Non-zero determinant, $\det A \neq 0$	51
4.4 Determinant equal to zero, $\det A = 0$	53
4.4.1 Non-degenerate case	53

4.4.2	Two zero amplitudes	57
4.4.3	Four zero amplitudes	58
	Four zero amplitudes and rank three	58
	Four zero amplitudes and rank two	59
	Six zero amplitudes	60
5	Limiting distribution and role of coin eigenstates	62
5.1	Velocity density for the eigenvector family	62
5.2	Velocity density for the eigenvalue family	65
5.3	Velocity density for the Wigner rotation matrices	72
5.3.1	Divergences of the Konno's density function	73
5.3.2	Elimination of the parameter γ	74
5.3.3	Construction of the suitable basis	74
5.3.4	Relation of the suitable basis to the eigensystem of the Wigner matrix	76
5.3.5	Three-state Wigner walk, $j=1$	78
5.3.6	Higher dimensions	85
	Four-state walk	85
	Five-state walk	87
	Appendices	97
A	Remarks on Wigner walks	98
A.1	Four-state Wigner walk	98
A.2	Five-state Wigner walk	99
A.3	Six-state Wigner walk	100
	Conclusions and outlook	107
	References	111
	List of publications	113
	Publications related to the thesis	113
	Other publications	113

Introduction

Classical random walks are well known as a tool describing processes in nature. The term random walks was first introduced by Karl Pearson in 1905 [1]. Their applications in physics, biology or chemistry have been found. Moreover, the concept gained its place even in different fields as economy for modelling stock markets, ecology or psychology. The wide range of applications in a classical world resulted in formation of its quantum counterpart as a model with a great promise to the future.

Quantum walks [2, 3, 4] were developed as a generalization of a classical random walk, where a quantum particle is propagating on a discrete lattice. It represents a concept with a great potential in particular with respect to its possible applications. Quantum walk based algorithms for the database search have been suggested [5]. Among others, one can find further applications in quantum information theory [6], transport theory [7] in photosynthetic systems [8] or use it as a universal tool for quantum computation [9]. Although it may seem that it is primarily a theoretical concept, a number of experimental realizations have been reported [10, 11, 12, 13]. The last significant achievement in this field was the experimental realization of a genuine two-dimensional quantum walk on a square lattice [14].

We can divide quantum walks into two classes. It is discrete-time and continuous-time walks. Continuous time quantum walks are driven by a given hamiltonian. On the other hand, the discrete-time quantum walks require implementation of an additional degree of freedom referred to as coin. Both of these types have some advantages and some disadvantages. For instance, continuous-time quantum walks are more convenient from computational perspective, but discrete-time quantum walks are easier to implement. One can read more about its similarities or differences in [24]. We will consider only discrete translationally invariant walks.

Compared to classical random walks, quantum walks has considerably different features. One can imagine simple classical discrete-time random walk as a Galton board. Sum of the individual paths any ball can go through results in the most probable final location of the ball being its starting position, i.e. binomial distribution. Change of pins in the board by beam splitters and balls by a laser beam behaves differently. The individual paths might subtract each other due to a phase change on the beam splitters and thus the most probable locations are shifted right and left from the origin. Mathematical description of such a discrete quantum walk requires additional degree of freedom, referred to as a coin. Without it, spreading of the walk would be trivial. Moreover, the resulting probability distribution is affected by a choice

of the initial state of this coin. There is nothing like an initial coin state classically and thus the quantum walks are better adaptable to special situations.

For translationally invariant walks, the shape of the position probability distribution can be analysed using similarities with the wave theory, namely the propagation of a wave packet. Further investigation of the time evolution is considerably simplified using the Fourier transform from the position to the momentum variable. The travelling peaks are associated with the continuous spectrum of the unitary evolution operator in the Fourier picture and the phases of the corresponding continuous spectrum are represented by the dispersion relation. The group velocity of spreading of the walk is given by the first derivative of the phase with respect to the momentum. It can be shown that the maximal peaks propagate with the maximal group velocity. This results from the stationary phase method [15] which says that the largest contributions to the probability distribution comes from points, where the derivative of the dispersion relation vanishes.

For certain quantum walks, the evolution operator has also non-empty point spectrum. This property results in one additional peak in the position probability distribution placed at the initial position of the particle. Similar effect occur also classically for so-called lazy random walks. Nevertheless, not all trapping walks have its classical counterpart. which is also our case. We emphasize that the existence of this extra peak is influenced by the initial state of the walk. For most of the walks we can find so-called escaping state, which is an initial state for which the additional peak is not observed. Further, a choice of a coin plays a crucial role in trapping, since it is the coin which specifies the exact form of the evolution operator driving a distribution of the probability over a given lattice. Trapping is also sensitive to the dimensionality of the lattice and the dimensionality of the walk. It was found for the three-state quantum walk on a line with the Grover coin [16, 17] (i.e. three-state Grover walk), that the point spectrum of the evolution operator contains an eigenvalue equal to one and thus the walk exhibits trapping. In this case by the three-state walk we mean that the walker can, excepts movements to the left and right, stay at the actual position. If we increase the dimensionality of the lattice and perform the three-state Grover walk on a honeycomb lattice [18], the trapping will not be observed. Staying on a line and decreasing the dimensionality of the walk to a two state walk leads to a non-trapping walk for any choice of a coin. Although it might seem that allowing the walker to stay at its actual position contributes to the existence of the trapping, there exist walks for which this is not required. The four-state Grover walk exhibits trapping on a line or a two-dimensional lattice regardless to the fact that the walker does not have the option to stay. By the four-state walk on a line we assume that the particle performs one and two steps to the right and left. On a two-dimensional lattice these four states are movements to the left, right, down and up.

In this work, we focus on finding conditions under which the point spectrum of the evolution operator exists. These conditions are restrictions on a choice of a coin, which in general depends on several parameters. We studied the role of the coin parameters, where we focused on a discrete time, translationally invariant quantum walk on a line and two-dimensional lattice. For example, we examined limiting distribution for certain types of

walks. The aim of limiting distribution is to provide an approximation of the probability distribution of quantum walk for large number of steps. It is very useful, since otherwise one has to calculate the probability distribution recursively using the results for the previous steps. The complexity of the calculations and resulting limiting distribution is influenced by the choice of the coin space basis. There exist a basis that is more suitable than the standard one. This choice provides much simpler resulting distribution formulas. In addition, suitable basis reveals some very interesting features that are otherwise hidden, respectively difficult to extract from other ones theoretically predicted expressions. In addition, calculation of the trapping probability at the vicinity of the origin is in the suitable basis much easier. As for the limiting distribution, interesting properties regarding trapping arising from the choice of the basis are observed.

The thesis is divided into five chapters and follows the work done during the doctoral studies. Most of the results provided in the thesis were already published and the original articles are listed in the list of publication at the end of the thesis. These papers are for better resolution in the text numbered by Roman numerals. Due to this fact, we provide a more detailed description and introduction into the problems than one can find in the papers. We devote more attention to the explanation of the problem, methods and partial results providing full solution. Considering the results, we often skip their explicit forms, if they are too space consuming and rather refer to the particular paper. Further, the structure of the thesis is not done in a way that every chapter corresponds to one paper. The topics of the individual articles partially overlap and are therefore rearranged in order to ensure a better flow of the text.

The first chapter of the thesis deals with the description of the discrete-time quantum walks with non-empty point spectrum with respect to the walks that will be studied in the following chapters. We provide an introduction to the trapping effect that accompanies us throughout the whole thesis. On a simple example, which is a two and a three-state walk on a line, we introduce notation, explain basic properties and concepts and show how the is the analysis of the quantum walks performed. Next we introduce Wigner walks on a line, which are defined for any dimension starting with two and thus cover walks with more than three allowed movements. By an increasing dimension we mean only a dimension of a coin space, i.e. number of possible movements. The lattice is still one-dimensional. A separate section is devoted to quantum walks on a two-dimensional lattice. Except a brief illustration of differences from a walk on a line, we illustrate a new phenomena called strong trapping. This feature neglects the importance of the initial state on the existence trapping. We provide an example of a strong trapping coin class and show that an escaping state for which the trapping is not observed does not exist.

Chapter two is devoted to the one-parameter deformations of the Grover walk. It describes the construction of these families and briefly summarizes some results from [I]. Although this work was done during master and not doctoral studies, we find these constructions very useful for the following work. We present only the most important results to which we will refer to in the following chapters. The results are two classes of coins preserving trapping

and these classes are further studied especially in the last chapter which discusses a limiting distribution. Since it was not clear whether these two families cover all three-state trapping coins. The investigation continues in the following section.

The third chapter extends the results from chapter two and provides a full classification of the trapping coins for the three-state quantum walks on a line. The starting point of the analysis is a general unitary coin on which we apply conditions, the trapping coin has to satisfy. We focus only on the non-trivial walks, i.e. the walks where none of the elements in the final trapping matrix is zero. This chapter follows arguments presented in [II], where one can also find situation for the trivial trapping cases. The final two non-trivial classes of coins have a significant number of free parameters. Nevertheless, not all of these parameters influence the spreading of the walk and the trapping. We show that these classes are generalization of the one-parameter families introduced in chapter two.

The classification of four-dimensional coins was addressed using different methods from that applied on the three-dimensional case. Therefore, we devote a whole chapter to this new method. The starting point in the analysis is, instead of a general unitary coin, a stationary state of the walk. It is the eigenstate corresponding to the constant eigenvalue of the evolution operator. Provided that the coin is not given, we cannot find an exact form of the stationary state. Nevertheless, we can restrict a wide region of the possible states using the knowledge that we are dealing with a trapping walk. This allows us to discover a maximal support on which the stationary state might exist. Since the evolution operator remains the stationary state unchanged, we can find conditions on the coin leading to the trapping. Further we have to keep in mind, that the coin has to be a unitary matrix. These all together give us unique parametrizations of the trapping coins. Here we have to distinguish between two non-trivial cases, where one of these cases equals strong trapping family of coins. Many trivial sub-cases arise here and we will discuss them in the last section of this chapter. This section contains unpublished results that are currently prepared for submission.

The most comprehensive chapter five deals with a limiting probability distribution and the role of the coin eigenstates on a simplification of this distribution. This approximative probability distribution was usually derived with respect to the standard coin space basis. Even though this choice is a natural one, it seems that there are better but not so obvious choices. We begin with the analysis of the limiting distribution for the two one-parameter families introduced in chapter two. We show that in this case, the coin space basis formed by the eigenvectors of the coin is a much better choice. In this basis, the limiting density gains a simple form and thus we call it suitable. Further, we do the similar analysis for the Wigner walks introduced in chapter one. Here the suitable basis is not given directly by the eigenstates of the coin. This helps us to understand what is really behind the simplification of the limiting density function and how to generally construct the suitable basis of the coin space. The main results of this chapter have been published in [III, IV]

The rest of the thesis provides conclusions summarizing the obtained results, outlook and one appendix providing technical support to the last chapter. The references are extended by a list of publications.

Chapter 1

Discrete-time quantum walks with non-empty point spectrum

Quantum walks can be divided into two classes. It is discrete-time and continuous-time walks. Continuous time quantum walks are driven by a given hamiltonian. On the other hand, the discrete-time quantum walks require implementation of an additional degree of freedom referred to as coin. Both of these types have some advantages and some disadvantages. For instance, continuous-time quantum walks are more convenient from computational perspective, but discrete-time quantum walks are easier to implement. One can read more about its similarities or differences in [24].

Throughout the entire thesis, we will assume only discrete-time and translationally invariant quantum walks. It means that the walker can make only discrete-time steps on a certain lattice type. The Hilbert space is given by a tensor product of a position and a coin space,

$$\mathcal{H} = \mathcal{H}_p \otimes \mathcal{H}_C. \quad (1.1)$$

The position space \mathcal{H}_p is spanned by all possible positions on a given lattice and the coin space \mathcal{H}_C is determined by the allowed local moves - local steps.

Every walk starts by the choice of the initial state $|\psi_0\rangle$. This choice can be arbitrary and might help to reach our goals. For example, the convenient choice for the quantum walk bases search algorithm might be superposition over all possible positions. The convenient choice for us is to start the walk at the origin. In general, quantum walks are translationally invariant and thus any single initial position can be assumed as a new origin. Therefore we will usually write the initial state as a tensor product

$$|\psi_0\rangle = |0\rangle \otimes |\psi_C\rangle = |0\rangle|\psi_C\rangle. \quad (1.2)$$

The initial coin state is an arbitrary state $|\psi_C\rangle$ from \mathcal{H}_C , satisfying the normalization condition $\langle\psi_C|\psi_C\rangle = 1$. Every single step of the walk is realized by the unitary evolution operator

$$\hat{U} = \hat{S}(\hat{I}_p \otimes \hat{C}), \quad (1.3)$$

where \hat{C} is a coin operator acting only on the coin Hilbert space \mathcal{H}_C , \hat{I}_p is an identity on the position space \mathcal{H}_p and \hat{S} is a step operator operator, acting on the tensor product of both spaces. Matrix representation of the coin operator \hat{C} is called coin and often labeled as C . The only requirement is that the coin has to be a unitary matrix.

After time t , it means after t steps, the state of the walker reads

$$|\psi(t)\rangle = \hat{U}^t |\psi_0\rangle.$$

The time evolution of the quantum walk is given by repeated action of the unitary evolution operator \hat{U} from Eq. (1.3). For better understanding, we omit further general description of the quantum walk behaviour and leave it to the specific examples, which will clarify the structure for all other types of discrete-time quantum walks. Therefore, we now turn to the two and three-state quantum walk on a line and provide introductory details regarding the analysis and the evolution of the walk. We introduce coin states and its matrix description and show how the coin acts on these states. Further, we define a step operator and for illustration describe an action of the coin and the step operators during first three steps of the walk. Fourier analysis as a powerful tool for studying the quantum walks is discussed in a separate subsection. The results coming from this analysis are further used during investigation of the spreading of the walk and will accompany us during the whole thesis. At the end of the following section, we introduce so-called Wigner walks as one of the models we will study later. Finally, we enlarge the lattice by another dimension and summarize our notation for the four-state walks on a two-dimensional lattice with particular interest in the four-state Grover walk. In the relation to this, effect of strong trapping is explained.

1.1 Quantum walks on a line

We start with a simple example which is a two-state quantum walk on a line. The walker can move only one step to the left or one step to the right at each discrete time moment. Due to the allowed movements of the walker, the coin Hilbert space is given by

$$\mathcal{H}_C = \text{Span}\{|L\rangle, |R\rangle\} = \mathbb{C}^2 = \text{Span}\left\{\begin{pmatrix} 1 \\ 0 \end{pmatrix}, \begin{pmatrix} 0 \\ 1 \end{pmatrix}\right\}. \quad (1.4)$$

Here $|L\rangle$ corresponds to the movement to the left and $|R\rangle$ to the movement to the right. In the last equality, we have used a matrix representation of the coin states. From it follows our notation that the left state corresponds to the first element in the vector. The same applies for the right state and the second element. Later we will work with so-called vector of probability amplitudes where this notation is important. The position Hilbert space is spanned by all possible locations of the particle on a line

$$\mathcal{H}_p = \text{Span}\{|x\rangle, x \in \mathbb{Z}\}.$$

As mentioned before, the walk is driven by a coin, here it is two-dimensional unitary matrix

$$C = \begin{pmatrix} C_{LL} & C_{LR} \\ C_{RL} & C_{RR} \end{pmatrix}.$$

The coin operator \hat{C} acts on the coin states via its matrix representation C as

$$\begin{aligned}\hat{C}|L\rangle &= \left(C_{LL}|L\rangle\langle L| + C_{RL}|R\rangle\langle L| \right) |L\rangle = C_{LL}|L\rangle + C_{RL}|R\rangle = \begin{pmatrix} C_{LL} \\ C_{RL} \end{pmatrix} = C \begin{pmatrix} 1 \\ 0 \end{pmatrix}, \\ \hat{C}|R\rangle &= \left(C_{LR}|L\rangle\langle R| + C_{RR}|R\rangle\langle R| \right) |R\rangle = C_{LR}|L\rangle + C_{RR}|R\rangle = \begin{pmatrix} C_{LR} \\ C_{RR} \end{pmatrix} = C \begin{pmatrix} 0 \\ 1 \end{pmatrix}.\end{aligned}$$

The step operator \hat{S} from Eq. (1.3) changes the position of the particle according to the internal coin state,

$$\begin{aligned}\hat{S}(|x\rangle \otimes |L\rangle) &= |x-1\rangle \otimes |L\rangle, \\ \hat{S}(|x\rangle \otimes |R\rangle) &= |x+1\rangle \otimes |L\rangle.\end{aligned}$$

A well known and extensively studied two-state quantum walk is called Hadamard walk [25]. It is a quantum walk with the coin given by the Hadamard matrix

$$C = H = \frac{1}{\sqrt{2}} \begin{pmatrix} 1 & 1 \\ 1 & -1 \end{pmatrix}.$$

If we measure the position probability of the Hadamard walk after each step, the resulting distribution is the same as for the classical random walk, which is binomial. For illustration we look at the first three steps of the Hadamard walk. For example, we choose the initial state to be $|\psi_0\rangle = |0\rangle \otimes |R\rangle$. Then

$$\begin{aligned}\text{1st step: } \hat{U}|\psi_0\rangle &= \hat{S}(\hat{I}_p \otimes \hat{C})|\psi_0\rangle = \hat{S} \left(|0\rangle \otimes \frac{1}{\sqrt{2}} (|L\rangle - |R\rangle) \right) = \\ &= \frac{1}{\sqrt{2}} | -1\rangle \otimes |L\rangle - \frac{1}{\sqrt{2}} |1\rangle \otimes |R\rangle,\end{aligned}$$

$$\begin{aligned}\text{2nd step: } \hat{U}^2|\psi_0\rangle &= \hat{S}(\hat{I}_p \otimes \hat{C}) \frac{1}{\sqrt{2}} (| -1\rangle \otimes |L\rangle - |1\rangle \otimes |R\rangle) = \frac{1}{2} \hat{S} | -1\rangle \otimes (|L\rangle + |R\rangle) + \\ &+ \frac{1}{2} \hat{S} |1\rangle \otimes (|L\rangle - |R\rangle) = \frac{1}{2} (|0\rangle|L\rangle + |0\rangle(|L\rangle + |R\rangle) - |2\rangle|R\rangle),\end{aligned}$$

$$\text{3rd step: } \hat{U}^3|\psi_0\rangle = \frac{1}{2\sqrt{2}} (| -3\rangle|L\rangle + | -1\rangle(2|L\rangle + |R\rangle) - |1\rangle|L\rangle + |3\rangle|R\rangle).$$

For the second and the third step, we omitted the sign for the tensor product. For instance we wrote $|2\rangle|R\rangle$ instead of $|2\rangle \otimes |R\rangle$. From now on, we will usually use this shorter notation without the tensor product sign. After t steps of the walk, we have

$$|\psi(t)\rangle = \hat{U}^t|\psi_0\rangle = \sum_{x=-t}^t \psi_x^L|x\rangle|L\rangle + \psi_x^R|x\rangle|R\rangle.$$

After tracing out the coin states we get that

$$p(x, t) = |\psi_x^L|^2 + |\psi_x^R|^2$$

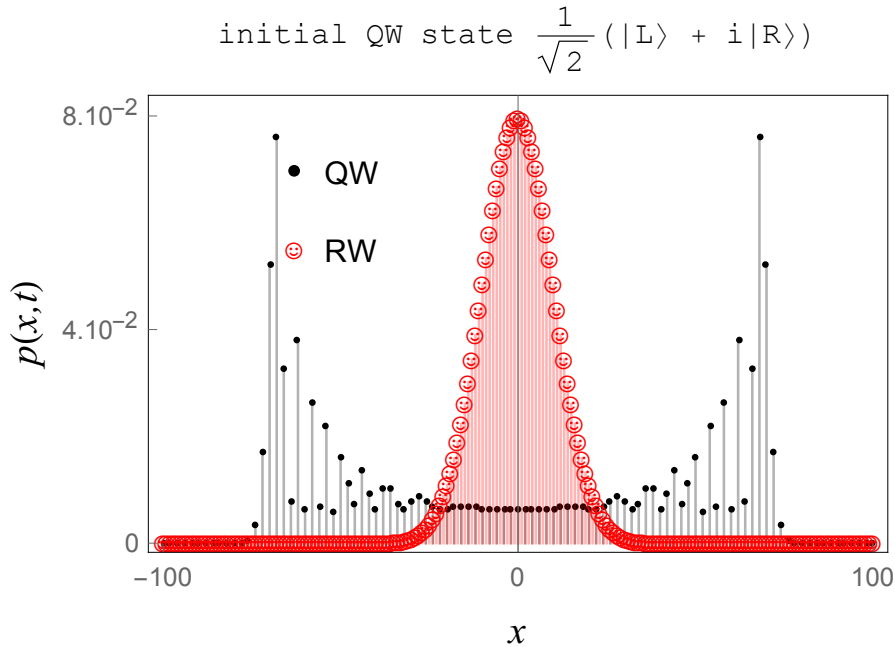


Figure 1.1: Position probability distribution of the quantum walk (QW) with the Hadamard coin and the classical random walk (RW) after $t = 100$ steps. The initial coin state of the quantum walk $|\psi_C\rangle = \frac{1}{\sqrt{2}}(|L\rangle + i|R\rangle)$ leads to a symmetric probability distribution with two peaks that move to the right or left with increasing number of steps. Probability around the origin decreases to zero. On the other hand we have classical unbiased random walk with equal probability of movements to the left or right. This results in a binomial probability distribution with highest value at the origin, which slowly vanishes with increasing distance from the origin.

is the probability that the particle is after t steps located at position x . We see that after the third step, the probability of being at positions $|\pm 1\rangle$ is not the same. This is in a striking difference to the ordinary random walk. The situation is depicted in the Fig. (1.1) for a symmetric initial state.

From this fact and the third step of the walk one can see, that with this initial state the walk inclines to the left, since the probability of being at the position -1 is higher than for position $+1$. This is different than for the classical unbiased random walk, where the position probability distribution is symmetric and the highest probability peak is located at the origin of the walk.

The lower dimensional quantum walks are rather well understood. However, depending on the dimensionality of the coin, they exhibit striking differences. As one from such effects we can list trapping. This manifest itself in additional peak in the position probability distribution which is stable and does not vanish with time approaching infinity. On the other hand, the travelling peaks depicted in Fig. (1.1) are getting smaller. Trapping can be observed already for a three-state quantum walk on a line.

1.1.1 Three-state Grover walk on a line

Another extensively studied types of walks are those driven by the Grover coin. The Grover coin $C_G^{(N)}$ is for a given dimension N defined as

$$C_G^{(N)} = 2|z\rangle\langle z| - I^{(N)}, \quad (1.5)$$

where $|z\rangle$ is equal superposition over all standard basis states $|i\rangle$,

$$|z\rangle = \frac{1}{\sqrt{N}} \sum_{i=1}^N |i\rangle, \quad (1.6)$$

and $I^{(N)}$ is N -dimensional identity matrix. If we choose appropriate lattice, Grover walks lead to the existence of trapping.

Let us look in more detail at the three-state Grover walk on line. The walk is performed on a line, therefore the position space is the same as we had for the two-state quantum walk on a line. The difference comes with the coin space \mathcal{H}_C , which is now three-dimensional and its standard basis consists of possible movements of the walker. In this case, by the three-state walk we mean that the walker can move one step to the left, one step to the right or stay on its actual position. Thus

$$\mathcal{H}_C = \mathbb{C}^3 = \text{Span}\{|L\rangle, |S\rangle, |R\rangle\} = \mathcal{C}^3 = \text{Span} \left\{ \begin{pmatrix} 1 \\ 0 \\ 0 \end{pmatrix}, \begin{pmatrix} 0 \\ 1 \\ 0 \end{pmatrix}, \begin{pmatrix} 0 \\ 0 \\ 1 \end{pmatrix} \right\}. \quad (1.7)$$

The time evolution is given by the unitary propagator

$$\hat{U} = \hat{S}(\hat{I}_p \otimes \hat{C}_G^{(3)}), \quad (1.8)$$

Eq. (1.3). We assume the coin $C_G^{(3)}$, i.e. matrix representation of the coin operator $\hat{C}_G^{(3)}$ to be three-dimensional Grover matrix,

$$C_G^{(3)} = \frac{1}{3} \begin{pmatrix} -1 & 2 & 2 \\ 2 & -1 & 2 \\ 2 & 2 & -1 \end{pmatrix}. \quad (1.9)$$

The step operator \hat{S} moves the particle on the lattice according to its coin state,

$$\begin{aligned} |x\rangle|L\rangle &\xrightarrow{\hat{S}} |x-1\rangle|L\rangle, \\ |x\rangle|S\rangle &\xrightarrow{\hat{S}} |x\rangle|S\rangle, \\ |x\rangle|R\rangle &\xrightarrow{\hat{S}} |x+1\rangle|R\rangle. \end{aligned} \quad (1.10)$$

and its explicit form reads

$$\hat{S} = \sum_{-\infty}^{\infty} (|x-1\rangle\langle x| \otimes |L\rangle\langle L| + |x\rangle\langle x| \otimes |S\rangle\langle S| + |x+1\rangle\langle x| \otimes |R\rangle\langle R|).$$

The time evolution is given by a repeated action of \hat{U} on the initial state $|\psi_0\rangle$. After t steps the walk reaches state

$$|\psi(t)\rangle = U^t|\psi_0\rangle = \sum_x |x\rangle(\psi_L(x,t)|L\rangle + \psi_S(x,t)|S\rangle + \psi_R(x,t)|R\rangle), \quad (1.11)$$

where the initial state is located at the origin and is of the form

$$|\psi_0\rangle = |0\rangle \otimes |\psi_C\rangle = |0\rangle \otimes (\psi_L(0,0)|L\rangle + \psi_S(0,0)|S\rangle + \psi_R(0,0)|R\rangle).$$

The initial coin state $|\psi_C\rangle$ is a superposition of the basic coin states and its amplitudes have to satisfy the normalization condition

$$|\psi_L(0,0)|^2 + |\psi_S(0,0)|^2 + |\psi_R(0,0)|^2 = \|\psi(0,0)\|^2 = \|\psi_0\|^2 = 1.$$

We call $\psi_{L,S,R}(x,t)$ probability amplitudes and from now on, let us call

$$\psi(x,t) = (\psi_L(x,t), \psi_S(x,t), \psi_R(x,t))^T \quad (1.12)$$

the vector of probability amplitudes. The probability of finding the particle at a position x after total number of steps t then reads

$$p(x,t) = \sum_{j=L,S,R} |\psi_j(x,t)|^2 = \|\psi(x,t)\|^2. \quad (1.13)$$

Fourier analysis

The time evolution of the initial state $|\psi(t)\rangle$, Eq. (1.11) can be efficiently handled by the Fourier analysis. Instead of working with a full state $|\psi(t)\rangle$, we use the probability amplitude vector $\psi(x,t)$, Eq. (1.12) providing the same information and apply the discrete Fourier transform on it. It is a transform from a discrete position variable x to a new continuous momentum variable k ,

$$\tilde{\psi}(k,t) = \sum_x e^{ixk} \psi(x,t), \quad k \in (0, 2\pi).$$

It is not difficult to check that $\tilde{\psi}$ evolves in time thanks to a new evolution operator $\tilde{U}(k)$ as

$$\tilde{\psi}(k,t) = \tilde{U}(k)\tilde{\psi}(k,t-1) = \tilde{U}(k)^t\tilde{\psi}(k,0) = \tilde{U}(k)^t\tilde{\psi}_0. \quad (1.14)$$

The last equality results from the fact that the vector $\tilde{\psi}(k,0)$ is the Fourier transform of the initial probability amplitude vector $\psi(0,0) = \psi_0$. Provided the walk starts at the origin of the lattice, both initial vectors $\tilde{\psi}(k,0)$ and ψ_0 are the same. It can be shown with some algebra [26] that the new evolution operator in the Fourier picture reads

$$\tilde{U}(k) = \begin{pmatrix} e^{-ik} & 0 & 0 \\ 0 & 1 & 0 \\ 0 & 0 & e^{ik} \end{pmatrix} \cdot C_G^{(3)}, \quad (1.15)$$

where $C_G^{(3)}$ is the Grover coin from Eq. (1.9). The diagonal matrix is the step operation in the Fourier picture and can be interpreted in the following way. The first diagonal element

e^{-ik} corresponds to kick to the left, the third one means kick to the right and the constant middle element says do nothing. This provides intuitive insight into the construction of the evolution \tilde{U} even for different types of walks.

Due to unitarity, we can rewrite Eq. (1.15) using spectral decomposition as,

$$\tilde{U}(k) = \sum_{j=1}^3 \lambda_j(k) v_j(k) v_j^\dagger(k)$$

where $\lambda_j(k)$, $v_j(k)$ are its eigenvalues and eigenvectors. The power of t than gives

$$\tilde{U}(k)^t = \sum_{j=1}^3 (\lambda_j(k))^t v_j(k) v_j^\dagger(k)$$

and therefore the time evolution, Eq. (1.14) gains the form

$$\tilde{\psi}(k, t) = \sum_{j=1}^3 \lambda_j(k)^t (v_j(k), \psi_0) v_j(k). \quad (1.16)$$

This is very simple sum compared to Eq. (1.11) with sum over all possible positions.

Further, it is very convenient to rewrite the eigenvalues $\lambda_j(k)$ of $\tilde{U}(k)$ from Eq. (1.15) in the exponential form

$$\lambda_j(k) = e^{i\omega_j(k)}. \quad (1.17)$$

For the Grover walk, the phases $\omega_j(k)$ read

$$\begin{aligned} \omega_{1,2}(k) &= \pm \arccos\left(-\frac{1}{3}(2 + \cos k)\right), \\ \omega_3(k) &= 0. \end{aligned} \quad (1.18)$$

This shows that that the point spectrum of the evolution operator $\tilde{U}(k)$ is indeed non-empty with the constant eigenvalue $\lambda_3(k) = 1$.

If we want to go back to the position variable x , we have to employ the inverse Fourier transform on $\tilde{\psi}(k, t)$ from Eq. (1.16). Then the position probability amplitude vector reads

$$\begin{aligned} \psi(x, t) &= \frac{1}{2\pi} \sum_{j=1}^3 \int_0^{2\pi} e^{-ixk} \tilde{\psi}(k, t) dk = \\ &= \frac{1}{2\pi} \sum_{j=1}^3 \int_0^{2\pi} e^{i(\omega_j(k) - \frac{x}{t}k)t} (v_j(k), \psi_0) v_j(k) dk. \end{aligned} \quad (1.19)$$

The last equality uses Eq. (1.16) and the exponential expression of the eigenvalues, Eq. (1.17). This formula allows us to calculate probability amplitude vector at a given position x . Moreover, in the following subsection we will use it for determination of peaks in the position probability distribution and analysis of their spreading through the lattice.

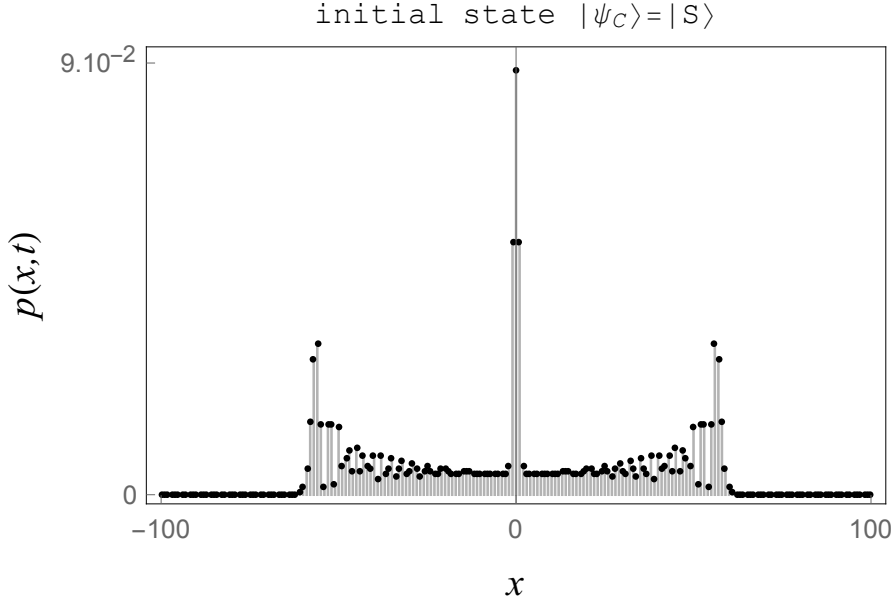


Figure 1.2: Position probability distribution of the Grover walk after $t = 100$ steps is depicted for the initial state $|\psi_0\rangle = |0\rangle \otimes |S\rangle$. Central trapping peak decreases exponentially with increasing distance from the origin of the lattice.

Calculation of the peak velocities and trapping

The Grover walk is special because it exhibits trapping. This property occurs due to the fact that one of the eigenvalues $\lambda_j(k)$ of the evolution operator $\tilde{U}(k)$ is independent of the momentum variable k . We now describe how this constant eigenvalue affects the probability distribution.

A typical probability distribution of the Grover walk is shown in Fig. (1.2). It has three dominant peaks and the central one is present due to the trapping effect. However, the presence of the peaks can be influenced by a choice of the initial coin state $|\psi_C\rangle$, Eq. (1.2). If we choose the initial state (initial probability amplitude vector) to be orthogonal to the eigenvector corresponding to the constant eigenvalue of $\tilde{U}(k)$, the central peak in the position probability distribution does not appear.

The integral from Eq. (1.19) can be analysed with the help of so-called stationary phase approximation. Here we will give only brief explanation of the method, for more details see for example [15].

Intuitively one can see, that the exponential function in the integral is rapidly oscillating, therefore increments cancel out each other. The most relevant increments come from points where the oscillations vanish. These points will be stationary points of the phase

$$\varphi_j(k) = \omega_j(k) - \frac{x}{t}k,$$

that is points where

$$\frac{d}{dk}\varphi_j(k) = \frac{d}{dk}\omega_j(k) - \frac{x}{t} = 0.$$

This implies that probable location of the particle depending on the momentum k is after t steps given by

$$x = \frac{d}{dk}\omega_j(k)t.$$

Therefore, k -dependent pseudo-velocity of the walk is equal to

$$v_j(k) = \frac{d}{dk}\omega_j(k). \quad (1.20)$$

Furthermore, higher order stationary point means larger increment. In other words, second order stationary point k_0 , for which

$$\left. \frac{d^2}{dk^2}\varphi_j(k) \right|_{k_0} = \left. \frac{d^2}{dk^2}\omega_j(k) \right|_{k_0} = \left. \frac{d}{dk}v_j(k) \right|_{k_0} = 0, \quad (1.21)$$

corresponds to the peak in the position probability distribution and

$$x_{max} = \underbrace{\left. \frac{d}{dk}\omega_j(k) \right|_{k_0}}_{v_{R,L}} t \quad (1.22)$$

is the position of the probability peak after t steps. We have denoted the velocities of the right and left travelling peaks as $v_{R,L}$.

To summarize, first derivative of the phase $\omega_j(k)$ expressed at point k_0 , which is the point where the second derivative of ω_j vanishes, gives velocities and therefore positions of the peaks in the position probability distribution.

In the case of the Grover walk we get that the highest probability peaks are found for the momentum

$$k_0 = 0,$$

and velocities of the travelling probability peaks are according to Eq. (1.22)

$$v_{R,L} = \lim_{k \rightarrow 0^+} \frac{d}{dk}\omega_{2,1}(k) = \pm \lim_{k \rightarrow 0^+} \frac{\sin k}{\sqrt{5 - 4 \cos k - \cos^2 k}} = \pm \frac{1}{\sqrt{3}}, \quad (1.23)$$

where $\omega_{1,2}(k)$ are given by Eq. (1.18). Note that the remaining phase $\omega_3 = 0$ immediately leads to stationary trapping peak with velocity $v_S = 0$, which is therefore centered at the origin. Moreover, since the point k_0 is the stationary point of the velocity, the peak velocity $v_{R,L}$ corresponds to the maximal velocity of spreading of the walk. This means that travelling probability peaks are the fastest parts in the position probability distribution, see Fig. (1.2).

Last but not least we have to note similarities with wave theory. Phases $\omega_j(k)$ from Eq. (1.18) can be assumed as dispersion relations. It is known that the first derivative of the dispersion relation with respect to wave-number corresponds to the group-velocity of spreading of the wave packet. Therefore, we might consider phases $\omega_j(k)$ as the dispersion relations, momentum k as a wave-number and the pseudo-velocities, Eq. (1.20) as the group velocity and its maximum is given by Eqs. (1.22) and (1.23).

1.1.2 Wigner walks

Wigner walks are a model of quantum walks on a one-dimensional lattice, where the coin is chosen as a Wigner rotation matrix. This type of a walk exists for any coin dimension starting with dimension two and provided that the dimension is odd, the trapping effect is observed. We emphasize that here by the dimension we mean a number of allowed movements. All the walks spread over a one-dimensional lattice, thus the dimension of the lattice is still the same.

The dimension of the Wigner rotation matrix is $2j + 1$, where j is a half-integer. The construction of these matrices comes from the quantum mechanical rotation operator and its irreducible matrix representation using Wigner formula [27, 28]. For each half-integer j , the $(2j + 1) \times (2j + 1)$ Wigner rotation matrix is a unitary matrix $R^{(j)}$ that provides a $2j + 1$ dimensional representation of the rotation group $SO(3)$. Since it corresponds to the matrix representation of the coin operator, from now on we will use more common designation for quantum coin as $C_W^{(j)}$ instead of $R^{(j)}$.

Considering the Hilbert space \mathcal{H} of the $2j + 1$ -dimensional walk from Eq.(1.1), $2j + 1$ allowed movements $|j\rangle, |j - 1\rangle, \dots, |-j\rangle$ form the standard basis of the coin Hilbert space \mathcal{H}_C . Note that since j can be also half-integer, the description of the walks is unified by setting the lengths of the individual step as $2m$, $m = -j, \dots, j$. Position Hilbert space is given as before by discrete positions on a one-dimensional lattice,

$$\mathcal{H}_p = \text{Span}\{|x\rangle, x \in \mathbb{Z}\}.$$

Coin $C_W^{(j)}$ is defined by the matrix elements ¹

$$(C_W^{(j)})_{mn}(\alpha, \gamma, \rho) = \langle m | \hat{C}^{(j)} | n \rangle$$

where $m, n = -j, -j + 1, \dots, j - 1, j$ and rotation $\hat{C}_W^{(j)}$ is the coin operator that is for the Wigner walks used in the evolution operator, Eq. (1.3). The matrix elements take the form

$$(C_W^{(j)})_{mn}(\alpha, \gamma, \rho) = e^{-iam} c_{mn}^{(j)}(\rho) e^{-i\gamma n}, \quad (1.24)$$

where

$$c_{mn}^{(j)}(\rho) = \sum_l \Gamma(j, m, n, l) \rho^{2j+m-n-2l} \sqrt{1 - \rho^2}^{2l-m+n}$$

and

$$\Gamma(j, m, n, l) = (-1)^l \frac{\sqrt{(j+m)!(j-m)!(j+n)!(j-n)!}}{(j-n-l)!(j+m-l)!(l+n-m)!l!}.$$

¹In [23] authors use parameter β instead of ρ . The relations between these two choices are $\cos \frac{\beta}{2} = \rho$, $\sin \frac{\beta}{2} = \sqrt{1 - \rho^2}$. Therefore, $|\rho|$ cannot exceed 1. Moreover, it is worth to assume that $|\rho| < 1$. The reason is that $\rho = \pm 1$ corresponds to the trivial walk with trivial dynamics. This notation is also more convenient for us since ρ corresponds to the maximal velocity of spreading, i.e. velocity of peaks in the position probability distribution.

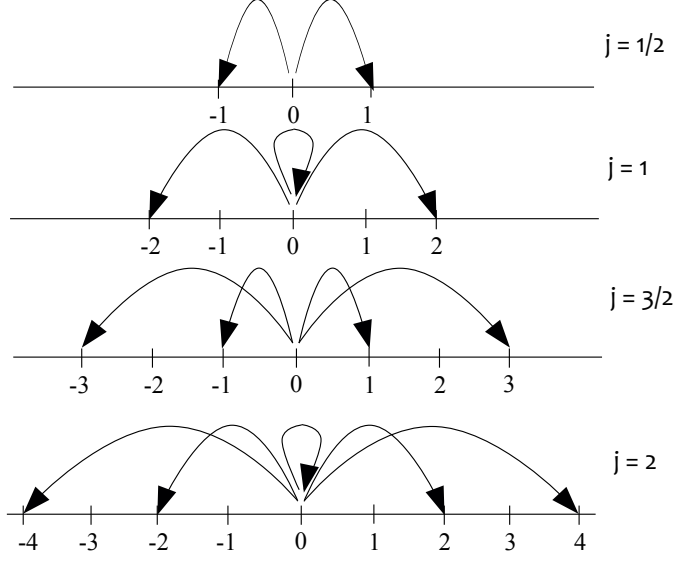


Figure 1.3: Allowed steps of $2j + 1$ -dimensional Wigner walk for different choices of j . If j is integer, we have odd-state walk where one of the possible movement is always to stay at the actual position. Both odd and even-state walks occupy only half of the positions on the lattice at each time.

The time evolution operator as described by Eq. (1.3) needs also a shift operator, which in the case of the Wigner walk has the form

$$\hat{S} = \sum_{x=-\infty}^{\infty} \sum_{m=-j}^j |x + 2m\rangle\langle x| \otimes |m\rangle\langle m|. \quad (1.25)$$

As we have mentioned above, this operator is defined in the way that the length of the step is not always equal to one, but can be larger and depends on the internal state of the coin m . The allowed movements are $2j$ steps to the right and left, $2(j - 1)$ steps to the right and left and so on. For integer j there is an odd number of steps allowed, therefore the walker may also stay on the actual position as one of the possibilities. Due to these movements, the walk occupies only half of the possible position at each time. The situation for the allowed steps of the Wigner walk and several choices of j is depicted in the Fig. (1.3).

The initial state of the walk $|\psi_0\rangle = |0\rangle \otimes |\psi_C\rangle$ evolves in time in a similar way as the three-state walk in Eq. (1.11). Therefore

$$|\psi(t)\rangle = \sum_x \sum_{m=-j}^j \psi_m^{(j)}(x, t) |x\rangle \otimes |m\rangle$$

and the probability of finding the particle at position x after t steps reads

$$p(x, t) = \sum_{m=-j}^j |\psi_m^{(j)}(x, t)|^2. \quad (1.26)$$

Note that the time evolution can be expressed also in a different way using position representation of a $(2j+1)$ -component probability amplitude vector $\psi^{(j)}(x, t) = (\psi_{-j}^{(j)}, \psi_{-j+1}^{(j)}, \dots, \psi_j^{(j)})$ and coin elements responsible for change of the coin states. Components of this vector evolves in time t as

$$\psi_m^{(j)}(x, t+1) = \sum_{n=-j}^j C_{mn}^{(j)} \psi_n^{(j)}(x+2n, t).$$

Further analysis is done similarly as among the lines presented in subsection 1.1.1. Using the Fourier transform we change the position to the momentum representation

$$\tilde{\psi}^{(j)}(k, t) = \sum_x e^{ikx} \psi^{(j)}(x, t).$$

It simplifies the calculation of the evolution of the probability amplitude vector to

$$\tilde{\psi}^{(j)}(k, t+1) = \tilde{U}(k) \tilde{\psi}^{(j)}(k, t) = \tilde{U}^t(k) \psi_0,$$

where $\tilde{U}(k)$ as the evolution operator in the Fourier picture read

$$\tilde{U}(k) = \text{Diag}\{e^{-2ikj}, e^{-2ik(j-1)}, \dots, e^{2ik(j-1)}, e^{2ikj}\} \cdot C_W^{(j)}.$$

Here Diag denotes diagonal matrix.

The importance of the introduced Wigner walks model sits in its suitable basis and the limiting distribution analysed in chapter 5. These walks helped us to understand physical meanings of the suitable basis and thus provided approach for its construction that can be applied for other types of walks.

By this final subsection, we have introduced all classes of quantum walks on a line whose properties will be later analysed. We do not limit ourselves only to a one-dimensional lattice and thus the next section is devoted to four-state quantum walks on a two-dimensional lattice. We introduce a notation and some properties we will refer to in the following chapters, especially chapter 2 and 4.

1.2 Quantum walks on a two-dimensional lattice

Let us start with a quantum walk on a two-dimensional lattice, where the walker can move in a plane to the left, right, down or up at each discrete time step. Therefore, the position Hilbert space

$$\mathcal{H}_p = \text{Span}\{|x, y\rangle; x, y \in \mathbb{Z}\}$$

is spanned by positions x on the horizontal lattice and y on the vertical lattice. Coin Hilbert space is given by

$$\mathcal{H}_C = \mathbb{C}^4 = \text{Span}\{|L\rangle, |R\rangle, |D\rangle, |U\rangle\} = \text{Span}\left\{\begin{pmatrix} 1 \\ 0 \\ 0 \\ 0 \end{pmatrix}, \begin{pmatrix} 0 \\ 1 \\ 0 \\ 0 \end{pmatrix}, \begin{pmatrix} 0 \\ 0 \\ 1 \\ 0 \end{pmatrix}, \begin{pmatrix} 0 \\ 0 \\ 0 \\ 1 \end{pmatrix}\right\},$$

denoting movements to the left, right, down and up.

Considering the time evolution, the evolution operator has the same form as before,

$$\hat{U} = \hat{S}(\hat{I}_p \otimes \hat{C})$$

and coin C is now an arbitrary four-dimensional unitary matrix of the general form

$$C = \begin{pmatrix} C_{LL} & C_{LR} & C_{LD} & C_{LU} \\ C_{RL} & C_{RR} & C_{RD} & C_{RU} \\ C_{DL} & C_{DR} & C_{DD} & C_{DU} \\ C_{UL} & C_{UR} & C_{UD} & C_{UU} \end{pmatrix}. \quad (1.27)$$

Further, the step operator reads

$$\begin{aligned} \hat{S} = \sum_{x,y} & |x-1, y\rangle\langle x, y| \otimes |L\rangle\langle L| + |x+1, y\rangle\langle x, y| \otimes |R\rangle\langle R| + \\ & + |x, y-1\rangle\langle x, y| \otimes |D\rangle\langle D| + |x, y+1\rangle\langle x, y| \otimes |U\rangle\langle U|. \end{aligned}$$

The time evolution of the probability amplitude vector after Fourier transform from positions x, y to momenta k, l is in complete analogy with Subsec. 1.1.1 and reads

$$\tilde{\psi}(k, l, t) = \tilde{U}(k, l)\psi(k, l, t-1) = \tilde{U}^t(k, l)\psi_0.$$

Here

$$\tilde{U}(k, l) = \text{Diag}\{e^{-ik}, e^{ik}, e^{-il}, e^{il}\} \cdot C, \quad (1.28)$$

is the evolution in the momentum Fourier representation. Since we are interested in the quantum walks with non-empty point spectrum, we describe one such a four-state walk, which is the Grover walk.

1.2.1 Four-state Grover walk on a two-dimensional lattice

In the case of the Grover walk, the coin is four-dimensional Grover matrix

$$C_G^{(4)} = \frac{1}{2} \begin{pmatrix} -1 & 1 & 1 & 1 \\ 1 & -1 & 1 & 1 \\ 1 & 1 & -1 & 1 \\ 1 & 1 & 1 & -1 \end{pmatrix}, \quad (1.29)$$

constructed according to Eq. (1.6).

Surprisingly, even though there is no option for the walk to stay at the the individual step, the trapping effect appears. The phases $\omega_j(k, l)$ of the eigenvalues $\lambda_j(k, l) = e^{i\omega_j(k, l)}$ of $\tilde{U}(k, l)$ from Eq. (1.28) with coin $C = C_G^{(4)}$ are equal to

$$\begin{aligned} \omega_{1,2}(k, l) &= \pm \arccos\left(-\frac{1}{2}(\cos k + \cos l)\right), \\ \omega_3(k, l) &= 0, \\ \omega_4(k, l) &= \pi. \end{aligned}$$

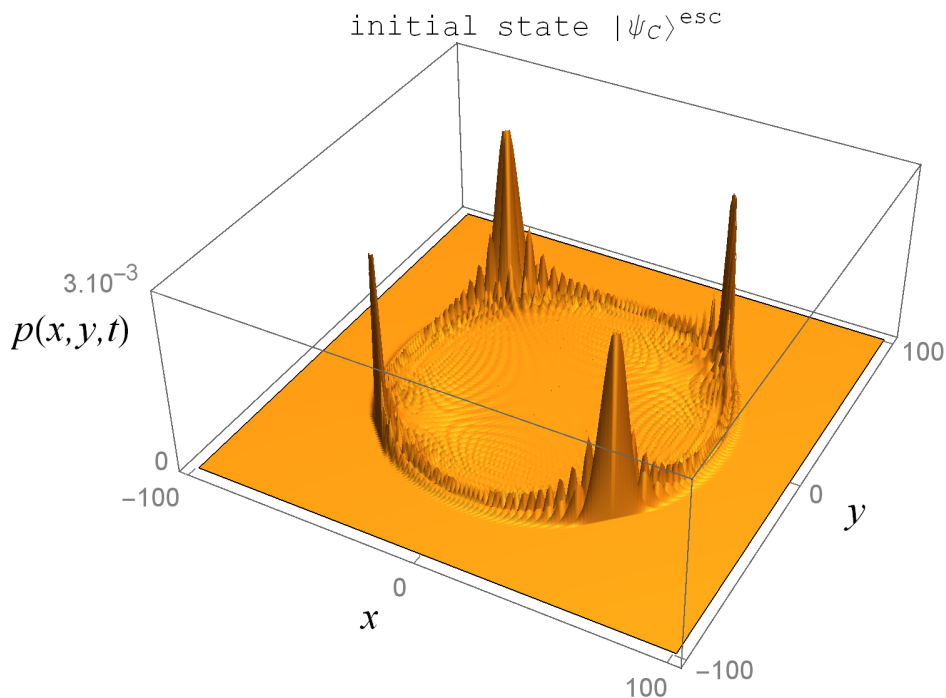


Figure 1.4: Position probability distribution of the four-state Grover walk on a two-dimensional lattice. Initial state is chosen to be the escaping state from Eq. (1.34). For the escaping state, trapping peak is not observed. The total number of steps is $t = 100$.

The existence of the constant phase ensures that the point spectrum of the walk is non-empty and therefore, the trapping at the vicinity of the origin appears.

We note that the eigenvectors corresponding to the constant eigenvalue $\lambda_{3,4} = \pm 1 = e^{i\omega_{3,4}(k,l)}$ read

$$v_{3,4}(k) = \frac{1}{n_{3,4}} \left(1 \pm e^{-il}, e^{ik}(\pm 1 + e^{-il}), (\pm 1 + e^{ik})e^{-il}, 1 \pm e^{ik} \right)^T, \quad (1.30)$$

with normalization factor

$$n_{3,4} = \pm 4 (\pm 2 + \cos k + \cos l).$$

The dependence of the trapping on the choice of the initial coin state is essential. For majority of the initial states, four-state Grover walk is trapped. Nevertheless, we can find an escaping state for which the trapping peak is not observed. It was found that certain coins lead to trapping quantum walks regardless of an initial state. Such walks are called strongly trapping.

1.2.2 Strong trapping

In [29], Kollár et al. introduced a completely new so-called strong trapping effect for two-dimensional quantum walks. Strong trapping manifest itself in the absence of an escaping state, that is initial coin state for which the trapping is not observed. The main importance of

this new phenomena sits in its possible applications in transport, efficiency and deposition of excitation in planar structures or spatial quantum search algorithms. In general, the existence of point spectrum of the time evolution operator $\tilde{U}(k, l)$ and the corresponding stationary states are responsible for trapping. Any initial coin state with non-zero overlap with the stationary state inevitably lead to the presence of the central trapping probability peak. The escaping state for which the trapping is not observed is the initial coin state orthogonal to trapping (stationary) state. For strong trapping coin class we cannot find such a state.

As an example of the main though let us first discuss the four-state Grover walk. This walk exhibits trapping but not strong trapping. The escaping state exists and has form

$$|\psi_C^{esc}\rangle = \frac{1}{2}(|L\rangle + |R\rangle - |D\rangle - |U\rangle), \quad (1.31)$$

which in the matrix representation read

$$\psi_C^{esc} = \frac{1}{2}(1, 1, -1, -1).$$

Indeed, the stationary states, Eq. (1.30), are the eigenstates of the evolution operator $\tilde{U}(k, l)$ corresponding to the constant eigenvalues ± 1 . The escaping initial state (initial probability amplitude vector) is independent of the momentum k , thus can be written as $\psi_0 = (\alpha, \beta, \gamma, \delta)^T$. It has to satisfy the condition

$$(v_{3,4}, \psi_0) = 0.$$

Comparison of the individual terms accompanying expressions $e^{if(k,l)}$, $f(k, l) = 0, k, l, \dots$ lead to the conditions

$$\begin{aligned} 1 &: & \alpha + \delta &= 0 \\ e^{-ik} &: & \beta + \delta &= 0 \\ e^{il} &: & \alpha + \gamma &= 0 \\ e^{i(l-k)} &: & \beta + \gamma &= 0 \end{aligned}$$

which provide the initial state,

$$\psi_0 = \frac{1}{2}(1, 1, -1, -1)^T = \psi_C^{esc} \Leftrightarrow |\psi_0\rangle = |0, 0\rangle \otimes \underbrace{\frac{1}{2}(|L\rangle + |R\rangle - |D\rangle - |U\rangle)}_{|\psi_C\rangle^{esc}}.$$

In [29] authors constructed non-trivial coin of the form

$$C^{ST} = \begin{pmatrix} e^{-i(\alpha_1+\alpha_2)}c_1c_2 & e^{-i(\beta_1+\beta_2+\varphi)}s_1s_2 & -e^{-i(\alpha_2+\beta_1)}c_2s_1 & -e^{-i(\alpha_1+\beta_2)}c_1s_2 \\ e^{i(\beta_1+\beta_2+\varphi)}s_1s_2 & e^{i(\alpha_1+\alpha_2)}c_1c_2 & e^{i(\alpha_1+\beta_2+\varphi)}c_1s_2 & e^{i(\alpha_2+\beta_1+\varphi)}c_2s_1 \\ e^{-i(\alpha_1+\alpha_2)}c_1s_2 & -e^{i(\alpha_2+\beta_2-\varphi)}c_2s_1 & -e^{-i(\beta_1-\beta_2)}s_1s_2 & e^{-i(\alpha_1-\alpha_2)}c_1c_2 \\ e^{-i(\alpha_2+\beta_1)}c_2s_1 & -e^{i(\alpha_1-\beta_2-\varphi)}c_1s_2 & e^{i(\alpha_1-\alpha_2)}c_1c_2 & -e^{i(\beta_1-\beta_2)}s_1s_2 \end{pmatrix}, \quad (1.32)$$

where

$$c_j = \cos \delta_j, \quad s_j = \sin \delta_j, \quad j = 1, 2.$$

Here the stationary states reads

$$v_{\lambda=\pm 1} = \frac{1}{2} \begin{pmatrix} e^{i\beta_1} s_1 \pm e^{i\ell} e^{i\beta_2} s_2 \\ e^{ik} e^{i\ell} e^{-i(\beta_1+\varphi)} s_1 \pm e^{ik} e^{-i(\beta_2+\varphi)} s_2 \\ e^{i\alpha_1} c_1 \mp e^{ik} e^{-i\alpha_2} c_2 \\ -e^{ik} e^{i\ell} e^{-i\alpha_1} c_1 \pm e^{i\ell} e^{i\alpha_2} c_2 \end{pmatrix} \quad (1.33)$$

It holds that for most of the C^{ST} -coins, arbitrary initial state

$$|\psi_0\rangle = |0, 0\rangle \otimes \underbrace{(\alpha|L\rangle + \beta|R\rangle + \gamma|D\rangle + \delta|U\rangle)}_{|\psi_C\rangle} \longrightarrow \tilde{\psi}_0 = \psi_0 = (\alpha, \beta, \gamma, \delta)^T$$

has non-zero overlap with the stationary state $v_{\lambda=\pm 1}$ and thus exhibits strong trapping effect. The only difference is the case where

$$\cos 2\delta_1 = \cos 2\delta_2,$$

for which we can find an escaping state. Also we have

$$\text{strong trapping} \Leftrightarrow \forall \psi_0, (v_{\lambda=\pm 1}, \psi_0) \neq 0 \Leftrightarrow \cos 2\delta_1 \neq \cos 2\delta_2.$$

In the case of $\cos 2\delta_1 = \cos 2\delta_2$, the escaping state is given by

$$\psi_0^{esc} = \psi_C^{esc} = \frac{1}{\sqrt{2}} \begin{pmatrix} e^{-i\beta_1} \cos \delta_1 \\ -e^{-i(\alpha_1+\alpha_2-\beta_2-\varphi)} \cos \delta_1 \\ -e^{-i\alpha_1} \sin \delta_1 \\ -e^{-i(\alpha_2+\beta_1-\beta_2)} \sin \delta_1 \end{pmatrix}.$$

Thus, initial state of the form

$$|\psi_0^{esc}\rangle = |0, 0\rangle \otimes \left(e^{-i\beta_1} \cos \delta_1 |L\rangle - e^{-i(\alpha_1+\alpha_2-\beta_2-\varphi)} \cos \delta_1 |R\rangle - \right. \\ \left. -e^{-i\alpha_1} \sin \delta_1 |D\rangle - e^{-i(\alpha_2+\beta_1-\beta_2)} \sin \delta_1 |U\rangle \right) \quad (1.34)$$

leads to a non-trapping walk.

In this section, we have introduced the concept of the four-state quantum walks on a two-dimensional lattice. We have showed that at least for the Grover walk, non-empty point spectrum and thus trapping effect exist. Moreover, for a specific coin class one can find a stronger version of trapping. It means that trapping is observed regardless the choice of the initial state. This feature is not observed for the Grover walk for which we can find a single initial state having zero overlap with the stationary state. We will return to the strong trapping effect in chapter 4 which is devoted to the classification of the trapping coins for four-state quantum walk on a two-dimensional lattice. We show that from all trapping families of coins, there exist no other strong trapping coin class besides C^{ST} .

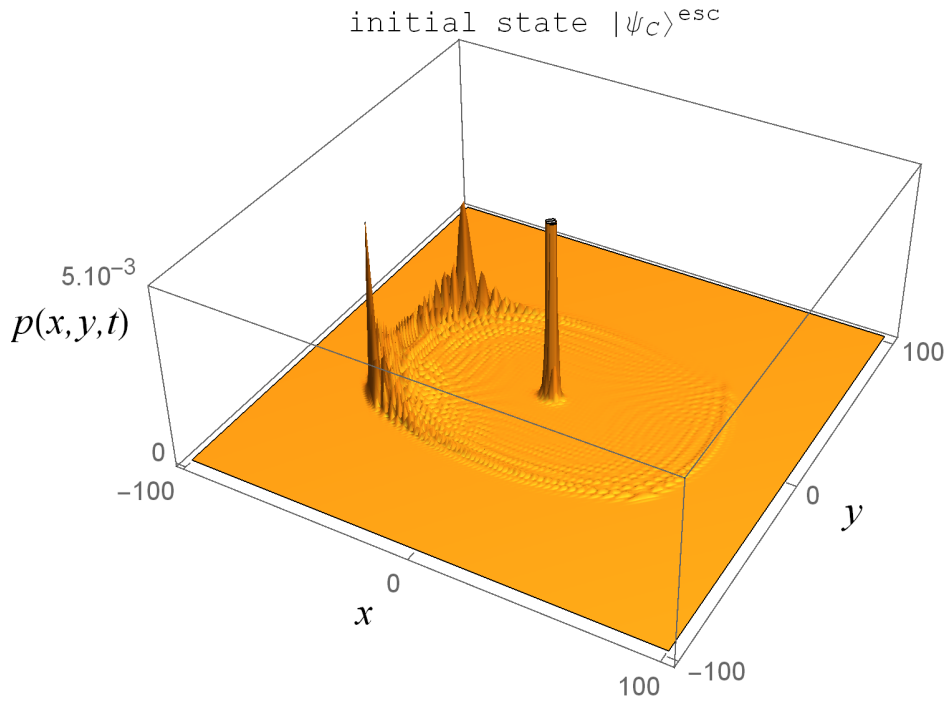


Figure 1.5: Position probability distribution of the quantum walk with strongly trapping coin class, Eq. (1.32). We have chosen parameters $\delta_1 = \pi/3$, $\delta_2 = \pi/4$ and all the phases $\alpha_{1,2} = \beta_{1,2} = \varphi = 0$. The initial coin state of the walk is the state which is for the Grover walk escaping, Eq. (1.34). This state was chosen for better comparison with Fig. (1.4). Strong trapping coin class exhibits trapping regardless of the initial state. Moreover, for this particular state the trapping peak is very thick and covers considerable part of the total probability. The central peak achieves value around 0.3 and exceeds the rest of the distribution significantly. Therefore, the plot range is cut. The total number of steps is $t = 100$.

Chapter 2

Continuous deformations of the Grover walk

Based on the trapping effect exhibited by the three-state quantum walk on a line with the Grover coin, we expect the existence of other coins or coin classes leading to trapping. We can immediately find a simple example of another trapping matrix. If we choose as a coin some trivial matrix, for instance the identity matrix, the walk will certainly satisfy the condition to exhibit non-empty point spectrum. We can see it directly for the three-state walk by choosing the initial coin state as "stay at your actual position", $|\psi_C\rangle = |S\rangle = (0, 1, 0)^T$. The action of the identity matrix leaves this state unchanged and trapped at the origin. The identity matrix does not mix coin states at all, there is no interference and the dynamics is trivial.

The question is whether there exist other non-trivial coins preserving the trapping effect and whether the already known coins are connected in some way. We show that such a connection can be established and the trivial matrices can be linked with the non-trivial ones. These connections lead to two one-parameter families of coins preserving the trapping effect. From the reasons that will be clear soon, let us call these two families as eigenvalue and eigenvector family.

Both resulting families of coins preserve the existence of the point spectrum of the time evolution operator in the Fourier picture. In other words, presented one-parameter families provide trapping walks for an arbitrary choice of the additional parameter. The advantage of the presented approach is that it can be easily extended to higher-dimensional quantum walks.

2.1 Eigenvalue family of coins

First, we describe the construction of the eigenvalue family for the three-state Grover walk on a line and apply the knowledge to the four-state Grover walk on a two-dimensional lattice. The approach is based on finding trivial matrices having full rank that commute with the Grover matrix. Therefore, their common eigenvectors can be found. This is not true for the eigenvalues which are different and we emphasize it by the name eigenvalue family.

2.1.1 Eigenvalue deformation of the three-state Grover walk on a line

The trivial matrix that plays a crucial role here is the anti-diagonal permutation matrix

$$P_\pi^{(3)} = \begin{pmatrix} 0 & 0 & 1 \\ 0 & 1 & 0 \\ 1 & 0 & 0 \end{pmatrix}. \quad (2.1)$$

Three-state quantum walk on a line with this permutation coin will only switch $|L\rangle \leftrightarrow |R\rangle$ in each step and state $|S\rangle$ remains unchanged. There is no mixing of the coin states, and the walker only jumps step to the right or left and then immediately back in the next step. Such a walk does not spread across the lattice.

This specific choice of the trivial coin is not arbitrary, since the spectrum of this matrix and the Grover matrix $C_G^{(3)}$, Eq. (1.9), differs only in a sign of one eigenvalue. Since the matrices $P_\pi^{(3)}$ and $C_G^{(3)}$ commute, their eigenvectors can be chosen the same. The change of sign can be solved by addition of a phase factor φ into the spectral decomposition of the Grover matrix. The decomposition of $C_G^{(3)}$ reads

$$C_G^{(3)} = \lambda_1 v_1 v_1^\dagger + \lambda_2 v_2 v_2^\dagger + \lambda_3 v_3 v_3^\dagger = -v_1 v_1^\dagger - v_2 v_2^\dagger + v_3 v_3^\dagger \quad (2.2)$$

where $v_{1,2,3}$ are the eigenvectors of the Grover matrix,

$$\begin{aligned} v_1 &= \frac{1}{\sqrt{6}} (1, -2, 1)^T \\ v_2 &= \frac{1}{\sqrt{2}} (1, 0, -1)^T \\ v_3 &= \frac{1}{\sqrt{3}} (1, 1, 1)^T, \end{aligned} \quad (2.3)$$

with the corresponding eigenvalues $\lambda_{1,2} = -1$, $\lambda_3 = 1$. On the other hand, due to a different sign of the first eigenvalue, the decomposition of $P_\pi^{(3)}$ reads

$$P_\pi^{(3)} = v_1 v_1^\dagger - v_2 v_2^\dagger + v_3 v_3^\dagger. \quad (2.4)$$

Adding a phase factor provides a continuous transfer between these two matrices,

$$P_\pi^{(3)} \xleftrightarrow{\varphi} C_G^{(3)}$$

as

$$C_{def_1}^{(3)}(\varphi) = -e^{2i\varphi} v_1 v_1^\dagger - v_2 v_2^\dagger + v_3 v_3^\dagger = \frac{1}{6} \begin{pmatrix} -1 + e^{2i\varphi} & 2(1 + e^{2i\varphi}) & 5 - e^{2i\varphi} \\ 2(1 + e^{2i\varphi}) & 2(1 - e^{2i\varphi}) & 2(1 + e^{2i\varphi}) \\ 5 - e^{2i\varphi} & 2(1 + e^{2i\varphi}) & -1 - e^{2i\varphi} \end{pmatrix}. \quad (2.5)$$

We call $C_{def_1}^{(3)}(\varphi)$ an eigenvalue family of coins.

From both, the construction and the final form of the eigenvalue family, it is easy to check that the choice $\varphi = \pi/2$ leads to the permutation matrix $P_\pi^{(3)}$. On the other hand, the choice $\varphi = 0$ gives the Grover matrix $C_G^{(3)}$, Eq. (1.9). The factor of 2 in the additional phase is not necessary, it is only convenient choice for further calculation. One can check quite easily that this new coin class preserves the trapping effect. Additional information and analysis regarding trapping and spreading of the walk is formulated in [I, 30].

2.1.2 Eigenvalue deformation of the four-state Grover walk on a two-dimensional lattice

In the same way as for the three-state walk, we can construct an eigenvalue family for the four-state quantum walk. We start from the four-dimensional Grover matrix from Eq. (1.29) and connect it with the permutation matrix of the form

$$P_\pi^{(4)} = \begin{pmatrix} 0 & 1 & 0 & 0 \\ 1 & 0 & 0 & 0 \\ 0 & 0 & 0 & 1 \\ 0 & 0 & 1 & 0 \end{pmatrix}. \quad (2.6)$$

This matrix switches only the coin states corresponding to the horizontal or vertical lattice,

$$|L\rangle \longleftrightarrow |R\rangle, \quad |D\rangle \longleftrightarrow |U\rangle. \quad (2.7)$$

The spectrum of the permutation matrix

$$\lambda_1^{P_\pi^{(4)}} = 1, \quad \lambda_2^{P_\pi^{(4)}} = -1, \quad \lambda_3^{P_\pi^{(4)}} = -1, \quad \lambda_4^{P_\pi^{(4)}} = 1, \quad (2.8)$$

differs from the spectrum of the Grover matrix

$$\lambda_1^{C_G^{(4)}} = -\lambda_1^{P_\pi^{(4)}} = -1, \quad \lambda_{2,3,4}^{C_G^{(4)}} = \lambda_{2,3,4}^{P_\pi^{(4)}}, \quad (2.9)$$

in the sign of the first eigenvalue. The common eigenvectors of the matrices $P_\pi^{(4)}$ and $C_G^{(4)}$ corresponding to the eigenvalues from Eqs. (2.8) and (2.9) read

$$\begin{aligned} v_1 &= \frac{1}{2}(1, 1, -1, -1)^T \\ v_2 &= \frac{1}{\sqrt{2}}(0, 0, 1, -1)^T \\ v_3 &= \frac{1}{\sqrt{2}}(1, -1, 0, 0)^T \\ v_4 &= \frac{1}{2}(1, 1, 1, 1)^T. \end{aligned} \quad (2.10)$$

The one-parameter family of trapping coins $C_{def_1}^{(4)}(\theta)$ with parameter $\theta \in \mathbb{R}$ connecting the Grover matrix and the permutation matrix \tilde{P}_π is constructed in the same way as in the previous section. Using the spectral decomposition we obtain

$$\begin{aligned} C_{def_1}^{(4)}(\theta) &= -e^{2i\theta} v_1 v_1^\dagger - v_2 v_2^\dagger - v_3 v_3^\dagger + v_4 v_4^\dagger = \\ &= \frac{1}{4} \begin{pmatrix} -(1 + e^{2i\theta}) & 3 - e^{2i\theta} & 1 + e^{2i\theta} & 1 + e^{2i\theta} \\ 3 - e^{2i\theta} & -(1 + e^{2i\theta}) & 1 + e^{2i\theta} & 1 + e^{2i\theta} \\ 1 + e^{2i\theta} & 1 + e^{2i\theta} & -(1 + e^{2i\theta}) & 3 - e^{2i\theta} \\ 1 + e^{2i\theta} & 1 + e^{2i\theta} & 3 - e^{2i\theta} & -(1 + e^{2i\theta}) \end{pmatrix}. \end{aligned} \quad (2.11)$$

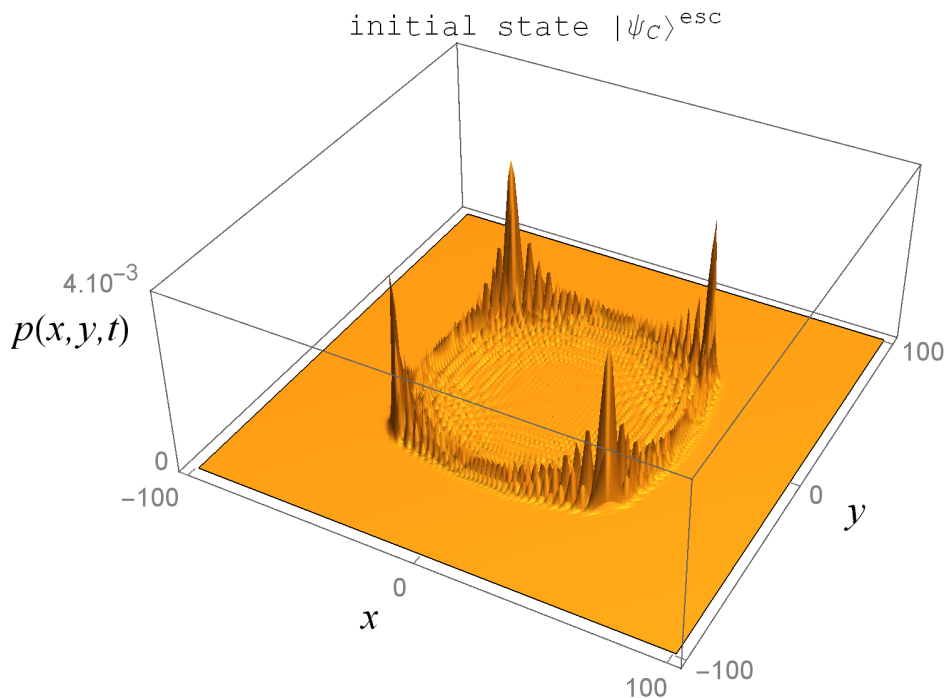


Figure 2.1: Position probability distribution for the four-state walk on a two-dimensional lattice with coin $C_1^{(4)}(\theta)$, Eq. (2.11). The initial state is a state which for which the Grover walk is non-trapping, Eq. (1.34). Parameter $\theta = \pi/8$ and the total number of steps $t = 100$.

It is seen that $C_{def_1}^{(4)}(0) = C_G^{(4)}$ and $C_{def_1}^{(4)}(\frac{\pi}{2}) = P_\pi^{(4)}$. Sometimes it is useful to multiply the eigenvalue family $C_{def_1}^{(4)}(\theta)$ by a global phase $e^{-i\theta}$ which changes many of the complex matrix elements to simple cosine function.

The new $C_{def_1}^{(4)}(\theta)$ family of coins preserves the presence of the constant eigenvalues of the evolution operator $\tilde{U}(k, l)$, Eq. (1.28). To show it, we write down their explicit forms, $\lambda_j(k, l, \theta) = e^{i\omega_j(k, l, \theta)}$, $j = 1, 2, 3, 4$, with phases

$$\begin{aligned}\omega_{1,2}(k, l, \theta) &= \theta \pm \arccos\left(-\frac{1}{2}(\cos k + \cos l) \cos \theta\right), \\ \omega_3(k, l, \theta) &= 0, \\ \omega_4(k, l, \theta) &= \pi.\end{aligned}$$

The constant eigenvalues are the same as for the Grover walk on a two-dimensional lattice, i. e. $\lambda_{3,4}(k, l, \theta) = \pm 1$.

Note that there exist other permutation matrices with one different eigenvalue. These matrices are, from our experience, not worth to use. They switch between the horizontal and the vertical lattice and do not lead to trapping.

2.1.3 Eigenvalue families for other types of higher-dimensional quantum walks

The application of the approach described in the previous subsections is not limited only to the three-state Grover walk on a line or the four-state Grover walk on a square lattice. We are convinced that it can be applied to any type of walk exhibiting trapping.

Due to the fact that there is no trapping for any two-state quantum walk on a line, we might assume that trapping exists only for odd-state walks on a line, where one of the allowed movement is to stay at the actual position. This feature was observed for the Wigner walks (subsection 1.1.2). Despite that, the four-state Grover walk on a line exhibits trapping. The possible movements are step to the left or right and two steps to the left or right. Then, in analogy with Eq. (1.15) and Eq. (1.28), the evolution operator in the Fourier picture reads

$$\tilde{U}(k) = \text{Diag}\{e^{-2ik}, e^{-ik}, e^{ik}, e^{2ik}\} \cdot C_G^{(4)}, \quad (2.12)$$

where $C_G^{(4)}$ is the four-dimensional Grover matrix, Eq. (1.29).

One can easily check, that the propagator $\tilde{U}(k)$ has two constant eigenvalues equal to ± 1 . Furthermore, a trivial walk with non-empty point spectrum needs to employ trivial coin in the form

$$\bar{P}_\pi = \begin{pmatrix} 0 & 0 & 0 & 1 \\ 0 & 0 & 1 & 0 \\ 0 & 1 & 0 & 0 \\ 1 & 0 & 0 & 0 \end{pmatrix}.$$

This anti-diagonal permutation matrix, whose eigenvalues differ from the eigenvalues of $C_G^{(4)}$ only in one sign, has common eigenvectors $p_i, i = 1, \dots, 4$ with $C_G^{(4)}$. These are

$$\begin{aligned} p_1 &= \frac{1}{2}(-1, 1, -1, 1), \\ p_2 &= \frac{1}{2}(-1, -1, 1, 1), \\ p_3 &= \frac{1}{2}(1, -1, -1, 1), \\ p_4 &= \frac{1}{2}(1, 1, 1, 1). \end{aligned}$$

Note that the choice of the eigenvectors is a bit different than in Eq. (2.10) due to different permutation matrices \bar{P}_π and $P_\pi^{(4)}$ from Eq. (2.6).

Now we can construct the eigenvalue family of coins similarly as in previous section, it is by a suitable addition of a phase factor $e^{i\vartheta}$ into the spectral decomposition. The resulting one-parameter family then reads

$$\begin{aligned} \bar{C}_{def_1}^{(4)}(\vartheta) &= -p_1 p_1^\dagger - p_2 p_2^\dagger - e^{2i\vartheta} p_3 p_3^\dagger + p_4 p_4^\dagger = \\ &= \frac{1}{4} \begin{pmatrix} -(1 + e^{2i\vartheta}) & 1 + e^{2i\vartheta} & 1 + e^{2i\vartheta} & 3 - e^{2i\vartheta} \\ 1 + e^{2i\vartheta} & -(1 + e^{2i\vartheta}) & 3 - e^{2i\vartheta} & 1 + e^{2i\vartheta} \\ 1 + e^{2i\vartheta} & 3 - e^{2i\vartheta} & -(1 + e^{2i\vartheta}) & 1 + e^{2i\vartheta} \\ 3 - e^{2i\vartheta} & 1 + e^{2i\vartheta} & 1 + e^{2i\vartheta} & -(1 + e^{2i\vartheta}) \end{pmatrix}, \end{aligned}$$

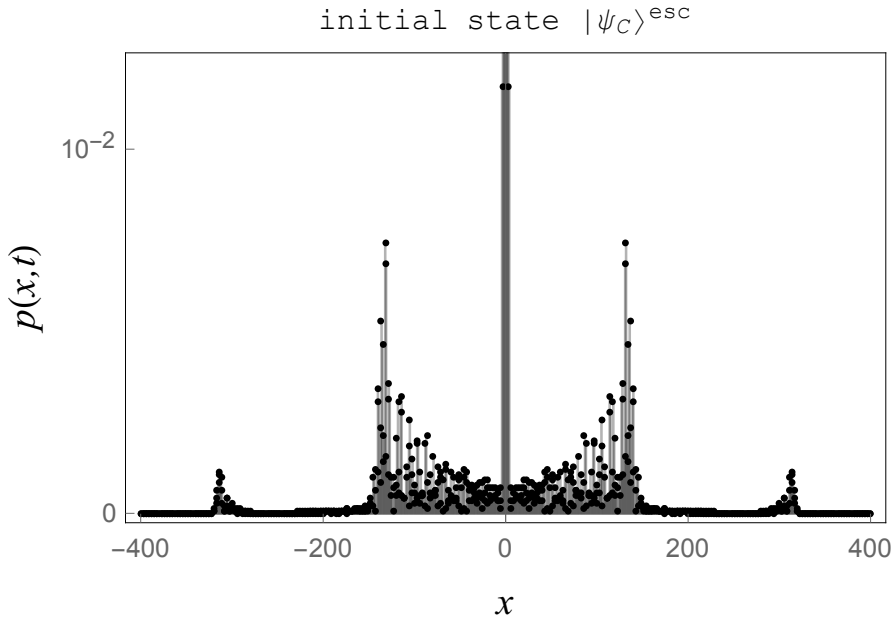


Figure 2.2: Position probability distribution for the four-state Grover walk on a line. As an initial state we have a state which is for the walk on a two-dimensional lattice escaping, Eq. (1.34). For the similar walk on a line, this initial state leads to trapping walk. The total number of steps is $t = 200$.

which is just a rearrangement of the eigenvalue family for the four-state walk on a 2D lattice, Eq. (2.11).

We have mentioned that the Grover matrix can be constructed in any dimension starting with dimension three, following Eq. (1.6). Therefore, we may construct eigenvalue families also for five and higher-state quantum walk on a line or a two-dimensional lattice. The key moment is to find a proper trapping trivial coin with spectrum differing only in a sign of one eigenvalue compared to the spectrum of the Grover matrix. This trivial coin depends on the dimensionality of the lattice. Such eigenvalue families will always preserve trapping.

2.2 Eigenvector family of coins

In the previous section we have described the construction of the eigenvalue family of trapping coins based on the sign difference in the spectrum. Nevertheless, there exist trivial matrices that have the same spectrum as the Grover matrix, but since these matrices do not commute with the Grover matrix, their eigenvectors cannot be chosen the same. We will show that the eigenvectors of the trivial and the Grover matrices can be parametrized in order to provide a continuous change from the trivial to the Grover matrix. Therefore, we call the new family of matrices eigenvector family of coins.

The idea of the parametrization of the eigenvectors is inspired by the work of Watabe et al. [31]. In this paper the authors studied a four-state quantum walk on a two-dimensional

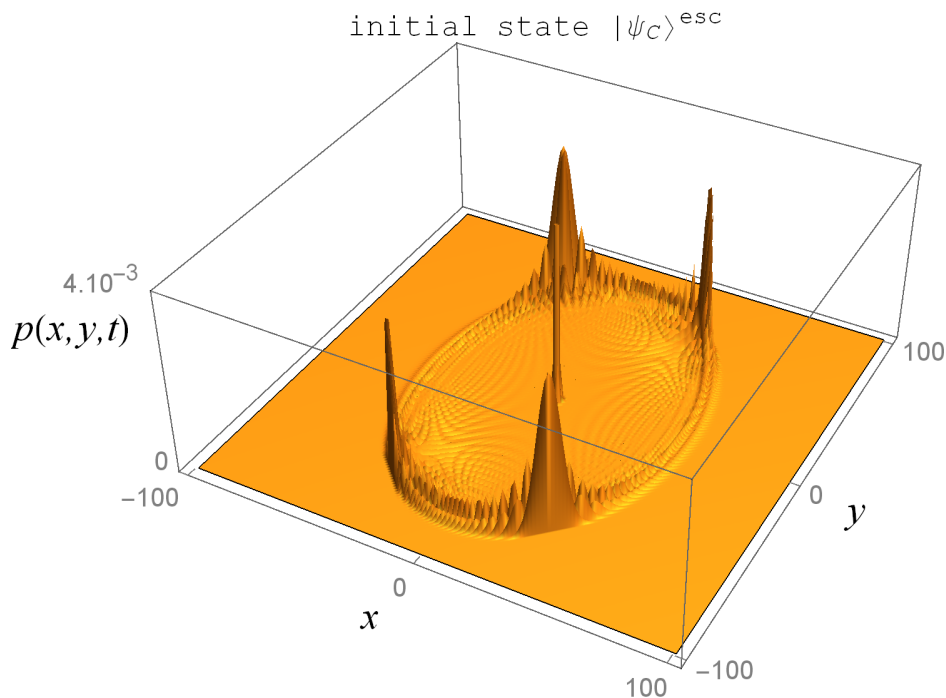


Figure 2.3: Position probability distribution for the four-state quantum walk on a two-dimensional lattice with the coin $C_{def_2}^{(4)}(p)$ results in elliptic spreading. We have chosen $p = 2/3$ and the initial state is given by Eq. (1.34). It is seen that this state is not an escaping state as it was for the Grover walk. The total number of steps is $t = 100$.

lattice with one parameter family of coins. This one-parameter family of coins has the form

$$C_{def_2}^{(4)}(p) = \begin{pmatrix} -p & q & \sqrt{pq} & \sqrt{pq} \\ q & -p & \sqrt{pq} & \sqrt{pq} \\ \sqrt{pq} & \sqrt{pq} & -q & p \\ \sqrt{pq} & \sqrt{pq} & p & -q \end{pmatrix}, \quad p + q = 1, \quad p \in \langle 0, 1 \rangle. \quad (2.13)$$

One can easily check that the spectrum of this matrix is the same as for the Grover matrix $C_G^{(4)}$ from Eq. (1.29). In fact, the choice $p = q = 1/2$ equals the Grover matrix $C_G^{(4)}$. Note that the choices $p = 0$ or $p = 1$ result in trivial matrices that switches the coin states only on the horizontal or vertical lattice, while the others remain unchanged.

This $C_{def_2}^{(4)}(p)$ family of coins exhibits trapping. Unfortunately, there was no explanation on the construction of the given family. We have analysed the family of coins, proposed the construction and employ it to define new types of walks. In the next subsection we provide, as an example, the eigenvector family for the three-state walk on a line. It will be seen that the described approach can be easily applied also to other types of walks. For more information about the spreading of these four-dimensional walks see [30].

2.2.1 Eigenvector deformation of the three-state Grover walk on a line

There exist two trivial matrices with the same spectrum as the Grover matrix $C_G^{(3)}$, Eq. (1.9), exhibiting trapping. These matrices T , T' are given by

$$T = \begin{pmatrix} 0 & 0 & 1 \\ 0 & -1 & 0 \\ 1 & 0 & 0 \end{pmatrix}, \quad T' = \begin{pmatrix} -1 & 0 & 0 \\ 0 & 1 & 0 \\ 0 & 0 & -1 \end{pmatrix}. \quad (2.14)$$

The coin T is very similar to the permutation matrix, Eq. (2.1), and leads to the same type of walk, where the particle jumps back and forth without spreading through the lattice. The coin T' does not even change the coin states at all and results in a similar type of walk as with the identity matrix. Therefore, initial coin state components $|L\rangle$ or $|R\rangle$ send the particle to the left or right at each step. After t steps, the particle can be found only at three possible positions, $x = 0$ and $x = \pm t$. Therefore, the velocity of spreading is equal to one, which is the maximum velocity any quantum walk can reach, provided that the particle moves to the neighbouring side on the lattice at each step, i.e. the length of the step is equal to one. Note that for the Wigner walks introduced in Subsec. (1.1.2) the steps can be larger and we have to multiply the basic velocity by the length of the step.

One can easily check that the eigenvalues of the trivial coins T and T' are the same as for the Grover matrix $C_G^{(3)}$, it is $\lambda_{1,2}^{T,T'} = -1$ and $\lambda_3^{T,T'} = 1$. On the other hand, these matrices do not commute with the Grover matrix and thus their eigenvectors cannot be chosen the same. For the trivial coin T the eigenvectors are given by

$$\begin{aligned} v_1^T &= (0, -1, 0)^T, \\ v_2^T &= \frac{1}{\sqrt{2}}(1, 0, -1)^T, \\ v_3^T &= \frac{1}{\sqrt{2}}(1, 0, 1)^T \end{aligned}$$

and for the matrix T' we have

$$\begin{aligned} v_1^{T'} &= \frac{1}{\sqrt{2}}(1, 0, 1)^T, \\ v_2^{T'} &= \frac{1}{\sqrt{2}}(1, 0, -1)^T, \\ v_3^{T'} &= (0, 1, 0)^T. \end{aligned}$$

Both trivial matrices have clearly different eigenvectors from the Grover coin, Eq. (2.3). Nevertheless, an appropriate parametrization of the eigenvectors leads to the transition

$$T \xleftrightarrow{\rho} G_3 \xleftrightarrow{\rho} T',$$

where ρ is a parameter connecting these three matrices, respectively their eigenvectors. The

parametrized eigenvectors read

$$v_1(\rho) = \left(\frac{\rho}{\sqrt{2}}, -\sqrt{1-\rho^2}, \frac{\rho}{\sqrt{2}} \right)^T \quad (2.15)$$

$$v_2(\rho) = \frac{1}{\sqrt{2}}(1, 0, -1)^T$$

$$v_3(\rho) = \left(\sqrt{\frac{1-\rho^2}{2}}, \rho, \sqrt{\frac{1-\rho^2}{2}} \right)^T, \quad (2.16)$$

where ρ ranges from 0 to 1.

The resulting eigenvector family of coins $C_{def_2}^{(3)}(\rho)$ is then formed as

$$\begin{aligned} C_{def_2}^{(3)}(\rho) &= -v_1(\rho)v_1^\dagger(\rho) - v_2(\rho)v_2^\dagger(\rho) + v_3(\rho)v_3^\dagger(\rho) = \\ &= \begin{pmatrix} -\rho^2 & \rho\sqrt{2(1-\rho^2)} & 1-\rho^2 \\ \rho\sqrt{2(1-\rho^2)} & 2\rho^2-1 & \rho\sqrt{2(1-\rho^2)} \\ 1-\rho^2 & \rho\sqrt{2(1-\rho^2)} & -\rho^2 \end{pmatrix}. \end{aligned} \quad (2.17)$$

To get the original Grover matrix we have to choose $\rho = 1/\sqrt{3}$ and the choices $\rho = 0$, $\rho = 1$ give the matrices T , T' . Note that for the three-state Grover walk, the velocity of spreading of the walk given by Eq. (1.23) is equal to $\pm 1/\sqrt{3}$. The trivial walk with coin T from Eq. (2.14) does not spread through the lattice at all, therefore its velocity equals zero. Further, the walk with T' coin, Eq. (2.14), spreads with the maximal velocity equal to one. It is not an accident that these velocities are the same as the choice of the parameter ρ . This additional parameter really corresponds to the rate of spreading of the walk. To show it we have to look at the phases $\omega_j(k, \rho)$ of the eigenvalues $\lambda_j(k, \rho)$ of the evolution operator

$$\tilde{U}(k, \rho) = \text{Diag}\{e^{-ik}, 1, e^{ik}\} \cdot C_{def_2}^{(3)}(\rho),$$

which is, up to the coin which is now $C_{def_2}^{(3)}(\rho)$, the same as Eq. (1.15). The phases of the eigenvalues of $\tilde{U}(k, \rho)$ read

$$\begin{aligned} \omega_{1,2}(k, \rho) &= \pm \arccos(\rho^2 - 1 - \rho^2 \cos k) \\ \omega_3(k, \rho) &= 0. \end{aligned} \quad (2.18)$$

Following the recipe given in the subsection 1.1.1 the velocities of spreading of the walk, i.e. the velocities of the probability peaks, are given by

$$v_{R,L}(\rho) = \left. \frac{\partial \omega_{2,1}(k, \rho)}{\partial \rho} \right|_{k_0} = \lim_{k \rightarrow 0^+} \frac{\partial \omega_{2,1}(k, \rho)}{\partial \rho} = \pm \rho \quad (2.19)$$

and

$$v_S(\rho) = 0.$$

We remind that $k_0 = 0$ is a point, where the second derivative of the dispersion relations $\omega_{1,2}(k, \rho)$ vanishes.

In this chapter we have shown that the Grover walk is not the only three-state or four-state walk exhibiting trapping. Nevertheless, the presented construction of the one-parameter families preserving trapping can be easily applied to higher dimensional walks, but does not allow us to make any statement about a completeness of these trapping classes. The following chapter is a step leading towards a full classification of the trapping three-state quantum walks on a line.

Chapter 3

Classification of trapping coins for three-state quantum walk on a line

In the previous chapter we have described an easy and intuitive constructions of trapping coins that can be used for more types of walks. The disadvantage of the construction of the eigenvector respectively eigenvalue families is that it does not say whether these two families cover all trapping coins or not. In this chapter we answer this question and show, how the most general trapping coin look like. We put the already found families into the context and comment how they form its subclasses. Since this is quite a complex problem, we have to limit ourselves to the three-state quantum walk on a line and will present a construction that covers all trapping coins. We will see that a general trapping coin for the three-state walk on a line contains more than one parameter. Nevertheless, even with higher number of parameters which ensure the existence of trapping, it is still a rare effect among all possible quantum walks.

3.1 Conditions on a non-empty point spectrum

We consider a three-state quantum walk on a line, for which the coin states are given by Eq. (1.7) and the time evolution operator, Eq. (1.15), has in the Fourier representation following form

$$\tilde{U}(k) = \text{Diag}\{e^{-ik}, 1, e^{ik}\}.C. \quad (3.1)$$

Here C is a general coin with matrix elements C_{ij} , $i, j = L, S, R$, thus

$$C = \begin{pmatrix} C_{LL} & C_{LS} & C_{LR} \\ C_{SL} & C_{SS} & C_{SR} \\ C_{RL} & C_{RS} & C_{RR} \end{pmatrix}. \quad (3.2)$$

Since we are interested in trapping at the vicinity of the origin, which is described by the non-empty point spectrum of the evolution operator $\tilde{U}(k)$, we can immediately write the eigenvalues of $\tilde{U}(k)$, as

$$\lambda_1(k) = e^{i\alpha}, \lambda_{2,3}(k) = e^{i\omega_{2,3}(k)}. \quad (3.3)$$

In order to ensure the trapping, one of the eigenvalues has to be constant. Here λ_1 is a constant eigenvalue and $\lambda_{2,3}$ depend on the momentum k . The characteristic equation of $\tilde{U}(k)$ from Eq. (3.1) reads

$$\det(\tilde{U}(k) - \lambda I) = (\lambda - \lambda_1(k))(\lambda - \lambda_2(k))(\lambda - \lambda_3(k)) = 0. \quad (3.4)$$

Here we assume that $\lambda_{1,2,3}(k)$ are the eigenvalues from Eq. (3.3). Now we compare terms with the same power of λ on the left and the right hand side of Eq. (3.4). The absolute term gives

$$\lambda^0 : e^{i(\alpha + \omega_2(k) + \omega_3(k))} = \det C,$$

which, due to k -independence of the coin C , results in

$$\begin{aligned} \omega_2(k) &= -\omega_3(k) = \omega(k), \\ \det C &= e^{i\alpha}. \end{aligned} \quad (3.5)$$

The first equation of Eqs. (3.5) shows that the eigenvalues $\lambda_{2,3}(k)$ of the evolution operator $\tilde{U}(k)$ from Eq. (3.1) are complex conjugate. The other two powers of λ in Eq. (3.4) give

$$\begin{aligned} \lambda^1 : 1 + e^{i\alpha}(e^{i\omega(k)} + e^{-i\omega(k)}) &= m_L e^{ik} + m_S + m_R e^{ik}, \\ \lambda^2 : e^{i\alpha} + e^{i\omega(k)} + e^{-i\omega(k)} &= C_{LL} e^{-ik} + C_{SS} + C_{RR} e^{ik}. \end{aligned} \quad (3.6)$$

Here we have used Eq. (3.5) and have denoted as m_j , $j = L, S, R$ sub-determinants of the coin C from Eq. (3.2) with crossed-out j th row and j th column. For example,

$$m_L = \begin{vmatrix} C_{SS} & C_{SR} \\ C_{RS} & C_{RR} \end{vmatrix} = C_{SS}C_{RR} - C_{SR}C_{RS}.$$

From Eqs. (3.6) we get that

$$\begin{aligned} \lambda^1 &\Rightarrow 2 \cos \omega(k) = e^{-i\alpha}(m_L e^{ik} + m_S + m_R e^{-ik} - 1), \\ \lambda^2 &\Rightarrow 2 \cos \omega(k) = C_{LL} e^{-ik} + C_{SS} + C_{RR} e^{ik}. \end{aligned} \quad (3.7)$$

These two equations provide us with the last constraints on the diagonal matrix elements of the general trapping coin C ,

$$\begin{aligned} C_{LL} &= e^{-i\alpha}(C_{LL}C_{SS} - C_{LS}C_{SL}), \\ C_{RR} &= e^{-i\alpha}(C_{RR}C_{SS} - C_{RS}C_{SR}), \\ C_{SS} - 1 &= e^{-i\alpha}(C_{LL}C_{RR} - C_{LR}C_{RL} - 1). \end{aligned} \quad (3.8)$$

These constraints ensure the existence of the point spectrum of $\tilde{U}(k)$. Moreover, from the second equation in Eqs. (3.7) and the fact that $\omega \in \mathbb{R}$ we see that the left hand side is real. Thus we get another requirements on the right hand side. The elements $C_{LL(RR)}$ staying at the right hand side have to compensate the imaginary parts of $e^{\pm ik}$. Thus we may conclude that $C_{LL} = C_{RR}^*$.

3.2 Unitarity

It is known that the coin C from Eq. (3.2) has to be unitary. Until now we did not use any requirement on the matrix elements $C_{ij}, i, j = L, S, R$ to ensure unitarity. We have only constraints on the existence of the point spectrum without exploiting unitarity of the matrix elements.

Since we want to find all trapping coins, our coin C has to be the most general three-dimensional unitary matrix. There exist several recursive methods for the construction of general unitary matrices. Nevertheless, even in the moderate dimension of three, the final matrix with nine real parameters has quite complicated form. The application of the conditions from Eq. (3.8) makes possible solutions unreadable. However we know that at least two solutions exist in the form of the one-parameter families, Eqs. (2.11, 2.17).

Let us now briefly describe a parametrization, which we use and modify in order to find a convenient unitary coin. It is known that every unitary matrix can be decomposed into a product of three unitary matrices [20], where two of them are diagonal. For the elements of the three-dimensional unitary matrix $U(3)$ we need nine real parameters that are hidden in the decomposition of the form

$$C = \text{Diag}\{e^{i\alpha_1}, e^{i\alpha_2}, e^{i\alpha_3}\}.V.\text{Diag}\{e^{i\alpha_4}, e^{i\alpha_5}, e^{i\alpha_6}\}. \quad (3.9)$$

Here Diag denotes diagonal matrix. Parameters $\alpha_i, i = 1, \dots, 6$ appear only in sums with some other $\alpha_j, j = 1, \dots, 6, j \neq i$ and therefore the diagonal matrices effectively give only five independent real parameters $\gamma_{1, \dots, 5}$ that will be specified later. The unitary matrix V includes the remaining four parameters and can be constructed recursively [20]. Nevertheless, this and most other recursive parametrisation would lead to the unsolvability as mentioned above. Fortunately, there is a way to solve this problem. Let us take as V so-called quark mixing matrix [32]

$$V = \begin{pmatrix} c_{12}c_{13} & s_{12}c_{13} & s_{13}e^{-i\delta} \\ -s_{12}c_{23} - c_{12}s_{23}s_{13}e^{i\delta} & c_{12}c_{23} - s_{12}s_{23}s_{13}e^{i\delta} & s_{23}c_{13} \\ s_{12}s_{23} - c_{12}c_{23}s_{13}e^{i\delta} & -c_{12}s_{23} - s_{12}c_{23}s_{13}e^{i\delta} & c_{23}c_{13} \end{pmatrix}, \quad (3.10)$$

which satisfy the requirement of four independent real parameters. Here $c_{ij} = \cos \theta_{ij}, s_{ij} = \sin \theta_{ij}, i = 1, 2, j = 2, 3$. Following the prescription from Eq. (3.9) we get unitary matrix with nine real independent parameters, which are

$$\delta, \theta_{12}, \theta_{13}, \theta_{23}, \gamma_1, \gamma_2, \gamma_3, \gamma_4, \gamma_5,$$

and

$$\gamma_1 = \alpha_1 + \alpha_4, \gamma_2 = \alpha_1 + \alpha_5, \gamma_3 = \alpha_1 + \alpha_6, \gamma_4 = \alpha_2 + \alpha_4, \gamma_5 = \alpha_3 + \alpha_4.$$

The general 9-parameter unitary coin in the convenient form then reads

$$C = \begin{pmatrix} e^{i\gamma_1} c_{12} c_{13} & e^{i\gamma_2} s_{12} c_{13} & s_{13} e^{i(\gamma_3 - \delta)} \\ -e^{i\gamma_4} (s_{12} c_{23} + c_{12} s_{23} s_{13} e^{i\delta}) & e^{i(\gamma_4 + \gamma_2 - \gamma_1)} (c_{12} c_{23} - s_{12} s_{23} s_{13} e^{i\delta}) & e^{-i(\gamma_1 - \gamma_3 - \gamma_4)} s_{23} c_{13} \\ e^{i\gamma_5} (s_{12} s_{23} - c_{12} c_{23} s_{13} e^{i\delta}) & e^{i(\gamma_5 + \gamma_2 - \gamma_1)} (-c_{12} s_{23} - s_{12} c_{23} s_{13} e^{i\delta}) & e^{i(\gamma_5 + \gamma_3 - \gamma_1)} c_{23} c_{13} \end{pmatrix}. \quad (3.11)$$

Now we can use this coin together with the conditions ensuring trapping. Applying the first two conditions from Eq. (3.8) on the matrix (3.11) imply

$$\begin{aligned} C_{LL} &\Rightarrow c_{13}(c_{12} - e^{-i(\gamma_3 + \gamma_5)} c_{23}) = 0, \\ C_{RR} &\Rightarrow c_{13}(c_{12} - e^{i(\gamma_3 + \gamma_5)} c_{23}) = 0. \end{aligned} \quad (3.12)$$

We have used the fact from Eq. (3.5) saying that the constant eigenvalue is equal to the determinant of the coin

$$\det C = e^{i\alpha} = e^{i(-\gamma_1 + \gamma_2 + \gamma_3 + \gamma_4 + \gamma_5)}.$$

To get a non-trivial solution, where by non-trivial we mean that no C_{ij} equals zero, all the θ_{ij} -parameters have to be non-zero. Trivial solutions will not be discussed here and one can find them in [II]. Following Eq. (3.12), we have to satisfy the conditions

$$\cos \theta_{12} = \cos \theta_{23} \quad \text{and} \quad \gamma_5 = -\gamma_3.$$

Let us note that the condition $\gamma_5 = -\gamma_3$ immediately follows also from the fact that $C_{LL} = C_{RR}^*$, which we have already mentioned below Eq. (3.7).

For the complete solution, we still have to use the last equation in Eqs. (3.8) which provide two final non-trivial solutions. Let us summarize the results:

$$\cos \theta_{12} = \cos \theta_{23}, \gamma_5 = -\gamma_3 \quad \text{and}$$

First solution

$$\delta = 0, \gamma_1 = \gamma_2 + \gamma_4$$

$$C_{full_1}^{(3)} = \begin{pmatrix} e^{i(\gamma_2 + \gamma_4)} c_{13} c_{23} & e^{i\gamma_2} s_{23} c_{13} & s_{13} e^{-i\gamma_5} \\ -e^{i\gamma_4} (s_{23} c_{23} + c_{23} s_{23} s_{13}) & c_{23}^2 - s_{23}^2 s_{13} & e^{-i(\gamma_2 + \gamma_5)} s_{23} c_{13} \\ e^{i\gamma_5} (s_{23}^2 - c_{23}^2 s_{13}) & e^{i(\gamma_5 + \gamma_4)} (-c_{23} s_{23} (1 - s_{13})) & e^{-i(\gamma_2 + \gamma_4)} c_{23} c_{13} \end{pmatrix}, \quad (3.13)$$

Second solution

$$\sin \theta_{13} = \frac{\sin(\gamma_1 - \gamma_2 - \gamma_4)}{\sin(\delta - \gamma_1 + \gamma_2 + \gamma_4)}, \quad \text{where } \delta \neq \gamma_1 - \gamma_2 - \gamma_4 \quad \text{and} \quad -1 \leq \sin \theta_{13} \leq 1$$

$$C_{full_2}^{(3)} = \begin{pmatrix} e^{i\gamma_1} c_{23} B & e^{i\gamma_2} s_{23} B & \sin \Gamma A e^{i(-\gamma_5 - \delta)} \\ -e^{i(\gamma_1 - \gamma_2)} A s_{23} c_{23} \sin \delta & e^{i\Gamma} c_{23}^2 + e^{i\Gamma} A s_{23}^2 \sin \Gamma & e^{-i(\gamma_1 + \gamma_5 - \gamma_4)} s_{23} B \\ e^{i\gamma_5} (s_{23}^2 + \sin \Gamma c_{23}^2 A e^{i\delta}) & e^{i(-\gamma_5 + \gamma_4)} A c_{23} s_{23} \sin \delta & e^{-i\gamma_1} c_{23} B \end{pmatrix},$$

where (3.14)

$$\Gamma = \gamma_2 + \gamma_4 - \gamma_1, \quad A = 1/\sin(\Gamma + \delta), \quad B = \sqrt{A^2 \sin(2\Gamma + \delta) \sin \delta}.$$

These two families $C_{full_1}^{(3)} = C_{full_1}^{(3)}(\theta_{13}, \theta_{23}, \gamma_2, \gamma_4, \gamma_5)$ and $C_{full_2}^{(3)} = C_{full_2}^{(3)}(\theta_{23}, \delta, \gamma_1, \gamma_2, \gamma_4, \gamma_5)$ cover all non-trivial three-dimensional coins that lead to the non-empty point spectrum of the evolution operator $\tilde{U}(k)$ from Eq.(3.1). Thus the trapping effect exists for an arbitrary choice of their parameters.

Each of these new families $C_{full_{1,2}}^{(3)}$ is a generalization of the previously found one-parameter families of coins that we derived in chapter 2 and called the eigenvalue and the eigenvector family. More precisely, the matrix $C_{full_1}^{(3)}$ from Eq. (3.13) is the generalized eigenvector family $C_{def_2}^{(3)}(\rho)$ from Eq. (2.17) and the same holds for $C_{full_2}^{(3)}$, Eq. (3.14), and the eigenvalue family $C_{def_1}^{(3)}(\varphi)$ from Eq. (2.11). Indeed, if we choose in $C_{full_1}^{(3)}(\theta_{13}, \theta_{23}, \gamma_2, \gamma_4, \gamma_5)$ the parameters as

$$\gamma_{2,4,5} = 0, \theta_{13} = \arcsin(1 - \rho^2), \theta_{23} = \arccos\left(-\frac{\rho}{\sqrt{2 - \rho^2}}\right) \quad (3.15)$$

we get the eigenvector family $C_{def_2}^{(3)}(\rho)$. Further for $C_{full_2}^{(3)}(\theta_{23}, \delta, \gamma_1, \gamma_2, \gamma_4, \gamma_5)$ we have to choose

$$\gamma_1 = \gamma_2 = \pi, \gamma_4 = \gamma_5 = -\varphi, \theta_{23} = -\arctan 2, \delta = \varphi + \arctan\left(\frac{2 \cot \varphi}{3}\right). \quad (3.16)$$

This choice give us, up to the irrelevant global phase factor $e^{i\varphi}$, the eigenvalue family $C_{def_1}^{(3)}(\varphi)$.

A general three-dimensional unitary matrix C from Eq. (3.11) has nine real parameters. We have reduced the number of parameters from nine to five resp. six in the case of $C_{full_1}^{(3)}$ resp. $C_{full_2}^{(3)}$ matrix. In the case of the eigenvalue and eigenvector family from Eqs. (2.5, 2.17), the additional parameters φ and ρ influence the rate of spreading of the walk. For general trapping coins $C_{full_{1,2}}^{(3)}$, there might exist parameters that can be ignored, since they do not influence the rate of spreading and the shape of the probability distribution. We analyse this feature in the same way as we did for the three-state Grover walk in the section 1.1.1. Some results are summarized and commented in the following subsection.

3.3 Spreading of a general three-state trapping quantum walk

Every quantum walk spreads across a given lattice with a certain speed. This velocity is calculated via dispersion relation and depends on a coin parameter. Dispersion relations arises from the eigenvalues of the evolution operator. Thus we have to begin with calculation

of the eigenvalues of $\tilde{U}(k) = \text{Diag}\{e^{-ik}, 1, e^{ik}\} \cdot C_{full_{1,2}}^{(3)}$, Eqs. (3.1). We consider as $C_{full_{1,2}}^{(3)}$ general trapping coins of the three-state walk, Eqs. (3.13, 3.14). In both cases, one eigenvalue will be independent of the momentum k . The existence of this eigenvalue is associated with the central non-moving peak in the probability distribution. Further, we have two complex conjugate eigenvalues $e^{\pm i\omega_{full_1}(k)}$ for the $C_{full_1}^{(3)}$ walk and $e^{\pm i\omega_{full_2}(k)}$ for the $C_{full_2}^{(3)}$ walk. These eigenvalues are related to the travelling peaks in the probability distribution.

The phases read

$$\begin{aligned}\omega_{full_1}(k) &= \arccos(\cos(\gamma_2 + \gamma_4 - k) \cos \theta_{13} \cos \theta_{23} + 1/2(\sin \theta_{13} - 1) \sin^2 \theta_{23}), \\ \omega_{full_2}(k) &= \arccos\left(\cos(\gamma_1 - k)A \cos \theta_{23} - \frac{\sin \delta \sin^2 \theta_{23}}{2 \sin(d - \gamma_1 + \gamma_2 + \gamma_4)}\right), \\ \text{where } A &= \sqrt{\frac{\sin \delta \sin(\delta - 2(\gamma_1 - \gamma_2 - \gamma_4))}{\sin^2(\delta - \gamma_1 + \gamma_2 + \gamma_4)}}.\end{aligned}\quad (3.17)$$

We emphasize that the phases (dispersion relations) $\omega_{full_{1,2}}(k)$, depend on less parameters than the original coins $C_{full_{1,2}}^{(3)}$, Eq. (3.13, 3.14). The parameters appearing in the dispersion relation are the only ones that influence the spreading of the walk. Any other parameter can be ignored. First of all we can ignore parameters shifting momentum k , i.e. $\gamma_{2,3}$ in ω_{full_1} and γ_1 in ω_{full_2} . In the case of $C_{full_1}^{(3)}$ walk, we end up with two parameters which are relevant

$$C_{full_1}^{(3)} : \theta_{13}, \theta_{23}.$$

From the same reasons, spreading of the walk with $C_{full_2}^{(3)}$ coin is influenced only by three parameters, one angle and two phases

$$C_{full_2}^{(3)} : \theta_{23}, \delta \text{ and } \kappa = (\gamma_1) - \gamma_2 - \gamma_4. \quad (3.18)$$

Since we have determined that the propagation of the trapping three-state walk depends only on two parameters in the case of $C_{full_1}^{(3)}$ coin, Eq. (3.13), or three parameters in the case of $C_{full_2}^{(3)}$ coin, Eq. (3.14), we can finally look how these parameters affects the spreading of the walk. To do that, we unify the marking. We can rewrite the dispersion relations from Eqs. (3.17) into the form

$$\omega_{full_{1,2}}(k) = \arccos(\alpha \cos k - \beta).$$

From Eq. (3.17) we see that

$$\begin{aligned}C_{full_1}^{(3)} : \quad \alpha &= \cos \theta_{13} \cos \theta_{23}, \\ \beta &= -1/2(\sin \theta_{13} - 1) \sin^2 \theta_{23}, \\ C_{full_2}^{(3)} : \quad \alpha &= A \cos \theta_{23}, \\ \beta &= \frac{\sin \delta \sin^2 \theta_{23}}{2 \sin(d - \gamma_1 + \gamma_2 + \gamma_4)}.\end{aligned}$$

Here we have ignored any parameter shifting the momentum k as discussed above. To get the point k_0 , for which the second derivative of the dispersion relation $\omega_{full_{1,2}}(k)$ vanishes, we have to solve the following equation,

$$\alpha\beta(1 + \cos^2 k) + (1 - \alpha^2 - \beta^2) \cos k = 0.$$

The solution to this equation reads

$$k_0 = \arccos \Delta,$$

where

$$\Delta = \frac{\alpha^2 + \beta^2 - 1 + \sqrt{(1 - \alpha^2 - \beta^2)^2 - 4\alpha^2\beta^2}}{2\alpha\beta}.$$

The velocities of the left and the right travelling peaks are then $v_{R,L} = \pm v^{max}$. Here

$$v^{max} = \rho \frac{\sqrt{1 - \Delta^2}}{\sqrt{1 - (\nu - \rho\Delta)^2}}. \quad (3.19)$$

These results are depicted in the Fig. 5.4 for both $C_{full_{1,2}}^{(3)}$ walks. For more information see [II].

We have showed how the individual parameters influence the spreading of the walk. The trapping peak does not spread at all and thus has to be analysed separately. Therefore, let us investigate a role of the coin parameters on the trapping. In general, the eigenvalues of $\tilde{U}(k)$ from Eq. (3.1) are $e^{i\alpha}$, $e^{\pm i\omega}$. Specifically, $\alpha = 0$, $\omega = \omega_{full_1}$ for quantum walk with $C_{full_1}^{(3)}$ coin and $\alpha = \Gamma$, $\omega = \omega_{full_2}$ for $C_{full_2}^{(3)}$ walk (see Eq. (3.17)). We can always multiply the coin by a global phase factor that does not change the dynamics of the walk. Let us choose the global phase as the inverse of the constant eigenvalue, $e^{-i\alpha}$. The eigenvalues of the propagator $\tilde{U}(k)$ now read

$$\lambda_1 = 1, \lambda_{2,3}(k) = e^{-i(\alpha \mp \omega(k))}.$$

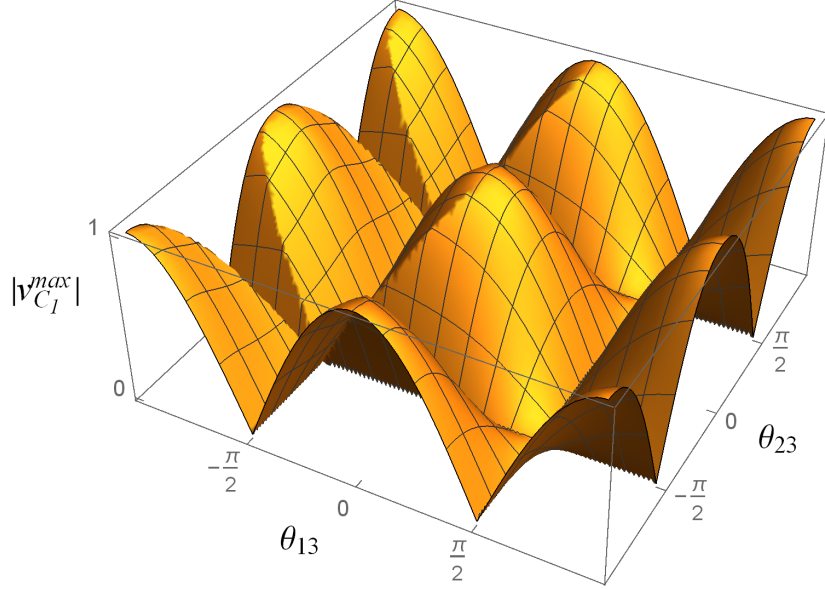
Further we have the eigenvector $v_1(k)$ corresponding to the constant eigenvalue $\lambda_1 = 1$ and $v_{2,3}(k)$ corresponding to the $\lambda_{2,3}(k) = e^{-i(\alpha \mp \omega(k))}$. We assume that all the eigenvectors are normalized. To calculate the trapping probability, we perform the inverse Fourier transform as shown in Eq. (1.16) back to position variable x

$$\psi(x, t) = \frac{1}{2\pi} \int_{-\pi}^{\pi} dk e^{-ixk} \tilde{\psi}(k, t) = \sum_{j=1}^3 \int_{-\pi}^{\pi} dk (e^{-i\frac{x}{t}k} \lambda_j)^t (v_j(k), \psi_0) v_j(k).$$

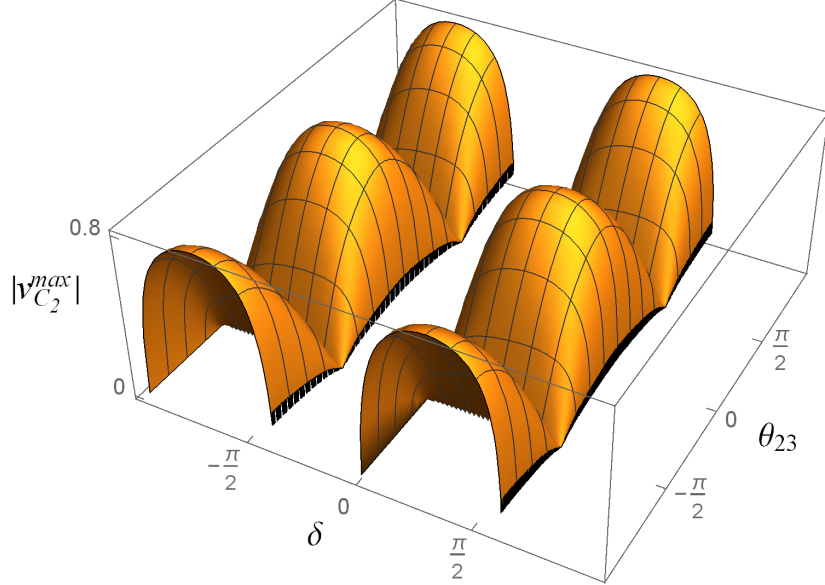
Here $\tilde{\psi}(k, t)$ is a probability amplitude vector at time t in the Fourier picture, which was introduced in Subsec. (1.1.1). On the left hand side we have probability amplitude vector in the position space $\psi(x, t)$. Using the form of the eigenvalues $\lambda_{1,2,3}(k)$ we get

$$\begin{aligned} \psi(x, t) &= \frac{1}{2\pi} \int_{-\pi}^{\pi} dk e^{-ixk} (v_1(k), \psi_0) v_1(k) + \\ &+ \frac{1}{2\pi} \left(\int_{-\pi}^{\pi} dk e^{-ixk} e^{-i(\alpha \pm \omega(k))t} (v_2(k), \psi_0) v_2(k) + \right. \\ &\left. + \int_{-\pi}^{\pi} dk e^{-ixk} e^{-i(\alpha \pm \omega(k))t} (v_3(k), \psi_0) v_3(k) \right). \end{aligned} \quad (3.20)$$

From the Riemann-Lebesgue lemma the last two time-dependent integral in (3.20) vanish when time t approaches infinity. In the limit of large time t (large number of performed



(a) Peak velocity for the quantum walk with coin $C_{full_1}^{(3)}$. The velocity depends only on two parameters θ_{13} and θ_{23} .



(b) Peak velocity for the quantum walk with coin $C_{full_2}^{(3)}$. In this case, the velocity depends on three parameters. One angle θ_{23} and two phases δ , $\kappa = (\gamma_1) - \gamma_2 - \gamma_4$. Here we have chosen $\kappa = \frac{\pi}{5}$. The empty regions are prohibited δ -regions. For every θ_{23} there is a condition adjacent to the $C_{full_2}^{(3)}$ solution, Eq. (3.14), which is $\sin \theta_{13} = \frac{\sin(\kappa)}{\sin(\delta - \kappa)}$. Since the value of the sine function is limited by one, $|\sin \theta_{13}| \leq 1$ and κ was chosen, restriction on δ naturally arises.

Figure 3.1: Velocity of the probability peak from Eq. (3.19) for the quantum walks with $C_{full_1}^{(3)}$ and $C_{full_2}^{(3)}$ coins, Eqs. (3.13, 3.14) in dependence on the coin parameters.

steps), the probability amplitude reads

$$\psi_\infty(x) = \lim_{t \rightarrow \infty} \psi(x, t) = \lim_{t \rightarrow \infty} \frac{1}{2\pi} \int_{-\pi}^{\pi} dk e^{-ixk} (v_1(k), \psi_0) v_1(k). \quad (3.21)$$

For the vector $v_1(k)$ holds

$C_{full_1}^{(3)}$:

$$v_1(k) = \frac{1}{n(k)} \begin{pmatrix} -e^{-i\gamma_5} s_{23} \left(\sin \frac{\theta_{13}}{2} + \cos \frac{\theta_{13}}{2} \right) \\ e^{i(k-\gamma_2-\gamma_5)} \left(\sin \frac{\theta_{13}}{2} - \cos \frac{\theta_{13}}{2} \right) + e^{i(\gamma_4-\gamma_5)} c_{23} \left(\sin \frac{\theta_{13}}{2} + \cos \frac{\theta_{13}}{2} \right) \\ -e^{ik} s_{23} \left(\sin \frac{\theta_{13}}{2} + \cos \frac{\theta_{13}}{2} \right), \end{pmatrix}$$

$$n(k) = 2 + s_{23}^2(1 + s_{13}) - 2c_{13}c_{23} \cos(k - \gamma_2 - \gamma_4) =$$

$$= a - 2b \cos(k - c),$$

$C_{full_2}^{(3)}$:

$$v_1(k) = \frac{1}{n(k)} \begin{pmatrix} e^{i(\gamma_2+\gamma_4)} s_\delta s_{23} \\ -e^{i(\gamma_1+\gamma_4)} s_\delta c_{23} + e^{i(k+\gamma_4)} \sqrt{s_\delta \sin(\delta + 2\kappa)} \\ e^{i(k+\gamma_1+\gamma_5)} s_\delta s_{23} \end{pmatrix},$$

$$n(k) = s_\delta \left(\sin(\delta + 2\kappa) + s_\delta(1 + s_{23}^2) - 2c_{23} \cos(k - \gamma_1) \sqrt{s_\delta \sin(\delta + 2\kappa)} \right) =$$

$$= a - 2b \cos(k - c). \quad (3.22)$$

We have denoted $\sin \delta = s_\delta$.

The corresponding probability of trapping at position x after infinitely many steps is given by the square of norm of the probability amplitude vector (see Eq. (5.26))

$$p_\infty(x) = \lim_{t \rightarrow \infty} |\psi(x, t)|^2 = |\psi_\infty(x)|^2 \quad (3.23)$$

and depends on the initial state of the walk. Due to the number of parameters in our coins, is not suitable to choose a general initial state. Since we want to focus only on the role of coin parameters on trapping we choose as a reference initial state maximally mixed state,

$$|\psi_0\rangle = |0\rangle \otimes \frac{1}{\sqrt{3}}(|L\rangle + |S\rangle + |R\rangle) \Rightarrow \psi_0 = \frac{1}{\sqrt{3}}(1, 1, 1)^T. \quad (3.24)$$

This is convenient choice because it covers all coin states with equal probability. It is known that the central peak decreases exponentially when we move away from the origin. Therefore, we take only the top of the peak corresponding to the position $x = 0$,

$$p_\infty = p_\infty(0).$$

For a maximally mixed state we then have

$$p_\infty = \frac{1}{3}(|\psi_{1,\infty}|^2 + |\psi_{2,\infty}|^2 + |\psi_{3,\infty}|^2),$$

where the elements of the probability amplitude vector $\psi_\infty = \psi_\infty(0) = (\psi_{1,\infty}, \psi_{2,\infty}, \psi_{3,\infty})^T$ are given by Eqs. (3.21) and (3.24). All the integrands in p_∞ can be expressed in the form

$$I_n = \int_{-\pi}^{\pi} \frac{e^{ink}}{2\pi(a - 2b \cos(k - c))} dk, \quad n = -1, 0, 1, \quad (3.25)$$

and then calculated with the help of the contour integration methods. We see that integral $I_{-1} = I_1^*$ and thus we have to calculate only integrals $I_{0,1}$. Note that the denominator in Eq. (3.25) follows from the normalization of the vector $v_1(k)$, Eq. (3.22) corresponding to the constant eigenvalue. For the $C_{full_1}^{(3)}$ walk we have

$$C_{full_1}^{(3)} : a = (1 + s_{13})s_{23}^2 + 2, \quad b = c_{13}c_{23}, \quad c = \gamma_2 + \gamma_4 \quad (3.26)$$

and for the $C_{full_2}^{(3)}$ walk

$$C_{full_2}^{(3)} : a = \left((1 + s_{23}^2 \sin \delta) + \sin(\delta + 2\kappa) \right) \sin \delta, \quad b = \sqrt{\sin \delta \sin(\delta + 2\kappa)} c_{23} \sin \delta, \quad c = \gamma_1. \quad (3.27)$$

Substitution $z = e^{ik}$ turns Eq. (3.25) into contour integration over a unit circle

$$I_n = -\frac{1}{2\pi i} \oint_{|z|=1} \frac{z^n}{be^{-ic}z^2 - az + be^{ic}} dz = \oint_{|z|=1} f(z) dz.$$

Here we can apply residue theorem that

$$I_n = \sum_{k, |z_k| < 1} Res(f, z_k).$$

For simple poles z_k of the function $f(z)$ the residue is given by

$$Res(f, z_k) = \lim_{z \rightarrow z_k} (z - z_k) f(z)$$

Here we deal only with simple poles in the form

$$z_{1,2} = e^{ic} \frac{a \pm \sqrt{a^2 - 4b^2}}{2b}.$$

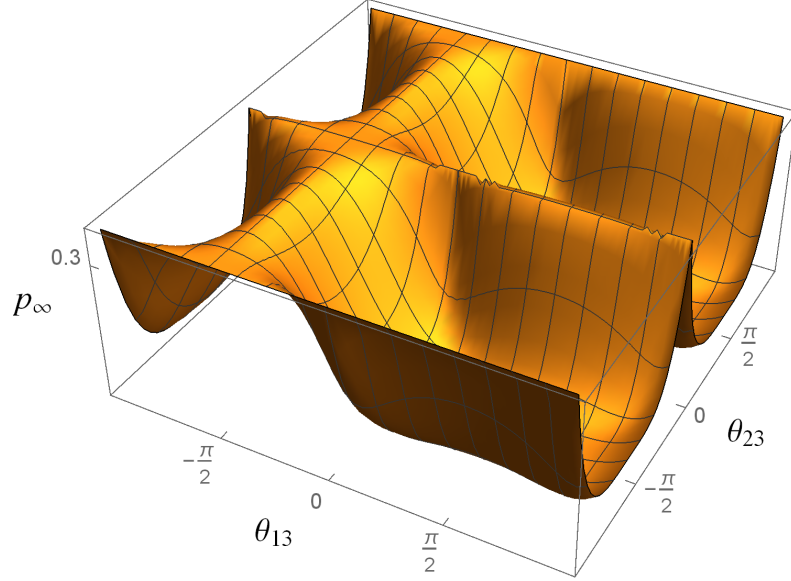
Note that in our case of a, b from Eqs. (3.26, 3.27), pole z_1 falls out of the unit circle region and therefore

$$I_n = Res(f, z_2) = \begin{cases} \frac{1}{\sqrt{a^2 - 4b^2}}, & n = 0, \\ \frac{e^{ic} \left(\frac{a}{\sqrt{a^2 - 4b^2}} - 1 \right)}{2b}, & n = 1. \end{cases} \quad (3.28)$$

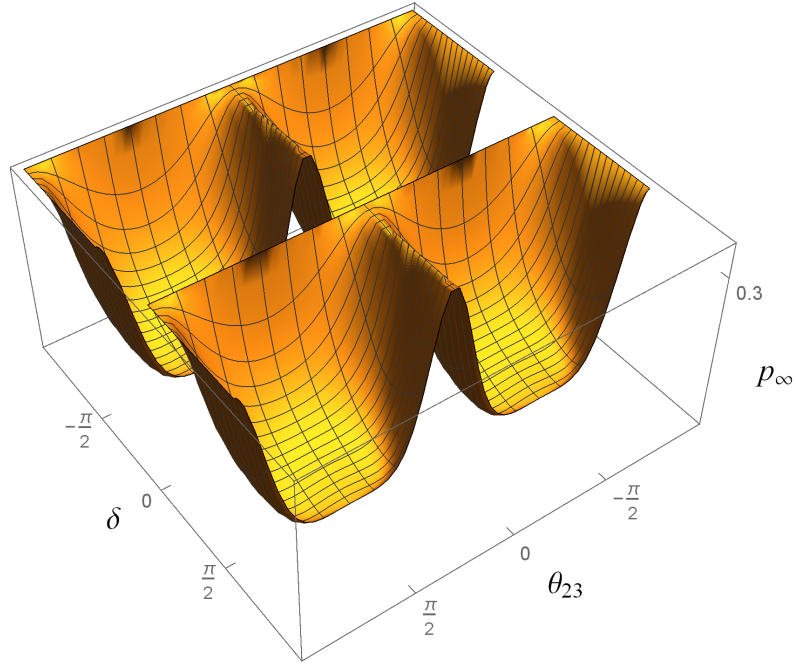
This general approach can be applied to both coins $C_{full_1}^{(3)}$ and $C_{full_2}^{(3)}$. Since the results are quite long [II], we will present them only graphically in Fig. 3.2. We emphasize that, as one might expected, the probability depends on the same reduced number of parameters as the velocity of spreading, it is θ_{13} and θ_{23} for $C_{full_1}^{(3)}$ walk, $\delta, \theta_{23}, \kappa = (\gamma_1) - \gamma_2 - \gamma_4$ for $C_{full_2}^{(3)}$ walk.

To conclude, after omitting cases containing at least one zero, there exist two classes of coins for three-state quantum walk on a line which lead to a non-empty point spectrum of the evolution operator in the Fourier picture $\tilde{U}(k)$. These classes have five resp. six free parameters, but only two resp. three are relevant and influence the dynamics. Both classes are generalizations of previously found one-parameter families of coins discussed in chapter 2. The results show that although we have enlarged the number of parameters, the trapping is for the three-state quantum walk on a line still quite a rare phenomena. Compared to nine real parameters general three-dimensional unitary coin contains, our special choices providing trapping are negligible.

$$\text{initial state } |\psi_C\rangle = \frac{1}{\sqrt{3}} (1, 1, 1)^T$$



(a) For the walk with $C_{full_1}^{(3)}$ coin, the limiting probability of finding the particle trapped at the origin depends on the same parameters as the peak velocity, on the angles θ_{13} and θ_{23} .



(b) The limiting trapping probability at the origin depends, for the walk with $C_{full_2}^{(3)}$ coin on the same parameters as the peak velocity, it is θ_{23} , δ , κ . Here we have chosen $\kappa = \frac{\pi}{5}$. The δ -region is limited by the condition $-1 \leq \sin \theta_{13} \leq 1$ as described for Fig. (3.1b)

Figure 3.2: Limiting probability p_∞ of finding the particle at the origin (position $m = 0$) when the number of steps t approaches infinity. The maximally mixed state from Eq. (3.24) was chosen as the initial state. The walks are driven by $C_{full_1}^{(3)}$ resp. $C_{full_2}^{(3)}$ coins from Eqs. (3.13, 3.14).

Chapter 4

Classification of trapping coins for four-state quantum walks on a two-dimensional lattice

In chapter 3, we have described the construction of all trapping coins for the three-state quantum walks on a line in. For that classification we have used a decomposition of the unitary matrices as a product of two diagonal and one $d^2 - (2d - 1)$ -parameter unitary matrix, where d is the dimension of the walk. For the three state walk $d = 3$. We used a trick since we did not use recurrent parametrization but found more suitable choice of the four-parameter matrix, which was the quark mixing matrix. In this case, we were able to find all solutions leading to trapping walks. Unfortunately, we have also found that this approach would almost certainly not be useful for higher dimensional quantum walks. Although there exist generalization of the mixing matrix to the dimension four, which reads [33]

$$M = \begin{pmatrix} s_1 s_3 s_5 & s_1 s_3 c_5 & s_1 c_3 & c_1 \\ M_{21} & M_{22} & M_{23} & -s_1 c_2 \\ M_{31} & M_{32} & M_{33} & -s_1 s_2 c_4 \\ M_{41} & M_{42} & M_{43} & -s_1 s_2 s_4 \end{pmatrix},$$

where the elements in the middle of the matrix are given by

$$\begin{aligned} M_{23} &= c_1 c_2 c_3 - s_2 s_3 c_6 e^{i\delta} \\ M_{33} &= c_1 s_2 c_3 c_4 + c_2 s_3 c_4 c_6 e^{i\delta} + s_3 s_4 s_6 e^{i\beta} \\ M_{22} &= c_1 c_2 s_3 c_5 + s_2 c_3 c_5 c_6 e^{i\delta} + s_2 s_5 s_6 e^{i\gamma} \\ M_{32} &= c_1 s_2 s_3 c_4 c_5 - c_2 c_3 c_4 c_5 c_6 e^{i\delta} - c_3 s_4 c_5 s_6 e^{i\beta} - c_2 c_4 c_5 c_6 e^{i\gamma} + s_4 s_5 c_6 e^{i(\beta+\gamma-\delta)} \end{aligned}$$

and the edge elements read

$$\begin{aligned}
M_{43} &= c_1 s_2 c_3 s_4 + c_2 s_3 s_4 c_6 e^{i\delta} - s_3 c_4 s_6 e^{i\beta} \\
M_{21} &= c_1 s_2 s_3 s_5 + s_2 c_3 s_5 c_6 e^{i\delta} - s_2 c_5 s_6 e^{i\gamma} \\
M_{42} &= c_1 s_2 s_3 s_4 c_5 - c_2 c_3 s_4 c_5 c_6 e^{i\delta} + c_3 c_4 c_5 s_6 e^{i\beta} - c_2 s_4 s_5 s_6 e^{i\gamma} - c_4 s_5 c_6 e^{i(\beta+\gamma-\delta)} \\
M_{31} &= c_1 s_2 s_3 c_4 s_5 - c_2 c_3 c_4 s_5 c_6 e^{i\delta} - c_3 s_4 s_5 s_6 e^{i\beta} + c_2 c_4 c_5 s_6 e^{i\gamma} - s_4 c_5 c_6 e^{i(\beta+\gamma-\delta)} \\
M_{41} &= c_1 s_2 s_3 s_4 s_5 - c_2 c_3 s_4 s_5 s_6 e^{i\delta} + c_3 c_4 s_5 s_6 e^{i\beta} + c_2 s_4 c_5 s_6 e^{i\gamma} + c_4 c_5 c_6 e^{i(\beta+\gamma-\delta)}
\end{aligned}$$

and its nine parameters make impossible to read out all the cases leading to a trapping quantum walk. Here s_j resp. c_j stands for $\sin \theta_j$ resp. $\cos \theta_j$, $j = 1, \dots, 6$.

One can definitely find some solutions leading to trapping when an approach similar to that of chapter 3 would be applied, but now for a four-dimensional mixing matrix M . For example, one solution is of the form

$$\begin{aligned}
c_2 = c_3, \quad s_2 = s_3, \quad c_6 = -c_1, \quad s_6 = s_1, \quad \delta = \beta = \sigma_1 = 0, \\
\gamma = \pi, \quad \sigma_2 = -\sigma_5, \quad \sigma_3 = \sigma_6, \quad \sigma_4 = -\sigma_7,
\end{aligned}$$

but many other possible solutions remain hidden in the complicated expressions and large number of parameters. Thus the completeness of the solutions would be impossible.

Since we want to find all trapping coins for the four-state quantum walk on a two-dimensional lattice, we have to develop a completely different approach. In [29] an alternative construction of one (strong) trapping coin class arising from the tensor product of unitary matrices. This alternative approach also does not lead to full classification. In fact the idea of a stationary state as the starting point is basis for further investigations that leads to desired result.

We devote the present chapter to the classification of four-dimensional walks. This chapter will be divided into several section. First we prove that the stationary state is restricted to a 2×2 subspace of the lattice. We can say that this is the key knowledge that provides, with some algebra, a full classification of the trapping coin classes.

4.1 Support of stationary states

As we have already mentioned, the analysis begin with a stationary state of a walk. It is a state which is invariant with respect to the action of the evolution operator. Knowledge of a coin controlling the walk leads to unique stationary state. If we do not know anything about the coin, it is hard to say something about the stationary state. Therefore, it is necessary to restrict a set of all possibly stationary states to those which are relevant. The restriction is done by specification of positions on which the state is trapped.

Trapping is caused by the existence of the constant eigenvalue $e^{i\phi}$ of the evolution operator

$$\tilde{U}(k, l) = \text{Diag}\{e^{-ik}, e^{ik}, e^{-il}, e^{il}\} \cdot C, \tag{4.1}$$

where C is an arbitrary 4×4 unitary matrix with its matrix elements as in Eq. (1.27). Multiplication of the coin C by a global phase $e^{-i\phi}$ only changes the eigenvalues of $\tilde{U}(k, l)$, but does not change the walk at all. Therefore, we can assume without loss of generality that the constant eigenvalue is always equal to one. It leads to equation

$$\tilde{U}(k, l)\psi = \psi$$

with $\psi = (\psi_1, \psi_2, \psi_3, \psi_4)^T$ being the eigenvector corresponding to the eigenvalue $\lambda = 1$. The vector ψ is found by solving the characteristic equation

$$\det \underbrace{(\tilde{U}(k, l) - I)}_W = 0$$

which says that the rows of W are not linearly independent. We denote the identity matrix as I . Thus, at least two rows of W are linearly dependent. Let us denote the rows of W as W_j , $j = 1, 2, 3, 4$ and assume that the first and the third row $W_{1,3}$ are linearly dependent. After omitting one of these rows we still have to get that

$$\begin{pmatrix} W_2 \\ W_3 \\ W_4 \end{pmatrix} \cdot \begin{pmatrix} \psi_2 \\ \psi_3 \\ \psi_4 \end{pmatrix} = 0, \quad \begin{pmatrix} W_1 \\ W_2 \\ W_4 \end{pmatrix} \cdot \begin{pmatrix} \psi_1 \\ \psi_2 \\ \psi_4 \end{pmatrix} = 0. \quad (4.2)$$

Plugging Eq. (4.1) into the Eq. (4.2) gives, in the case of eliminated W_1 , three equations for ψ_j , $j = 1, \dots, 4$. Solving these equations leads to expressions consisting of the elements depending on momenta k, l only in the exponential form. Thus the solution the most generally depends on momenta in the form

$$\text{omitted } W_1 : \underbrace{1}_{|x,y\rangle}, \underbrace{e^{ik}}_{|x+1,y\rangle}, \underbrace{e^{il}}_{|x,y+1\rangle}, \underbrace{e^{i(k+l)}}_{|x+1,y+1\rangle}, \underbrace{e^{i(k+2l)}}_{|x+1,y+2\rangle}, \underbrace{e^{i2l}}_{|x,y+2\rangle}.$$

Hence the stationary state occupies maximally a 2×3 lattice region. Nevertheless, the solution without W_3 leads to expressions with momenta of the form

$$\text{omitted } W_3 : \underbrace{1}_{|x,y\rangle}, \underbrace{e^{ik}}_{|x+1,y\rangle}, \underbrace{e^{il}}_{|x,y+1\rangle}, \underbrace{e^{i(k+l)}}_{|x+1,y+1\rangle}, \underbrace{e^{i(2k+l)}}_{|x+2,y+1\rangle}, \underbrace{e^{i2k}}_{|x+2,y\rangle}$$

and thus a 3×2 support. There should be no difference in the solution between omitting W_1 or W_3 row since these two choices are completely equivalent. This leads us to the conclusion that the stationary state occupies maximally a 2×2 region on the lattice. Therefore, we can write a general stationary state for any trapping four-state walk as

$$|\psi^{stat}\rangle = |x, y\rangle \otimes |\xi_{x,y}\rangle + |x+1, y\rangle \otimes |\xi_{x+1,y}\rangle + |x, y+1\rangle \otimes |\xi_{x,y+1}\rangle + |x+1, y+1\rangle \otimes |\xi_{x+1,y+1}\rangle \quad (4.3)$$

with $|\xi_{i,j}\rangle$, $i(j) = x(y), x(y) + 1$ being the coin state. Its general form reads

$$|\xi_{i,j}\rangle = \xi_{i,j}^{(L)}|L\rangle + \xi_{i,j}^{(R)}|R\rangle + \xi_{i,j}^{(D)}|D\rangle + \xi_{i,j}^{(U)}|U\rangle.$$

Note that the exact form of the coefficients $\xi_{i,j}^{(\cdot)}$ of the coin states $|\xi_{i,j}\rangle$ are strictly given by the stationary state requirements and their exact forms will be specified later.

In Eq. (4.2), we have chosen rows $W_{1,3}$ to be linearly dependent and this choice was not unreasonable. According to our notation from Eq. (4.1), the first and the second row of $W = \tilde{U}(k, l) - I$ is k -dependent and thus responsible for the kicks on the horizontal part of the 2D lattice. On the other hand, l -dependent $W_{3,4}$ are related to the vertical part of the lattice. Picking one k -dependent W_1 or W_2 and one l -dependent W_3 or W_4 sample and assuming their linear dependence is sufficient for a first half of the proof. It is the part where we study support of stationary states provided that the k -dependent (horizontal) lines $W_{1,2}$ are gained by multiplication of the l -dependent (vertical) lines $W_{3,4}$ by a k, l -dependent factor. Indeed one can check that for instance a choice of W_2 and W_3 as linearly dependent rows leads to 2×2 support similarly as we have shown for W_1 and W_3 .

Due to this limitation, one might become suspicious about the completeness of the proof. By now, we have not assumed that k -dependent rows W_1 and W_2 or l -dependent rows $W_{3,4}$ can be linearly dependent. Therefore, we look at this situation and reveal that it does not enlarge the 2×2 support proved in the previous paragraphs. Here we can even calculate the explicit form of the coin as a direct sum of two unitary matrices.

Now we describe the second half of the proof. Let us assume that $W_{1,2}$ are linearly dependent, it is $W_1 = KW_2$, where K is in general function of a momentum k . Then

$$\begin{aligned} 0 &= W_1 - KW_2 = \\ &= \left(-1 + e^{-ik}C_{LL} - Ke^{ik}C_{RL}, e^{-ik}C_{LR} - K(-1 + e^{ik}C_{RR}), \right. \\ &\quad \left. e^{-ik}C_{LD} - Ke^{ik}C_{RD}, e^{-ik}C_{LU} - Ke^{ik}C_{RU} \right). \end{aligned} \quad (4.4)$$

Here we have to keep in mind that the matrix elements $C_{i,j}$, $i, j = L, R, D, U$ (see Eq. (1.27)) are independent of k . The last two equations can be solved as

$$\begin{cases} \text{either} & K = e^{-2ik} \frac{C_{LD}}{C_{RD}} = e^{-2ik} \frac{C_{LU}}{C_{RU}} \quad \wedge \quad C_{RD}, C_{RU} \neq 0 \quad \Rightarrow \quad K \sim e^{-2ik}, \\ \text{or} & C_{LD} = C_{RD} = C_{LU} = C_{RU} = 0 \quad \Rightarrow \text{correct solution.} \end{cases} \quad (4.5)$$

We have already marked that the second solution is correct. Indeed, the first solution with $K \sim e^{-2ik}$ does not work since it requires dependence of the matrix element C_{ij} on momentum k . If we plug the first solution from Eq. (4.5) into the first two elements from (4.4) we immediately see that we cannot satisfy these equation with elements of the coin C being momentum independent. These arguments clearly confirm that the correct solution is the second one from Eq. (4.5). Due to unitarity, since $C_{LD} = C_{RD} = C_{LU} = C_{RU} = 0$ than also $C_{DL} = C_{DR} = C_{UL} = C_{UR} = 0$. All the coin elements responsible for mixing of the horizontal $|L\rangle, |R\rangle$ and the vertical $|D\rangle, |U\rangle$ coin states are equal to zero. Therefore, the final coin is a direct sum of two two-dimensional unitary matrices describing separate spreading horizontally and vertically,

$$C = \begin{pmatrix} U_1 & 0 \\ 0 & U_2 \end{pmatrix}.$$

The most general two-dimensional unitary matrix is of the form

$$U_i = \begin{pmatrix} e^{i\alpha_i} \cos \delta_i & e^{-i\beta_i} \sin \delta_i \\ e^{i\beta_i} \sin \delta_i & -e^{-i\alpha_i} \cos \delta_i \end{pmatrix}, \quad i = 1, 2. \quad (4.6)$$

This parametrization together with the first two components from Eq. (4.4) gives, after some algebra, additional conditions that $\delta_1 = \pi/2$ and $K = e^{-i(k+\beta)}$. Finally we constructed a coin

$$C = \begin{pmatrix} 0 & e^{-i\beta_1} & 0 & 0 \\ e^{i\beta_1} & 0 & 0 & 0 \\ 0 & 0 & e^{i\alpha_2} \cos \delta_2 & e^{-i\beta_2} \sin \delta_2 \\ 0 & 0 & e^{i\beta_2} \sin \delta_2 & -e^{-i\alpha_2} \cos \delta_2 \end{pmatrix}. \quad (4.7)$$

Now it is easy to check that the support of a stationary state of the walk with this coin remains 2×2 . We have assumed that the first two rows $W_{1,2}$ are linearly dependent. For assumption of the linear dependence of W_3 and W_4 , we can prove that the support does not exceed 2×2 region analogously. Now we have covered all the cases resulting from the linear dependence of $W = \tilde{U}(k, l) - I$ and thus completed the proof.

4.2 Conditions on the trapping coins

The stationary state $|\psi^{stat}\rangle$ from Eq. (4.3) remains during the time evolution unchanged. Therefore, it has to satisfy

$$\hat{U}|\psi^{stat}\rangle = \hat{S}(\hat{I}_p \otimes \hat{C})|\psi^{stat}\rangle = |\psi^{stat}\rangle.$$

This relation can be written using reverse of the step operator as

$$\hat{S}^{-1}|\psi^{stat}\rangle = (\hat{I}_p \otimes \hat{C})|\psi^{stat}\rangle. \quad (4.8)$$

The right hand side of this equation only changes the coin state and not positions,

$$\begin{aligned} (\hat{I}_p \otimes \hat{C})|\psi^{stat}\rangle &= |x, y\rangle \otimes |\xi_{x,y}^{\hat{C}}\rangle + |x+1, y\rangle \otimes |\xi_{x+1,y}^{\hat{C}}\rangle + \\ &+ |x, y+1\rangle \otimes |\xi_{x,y+1}^{\hat{C}}\rangle + |x+1, y+1\rangle \otimes |\xi_{x+1,y+1}^{\hat{C}}\rangle, \end{aligned}$$

where $|\xi_{i,j}^{\hat{C}}\rangle = \hat{C}|\xi_{i,j}\rangle$, $i, j = L, R, D, U$. On the other hand, the left hand side changes positions according to the coin states. Thus we have to eliminate these coefficients $\xi_{i,j}^{(\cdot)}$ from Eq. 4.3 that would take us outside of the 2×2 region $|m, n\rangle$, $m = x, x+1$, $n = y, y+1$. For instance

$$\hat{S}^{-1} \left(\xi_{x,y}^{(R)} |x, y\rangle \otimes |R\rangle \right) = \underbrace{|x-1, y\rangle \otimes |R\rangle}_{\notin 2 \times 2} \Rightarrow \xi_{x,y}^{(R)} = 0.$$

Therefore

$$\begin{aligned}
\hat{S}^{-1}|\psi^{stat}\rangle = & \underbrace{\xi_{x,y}^{(R)}}_f |x, y, R\rangle + \underbrace{\xi_{x,y}^{(U)}}_d |x, y, U\rangle + \underbrace{\xi_{x,y+1}^{(R)}}_h |x, y+1, R\rangle + \\
& + \underbrace{\xi_{x,y+1}^{(D)}}_b |x, y+1, D\rangle + \underbrace{\xi_{x+1,y}^{(L)}}_a |x+1, y, L\rangle + \underbrace{\xi_{x+1,y}^{(U)}}_g |x+1, y, U\rangle + \\
& + \underbrace{\xi_{x+1,y+1}^{(L)}}_c |x+1, y+1, L\rangle + \underbrace{\xi_{x+1,y+1}^{(D)}}_e |x+1, y+1, D\rangle \quad (4.9)
\end{aligned}$$

and thus

$$\begin{aligned}
|\psi^{stat}\rangle = & |x, y\rangle \otimes (a|L\rangle + b|D\rangle) + |x, y+1\rangle \otimes (c|L\rangle + d|U\rangle) + \\
& + |x+1, y\rangle \otimes (e|D\rangle + f|R\rangle) + |x+1, y+1\rangle \otimes (g|U\rangle + h|R\rangle) \quad (4.10)
\end{aligned}$$

From Eqs. (4.8-4.10) we have that the coin operator changes the coin states of the stationary state as

$$\begin{aligned}
a|L\rangle + b|D\rangle & \xrightarrow{\hat{C}} f|R\rangle + d|U\rangle \\
c|L\rangle + d|U\rangle & \xrightarrow{\hat{C}} h|R\rangle + e|D\rangle \\
e|L\rangle + f|D\rangle & \xrightarrow{\hat{C}} a|L\rangle + g|U\rangle \\
g|L\rangle + h|D\rangle & \xrightarrow{\hat{C}} c|L\rangle + e|D\rangle
\end{aligned}$$

or in matrix form as

$$\begin{aligned}
C \begin{pmatrix} a \\ 0 \\ b \\ 0 \end{pmatrix} &= \begin{pmatrix} 0 \\ f \\ 0 \\ d \end{pmatrix}, & C \begin{pmatrix} 0 \\ f \\ e \\ 0 \end{pmatrix} &= \begin{pmatrix} a \\ 0 \\ 0 \\ g \end{pmatrix}, \\
C \begin{pmatrix} c \\ 0 \\ 0 \\ d \end{pmatrix} &= \begin{pmatrix} 0 \\ h \\ b \\ 0 \end{pmatrix}, & C \begin{pmatrix} 0 \\ h \\ 0 \\ g \end{pmatrix} &= \begin{pmatrix} c \\ 0 \\ e \\ 0 \end{pmatrix}. \quad (4.11)
\end{aligned}$$

The coin C is a matrix representation of the coin operator \hat{C} with matrix elements C_{ij} , $i, j = L, R, D, U$ and we respect the ordering introduced in Sec. 1.2.

The conditions from Eq. (4.11) can be further rewritten as

$$C \underbrace{\begin{pmatrix} a & 0 & c & 0 \\ 0 & f & 0 & h \\ b & e & 0 & 0 \\ 0 & 0 & d & g \end{pmatrix}}_A = \underbrace{\begin{pmatrix} 0 & a & 0 & c \\ f & 0 & h & 0 \\ 0 & 0 & b & e \\ d & g & 0 & 0 \end{pmatrix}}_B. \quad (4.12)$$

If the determinant of the matrix A is non-zero than we can invert it and find solution for the coin C as $C = B.A^{-1}$. Nevertheless, it may happen that $\det A = 0$. In the following two sections we will discuss these two possibilities in more detail. Before we do that, we can derive some conditions the parameters $a, -, h$ have to satisfy.

We know that coin C is unitary, therefore $C^\dagger C = I$ and

$$\begin{aligned}
0 &= B^\dagger B - B^\dagger B = A^\dagger C^\dagger C A - B^\dagger B = A^\dagger A - B^\dagger B = \\
&= \begin{pmatrix} |a|^2 + |b|^2 - & & & \\ -|d|^2 - |f|^2 & eb^* - gd^* & ca^* - hf^* & 0 \\ be^* - dg^* & |e|^2 + |f|^2 - |a|^2 - |g|^2 & 0 & hf^* - ca^* \\ ac^* - fh^* & 0 & |c|^2 + |d|^2 - |b|^2 - |h|^2 & gd^* - eb^* \\ 0 & fh^* - ac^* & dg^* - be^* & |g|^2 + |h|^2 - \\ & & & -|c|^2 - |e|^2 \end{pmatrix}.
\end{aligned} \tag{4.13}$$

From Eq. (4.13) one can see that $0 = A^\dagger A - B^\dagger B$ is equivalent to conditions:

$$|a|^2 + |b|^2 = |d|^2 + |f|^2, \tag{4.14}$$

$$|g|^2 + |h|^2 = |c|^2 + |e|^2, \tag{4.15}$$

$$|c|^2 + |d|^2 = |b|^2 + |h|^2, \tag{4.16}$$

$$ac^* = fh^*, \tag{4.17}$$

$$be^* = dg^*. \tag{4.18}$$

Here we ignore condition $|e|^2 + |f|^2 = |a|^2 + |g|^2$ in the second row and column of the matrix (4.13) which is already governed in Eqs. (4.14-4.16). Equation (4.17) implies $|ac| = |fh|$ and

Eq. (4.18) implies $|be| = |dg|$. This can be used further in Eq. (4.16) from which we obtain:

$$\begin{array}{ll}
|c|^2 + |d|^2 = |b|^2 + |h|^2 & |c|^2 + |d|^2 = |b|^2 + |h|^2 \\
\Downarrow \cdot |a|^2 & \Downarrow \cdot |g|^2 \\
|a|^2|c|^2 + |a|^2|d|^2 = |a|^2|b|^2 + |a|^2|h|^2 & |g|^2|c|^2 + |g|^2|d|^2 = |g|^2|b|^2 + |g|^2|h|^2 \\
\Updownarrow (|ac| = |fh|) & \Updownarrow (|be| = |dg|) \\
|f|^2|h|^2 + |a|^2|d|^2 = |a|^2|b|^2 + |a|^2|h|^2 & |g|^2|c|^2 + |e|^2|b|^2 = |g|^2|b|^2 + |g|^2|h|^2 \\
\Updownarrow & \Updownarrow \\
|h|^2 (|f|^2 - |a|^2) = |a|^2 (|b|^2 - |d|^2) & |g|^2 (|c|^2 - |h|^2) = |b|^2 (|g|^2 - |e|^2) \\
\Updownarrow (\text{by (4.14)}) & \Updownarrow (\text{by (4.15)}) \\
0 = (|h|^2 - |a|^2) (|f|^2 - |a|^2) & 0 = (|g|^2 - |b|^2) (|g|^2 - |e|^2) \\
\Updownarrow & \Updownarrow \\
0 = (|h| - |a|) (|f| - |a|) & 0 = (|g| - |b|) (|g| - |e|) \\
\Updownarrow (\text{by (4.14) - (4.15)}) & \Updownarrow (\text{by (4.14) - (4.15)}) \\
\left\{ \begin{array}{l} \text{either } |a| = |h| \text{ and } |c| = |f| \\ \text{or } |a| = |f| \text{ and } |c| = |h| \\ \text{and } |b| = |d| \text{ and } |g| = |e| \end{array} \right. & \left\{ \begin{array}{l} \text{either } |g| = |b| \text{ and } |d| = |e| \\ \text{or } |g| = |e| \text{ and } |b| = |d| \\ \text{and } |c| = |h| \text{ and } |a| = |f| \end{array} \right.
\end{array}$$

thus there are two possibilities,

$$\text{I) } |a| = |h| \text{ and } |c| = |f| \text{ and } |g| = |b| \text{ and } |d| = |e|, \quad (4.19)$$

$$\text{II) } |a| = |f| \text{ and } |c| = |h| \text{ and } |b| = |d| \text{ and } |g| = |e|. \quad (4.20)$$

Note that the determinant of the matrix A from Eq. (4.12) reads

$$\det A = adeh - bcfg.$$

It is easy to check that the situation I) from Eq. (4.19) corresponds to $\det A \neq 0$. On the other hand, the situation II) from Eq. (4.20) results in $\det A = 0$. This supports our suspicion that we have to distinguish between zero or non-zero value of the determinant of the matrix A and we can now proceed to the detail analysis of these two cases.

4.3 Non-zero determinant, $\det A \neq 0$

First we look at the non-zero determinant corresponding to the situation I) from Eq. (4.19). This reduces the conditions from Eqs. (4.14-4.16) to

$$|a|^2 + |b|^2 = |c|^2 + |d|^2. \quad (4.21)$$

We can assume without loss of generality that the norm of $|\psi^{stat}\rangle$ from Eq. (4.10) is 2. It implies, due to Eq. (4.21) that $|a|^2 + |b|^2 = |c|^2 + |d|^2 = 1$. This allows us to write $|a|, |b|, |d|, |f|$ as sine and cosine functions,

$$|a| = \sin \delta_1 = |h| \quad |b| = \cos \delta_1 = |g| \quad |c| = \sin \delta_2 = |f| \quad |d| = \cos \delta_2 = |e|. \quad (4.22)$$

Note that since we assumed that Eq. (4.20) does not hold, it follows that the parameters $\delta_{1,2}$ has to be different, $\delta_1 \neq \delta_2$. Different parameters imply $|bcfg| \neq |adeh|$, and therefore $\det A \neq 0$.

Since the determinant of the matrix A , Eq. (4.12) is non-zero, we may invert A and calculate $C = B.A^{-1}$. This is uniquely determined by the amplitudes a, b, c, d , Eq. (4.22), of $|\psi^{stat}\rangle$ from Eq. (4.10). Let us check that this construction of the coin C satisfies unitarity. Matrix C is unitary if and only if $I = C^\dagger C = (A^\dagger)^{-1} B^\dagger B A^{-1}$. Since A is invertible, we can multiply this with A^\dagger and A from left and right. This leads us to condition $B^\dagger B = A^\dagger A$. We have already met this condition in Eq. (4.13) which is equivalent to (4.14)-(4.18). Therefore, any solution to these equations leads to a valid unitary coin.

From Eq. (4.22) we know the amplitudes of $a, -, h$. Every complex parameter p can be written using its magnitude and phase as $p = |p|e^{i\phi_p}$, $p = a, -, h$. Eq. (4.17) shows that we can assume without loss of generality that $\phi_a - \phi_c = \phi_f - \phi_h$, and similarly $\phi_b - \phi_e = \phi_d - \phi_g$ by Eq. (4.18). Since we can multiply everything by a global phase we can also assume $\phi_a = 0$. We can combine this phase information with our knowledge on the magnitudes (4.22) to conclude that all possible unitary values of $C = B.A^{-1}$ can be obtained using the following parametrisation:

$$\begin{aligned} a &= \sin \delta_1, & b &= e^{i(\phi_d + \phi_e - \phi_g)} \cos \delta_1, & c &= e^{i(\phi_h - \phi_f)} \sin \delta_2, & d &= e^{i\phi_d} \cos \delta_2, \\ e &= e^{i\phi_e} \cos \delta_2, & f &= e^{i\phi_f} \sin \delta_2, & g &= e^{i\phi_g} \cos \delta_1, & h &= e^{i\phi_h} \sin \delta_1. \end{aligned}$$

One can check that this parametrization provides, up to a global phase, the same stationary state as we had in Eq. (1.33).

Finally, the first class of the four-dimensional coins leading to trapping at the vicinity of the origin read

$$\begin{aligned} C_{full_1}^{(4)} &= C = B \cdot A^{-1} = \\ &= \begin{pmatrix} e^{-i(\alpha_1 + \alpha_2)} c_1 c_2 & -e^{-i(\alpha_2 + \beta_1)} s_1 c_2 & -e^{-i(\alpha_1 + \beta_2)} c_1 s_2 & e^{-i(\beta_1 + \beta_2 + \varphi)} s_1 s_2 \\ e^{-i(\alpha_1 - \beta_2)} c_1 s_2 & -e^{-i(\beta_1 - \beta_2)} s_1 s_2 & e^{-i(\alpha_1 - \alpha_2)} c_1 c_2 & -e^{i(\alpha_2 - \beta_1 - \varphi)} s_1 c_2 \\ e^{-i(\alpha_2 - \beta_1)} s_1 c_2 & e^{i(\alpha_1 - \alpha_2)} c_1 c_2 & -e^{i(\beta_1 - \beta_2)} s_1 s_2 & -e^{i(\alpha_1 - \beta_2 - \varphi)} c_1 s_2 \\ e^{i(\beta_1 + \beta_2 + \varphi)} s_1 s_2 & e^{i(\alpha_1 + \beta_2 + \varphi)} c_1 s_2 & e^{i(\alpha_2 + \beta_1 + \varphi)} s_1 c_2 & e^{i(\alpha_1 + \alpha_2)} c_1 c_2 \end{pmatrix}, \end{aligned} \quad (4.23)$$

where

$$\begin{aligned} s_1 &= \sin \delta_1, \quad c_1 = \cos \delta_1, \quad s_2 = \sin \delta_2, \quad c_2 = \cos \delta_2, \\ \alpha_1 &= \phi_g - \frac{\phi_d + \phi_e + \pi}{2}, \quad \alpha_2 = -\frac{\phi_d - \phi_e + \pi}{2}, \\ \beta_1 &= \frac{\phi_d + \phi_e - \pi}{2}, \quad \beta_2 = \phi_f - \phi_h + \frac{\phi_d + \phi_e - \pi}{2}, \quad \varphi = -\phi_d - \phi_e + \phi_h + \pi. \end{aligned} \quad (4.24)$$

When omitting a global phase ϕ_a , this trapping coin class has 7 real parameters. Let us remind that this coin class was already derived in [29] using an alternative construction. More importantly, this is a strongly trapping coin class, already described in section 1.2.2,

$$C_{full_1}^{(4)} = C^{ST}.$$

It means that four-state quantum walks with this coin are trapped regardless of the initial coin state. This is satisfied provided that $\cos 2\delta_1 \neq \cos 2\delta_2$. We remind that for $\cos 2\delta_1 = \cos 2\delta_2$ such a strong trapping can be avoided using the escaping initial state, Eq. (1.34). One particular situation of spreading is depicted in subsection 1.2.2, Fig. (1.5).

Note that the parametrization and the resulting coin, Eq. (4.23), is still valid if one of the parameters $a, -, h$ is equal to zero. More precisely, due to Eq. (4.22) if one parameter is zero, then some other one is zero as well and thus we always have even number of zeros. If only two parameters are zero, we still have $\det A \neq 0$ and the approach described above is still valid. Different situation comes with four parameters being equal to zero, since then we fall under situation II) from Eq. (4.20), which will be analysed later.

4.4 Determinant equal to zero, $\det A = 0$

Let us turn to the situation II) given by Eq. (4.20). This case results in $\det A = 0$. To see this, multiply the two equations (4.17) and (4.18) to get

$$adc^*g^* = bfe^*h^*.$$

Now multiply both sides with $cgeh$ and use conditions (4.20) to get

$$adeh|cg|^2 = bcfg|eh|^2.$$

This is further equivalent to

$$0 = |cg|^2 \underbrace{(adeh - bcfg)}_{\det A} = 0,$$

which implies

$$\det A = 0$$

even in the case when c or g is equal to zero. This results in the fact that the matrix A is not invertible and we cannot follow the construction from the previous section. Moreover, here we have to distinguish between several cases since there are more ways of getting a zero determinant of the matrix A . As one of the trivial cases we can for instance choose $a = 0$. Then from Eq. (4.20) also $f = 0$ which immediately results in $\det A = 0$. Nevertheless, there exist also a non-trivial case that occurs provided that the parameters $a, b, c, e \neq 0$ and $adeh = bcfg$. Let us first analyse the non-trivial case and then turn back to the trivial ones.

4.4.1 Non-degenerate case

The non-degenerate case occurs when all amplitudes of $|\psi^{stat}\rangle$, Eq. (4.10), are non-zero. Due to constraints from Eq. (4.20) it is sufficient to assume that

$$a, b, c, e \neq 0$$

Further, since $\det A = 0$, the elements have to satisfy condition

$$adeh = bcfg. \quad (4.25)$$

Due to zero determinant, matrix A is not invertible and thus we cannot get C directly by inverting A . However, since no coefficients are zero we can see that the last 3 columns of A are linearly independent and their linear combination together with the determinant condition from Eq. (4.25) provides the first column of A . Therefore the columns of A span a three-dimensional subspace. It is now easy to find a vector orthogonal to all columns of A in the form

$$v_A = (deh, ceg, -cfg, -ceh). \quad (4.26)$$

Because the coin C is unitary, it reflects three-dimensional subspace of A to three-dimensional subspace of B . Therefore, the columns of the matrix B from Eq. (4.12) are not linearly independent as well and its one dimensional orthogonal subspace is spanned by the vector

$$v_B = (egh, bcg, -cgh, -aeh). \quad (4.27)$$

Again from unitarity, we know that C reflects the orthogonal subspace v_A of A to orthogonal subspace v_b of the matrix B . We have that

$$v_A A = 0, \quad v_B B = 0$$

and from Eq. (4.20) also

$$\|v_A\| = \|v_B\|.$$

This allows us to assume that

$$C v_A^\dagger = e^{is} v_B^\dagger$$

and define $A, B \rightarrow \tilde{A}, \tilde{B}$ by replacing the first columns with $v_A^\dagger, e^{is} v_B^\dagger$. It is

$$\begin{aligned} A_{\bullet 1} &\rightarrow v_A^\dagger = \tilde{A}_{\bullet 1}, & B_{\bullet 1} &\rightarrow e^{is} v_B^\dagger = \tilde{B}_{\bullet 1}, \\ A_{\bullet j} &\rightarrow \tilde{A}_{\bullet j}, & B_{\bullet j} &\rightarrow \tilde{B}_{\bullet j}, \quad j = 2, 3, 4. \end{aligned}$$

The explicit form of the new matrices read

$$\tilde{A} = \begin{pmatrix} (deh)^\dagger & 0 & c & 0 \\ (ceg)^\dagger & f & 0 & h \\ -(cfg)^\dagger & e & 0 & 0 \\ -(ceh)^\dagger & 0 & d & g \end{pmatrix}, \quad \tilde{B} = \begin{pmatrix} e^{is}(egh)^\dagger & a & 0 & c \\ e^{is}(bcg)^\dagger & 0 & h & 0 \\ -e^{is}(cgh)^\dagger & 0 & b & e \\ -e^{is}(aeh)^\dagger & g & 0 & 0 \end{pmatrix}. \quad (4.28)$$

This results in the alternative to Eq. (4.12) in the form $C\tilde{A} = \tilde{B}$. Since \tilde{A} has now full column rank it can be inverted and therefore we can write

$$C = \tilde{B}\tilde{A}^{-1}.$$

Similarly as in section 4.3, we can assume without loss of generality that the norm of $|\psi^{stat}\rangle$, Eq. (4.10) is $\sqrt{2}$ and that $a \in \mathbb{R}$ (the phase of a can be assumed as a global phase

and thus eliminated). This provides, together with conditions from Eq. (4.20), additional restriction of the form

$$\langle \psi^{stat} | \psi^{stat} \rangle = 2 \quad \Rightarrow \quad |a|^2 + |b|^2 + |c|^2 + |e|^2 = 1.$$

It is seen that we need three angles $\delta_{1,2,3}$ to parametrize $|a|, |b|, |c|, |e|$ in sine and cosine form. Additional phases are chosen to satisfy Eqs. (4.17)-(4.18). At the end we have the following parametrisation:

$$\begin{aligned} a &= s_1 s_3, & b &= c_1 s_2 e^{i(\phi_d + \phi_e - \phi_g)}, & c &= s_1 c_3 e^{i(\phi_h - \phi_f)}, & d &= c_1 s_2 e^{i\phi_d}, \\ e &= c_1 c_2 e^{i\phi_e}, & f &= s_1 s_3 e^{i\phi_f}, & g &= c_1 c_2 e^{i\phi_g}, & h &= s_1 c_3 e^{i\phi_h}, \end{aligned} \quad (4.29)$$

where δ_k ranges from 0 to 2π , $s_k = \sin \delta_k$ and $c_k = \cos \delta_k$ where $k = 1, 3, 4$.

Using this parametrisation, we get our new coin class as

$$C_{full_2}^{(4)} = C = \tilde{B} \tilde{A}^{-1} = \begin{pmatrix} e^{i(\alpha+\gamma_3)} \Xi c_1^2 c_2 s_2 & e^{i\alpha} (\Xi c_1^2 c_2^2 + 1) & e^{i(\alpha-\gamma_1+\gamma_3)} \Xi c_1 c_2 s_1 s_3 & e^{i(\alpha-\gamma_2+\gamma_3)} \Xi c_1 c_3 c_2 s_1 \\ e^{-i\alpha} (\Xi c_1^2 s_4^2 + 1) & e^{-i(\alpha+\gamma_3)} \Xi c_1^2 c_2 s_2 & e^{-i(\alpha+\gamma_1)} \Xi c_1 s_1 s_3 s_2 & e^{-i(\alpha+\gamma_2)} \Xi c_1 c_3 s_1 s_2 \\ e^{i(\beta+\gamma_2)} \Xi c_1 c_3 s_1 s_2 & e^{i(\beta+\gamma_2-\gamma_3)} \Xi c_1 c_3 c_2 s_1 & e^{i(\beta-\gamma_1+\gamma_2)} \Xi c_3 s_1^2 s_3 & e^{i\beta} (\Xi c_3^2 s_1^2 + 1) \\ e^{-i(\beta-\gamma_1)} \Xi c_1 s_1 s_3 s_2 & e^{-i(\beta-\gamma_1+\gamma_3)} \Xi c_1 c_2 s_1 s_3 & e^{-i\beta} (\Xi s_1^2 s_3^2 + 1) & e^{-i(\beta-\gamma_1+\gamma_2)} \Xi c_3 s_1^2 s_3 \end{pmatrix}, \quad (4.30)$$

where $\Xi = (e^{is} - 1)$, $\alpha = -\phi_f$, $\beta = \phi_e - \phi_g$,

$$\gamma_1 = \phi_d + \phi_e - \phi_g + \pi, \quad \gamma_2 = \phi_d + \phi_f - \phi_h + \pi, \quad \gamma_3 = \phi_d + \phi_f - \phi_g + 2\pi. \quad (4.31)$$

This new coin class is not a strongly trapping coin class and we can therefore find an escaping initial state that leads to the non-trapping type of walk. This escaping state has already been revealed during the construction of the coin class from Eq. (4.30), respectively matrix \tilde{A} , and is proportional to

$$\psi_C^{esc} \sim v_A^\dagger = (deh, ceg, -cfg, -ceh)^\dagger.$$

Due to constraints from Eq. (4.20) and parametrization from Eq. (4.29) we can simplify the amplitudes to

$$v_A^\dagger \sim \left(b^\dagger e^{-i(\phi_g + \phi_h)}, e^\dagger e^{-i(\phi_h + \phi_g - \phi_f)}, -a^\dagger e^{-i(\phi_g + \phi_h)}, -c^\dagger e^{-i(\phi_e + \phi_h)} \right).$$

Finally, multiplication of the amplitudes by a global phase $e^{i(\phi_d + \phi_e + \phi_h)}$ and parametrization (Eq:paramZeroDet) provides the escaping state in the form

$$|\psi^{esc}\rangle = \cos \delta_1 \sin \delta_2 |L\rangle + \cos \delta_1 \cos \delta_2 e^{i\gamma_3} |R\rangle + \sin \delta_1 \sin \delta_3 e^{i\gamma_1} |D\rangle + \sin \delta_1 \cos \delta_3 e^{i\gamma_2} |U\rangle. \quad (4.32)$$

Here we have used for $\gamma_{1,2,3}$ notation from Eq. (4.31).

Now we turn to the cases when there are some zero amplitudes. Note that there is always even number of zero parameters. This is due to Eq. (4.20) containing conditions on the magnitudes of the parameters $a, -, h$.

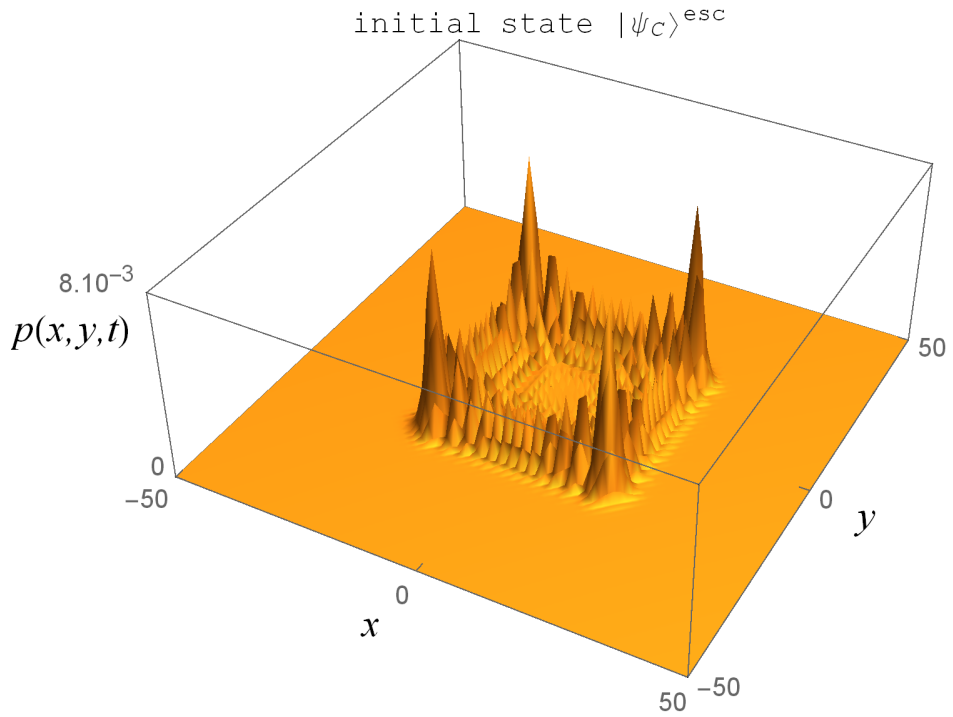


Figure 4.1: Four-state quantum walk on a 2D lattice with the coin class from Eq. (4.30). The parameters are $\alpha = \beta = \gamma_3 = 0$, $\gamma_1 = \gamma_2 = \pi$, $\delta_1 = \delta_2 = \delta_3 = s = \pi/4$ and are chosen so that the escaping state (4.32) as the initial state is the same as the escaping state for the Grover walk, Eq. (1.34). Number of steps is $t = 100$. Since the spreading is slow, the plot range is cut to the relevant area.

4.4.2 Two zero amplitudes

Suppose that there are two zero elements. Without loss of generality we can assume $a = 0 = f$. Then the determinant of \tilde{A} from Eq. (4.28) is non-zero and we can use the approach described above. This leads to the matrix $C_{full_2}^{(4)}$ from Eq. (4.30) with some of the sine or cosine functions equal to zero. For $a = 0 = f = s_1 s_3$ we have only one choice, since the other one leads to more than two zeros:

$$\underbrace{\sin \delta_1 = 0}_{\Rightarrow c=h=0} \quad \text{or} \quad \underbrace{\sin \delta_3 = 0}_{\checkmark}. \quad (4.33)$$

It is seen that the first choice $s_1 = 0$ leads to four zero elements and will be therefore analysed later. Thus we can conclude that situation

$$a = f = 0 \wedge b, c, d, e, h, g \neq 0 \quad \Leftrightarrow \quad \sin \delta_3 = 0$$

focuses only on the second case with $\sin \delta_3 = 0$. The same analysis can be done for b, c and e equal to zero,

$$\begin{aligned} b = d = 0 \wedge a, c, e, f, g, h \neq 0 &\quad \Leftrightarrow \quad \sin \delta_2 = 0, \\ c = h = 0 \wedge a, b, d, e, f, g \neq 0 &\quad \Leftrightarrow \quad \cos \delta_3 = 0, \\ e = g = 0 \wedge a, b, c, d, f, h \neq 0 &\quad \Leftrightarrow \quad \cos \delta_2 = 0. \end{aligned} \quad (4.34)$$

Even though this set of equations indeed summarizes all two-zero cases, careful reader might discover problem with the determinant of \tilde{A} which we are now going to discuss and discover its elimination. Let us remind that during the construction of the matrix \tilde{A} , Eq. (4.28), we have chosen one particular column of the matrix A and replaced it. In \tilde{A} we have replaced the first column of the matrix A . In general, there was no specific reason for choosing this particular column and we could have replaced different column instead. The reason for mentioning this becomes clear in the following paragraphs, here we mention only a motivation. Since we are dealing with two-zero case we find out that the value of $\det \tilde{A}$ varies in dependence on its parameters. Special choices even lead to $\det \tilde{A} = 0$. This inconvenient situation can be resolved by an alternative modification of the matrix A .

Although we claimed that $\det \tilde{A} \neq 0$ for $a = f = 0$ it is actually not true for example for $c = h = 0$ where $\det \tilde{A} = 0$. It is due to a fact that $v_A = 0$ as well. Thus it seems that we cannot use results from Eq. (4.30) and have to find a different approach instead. Let us now explain the solution to this problem in more detail. One can easily check that

$$\begin{aligned} \left. \begin{aligned} a = f = 0 \\ b = d = 0 \end{aligned} \right\} \det \tilde{A} \neq 0 \\ \left. \begin{aligned} c = h = 0 \\ e = g = 0 \end{aligned} \right\} \det \tilde{A} = 0. \end{aligned} \quad (4.35)$$

The issue with zero determinant in the last two cases of Eq. (4.35) can be easily solved. It initially arises from the construction of the \tilde{A} matrix, where we have removed the first column

of the matrix A from Eq. (4.12) and have it replaced by v_A^\dagger , which is orthogonal complement to the columns of A and v_A is given by Eq. (4.26). Since the columns of the matrix A are linearly dependent, we could have, without loss of generality, replaced the last column of A by a vector orthogonal to its columns in a different form,

$$u_A^\dagger = (bdf, -adf, -bcf, +ade)^\dagger.$$

This vector is non-zero for $c = h = 0$ and $e = g = 0$ and gives rise to u_B^\dagger of the form

$$u_B^\dagger = (bfg, -adh, -abf, +abd)^\dagger$$

satisfying

$$Cu_A^\dagger = e^{is}u_B^\dagger.$$

Vector u_B^\dagger is of course orthogonal to the first three columns of the matrix B . Let us note A_u, B_u matrices A, B with replaced fourth column by u_A^\dagger and $e^{is}u_B^\dagger$. Now we can write instead of Eq. (4.12) that $CA_u = B_u$. Matrix A_u is invertible and from its completely equivalent construction it is no surprise that it provides the same result as \tilde{A} , it is

$$C_{full_2}^{(4)} = C = B_u A_u^{-1} = \tilde{B} \tilde{A}^{-1}. \quad (4.36)$$

Let us remind that the aim of this equivalent construction was to get rid of the zero determinant from Eq. (4.35). We have reached the goal and for $c = h = 0$ and $e = g = 0$ hold that $\det A_u \neq 0$ and thus A_u remains invertible. Nevertheless, with $a = f = 0$ or $b = d = 0$ we get $\det A_u = 0$ since also $u_A^\dagger = 0$. Let us summarize and conclude two-zero subsection by the following diagram:

$$\left. \begin{array}{l} a = f = 0 \\ b = d = 0 \\ c = h = 0 \\ e = g = 0 \end{array} \right\} \left. \begin{array}{l} \det \tilde{A} \neq 0 \\ \det A_u \neq 0 \end{array} \right\} \text{class } C_{full_2}^{(4)} \text{ Eq.(4.30)} \left\{ \begin{array}{l} \sin \delta_3 = 0 \\ \sin \delta_2 = 0 \\ \cos \delta_3 = 0 \\ \cos \delta_2 = 0. \end{array} \right. \quad (4.37)$$

4.4.3 Four zero amplitudes

One can guess from the previous subsection and the construction of the matrices \tilde{A}, A_u that we will have to distinguish between several sub-cases as well. For example, if $a = f = 0$ and $b = d = 0$, it is $\sin \delta_3, \sin \delta_2 = 0$, (see Eqs. (4.33, 4.34)) it still holds that $\det \tilde{A} \neq 0$ since the rank of A remains three. More precisely, the first row of A is given only by zeros and we appropriately replace this first column in the construction of \tilde{A} . Nevertheless, if $a = f = 0$ through $\sin \delta_1 = 0$, we get that also $c = h = 0$, Eq. (4.33). This situation leads to $\text{rank} A = 2$ and therefore we cannot use results from Eq. (4.30) and have to solve it separately.

Four zero amplitudes and rank three

This situation is already covered in the solution $C_{full_2}^{(4)}$ from Eq. (4.30), with some of the elements being set to zero. We get four different combinations of the zero amplitudes satisfying rank condition, which are discussed below.

As we have already mentioned, rank three is achieved for

$$I) \quad \sin \delta_3 = \sin \delta_2 = 0 \text{ i.e } a = f = b = d = 0, \quad c = h = e = g \neq 0.$$

Similarly, according to Eq. (4.37) we can combine cosines,

$$II) \quad \cos \delta_3 = \cos \delta_2 = 0 \text{ i.e } c = h = e = g = 0, \quad a = f = b = d \neq 0.$$

These two cases give us stationary states, Eq. (4.10) of the form

$$\begin{aligned} |\psi^{stat}\rangle &= c|x, y+1\rangle \otimes |L\rangle + e|x+1, y\rangle \otimes |D\rangle + |x+1, y+1\rangle \otimes (g|U\rangle + h|R\rangle), \\ |\psi^{stat}\rangle &= |x, y\rangle \otimes (a|L\rangle + b|D\rangle) + d|x, y+1\rangle \otimes |U\rangle + f|x+1, y\rangle \otimes |R\rangle, \end{aligned}$$

living on a smaller "corner-like" support. From Eq. (4.10) we see that another two corner-like cases are allowed,

$$III) \quad \sin \delta_3 = \cos \delta_2 = 0 \text{ i.e } a = f = e = g = 0, \quad b = d = c = h \neq 0,$$

$$IV) \quad \sin \delta_2 = \cos \delta_3 = 0 \text{ i.e } b = d = c = h = 0, \quad a = f = e = g \neq 0.$$

The cases *III*), *IV*) correspond to $\text{rank}(A) = 3$. The only problem and also a reason why we have separated these two situations is the determinant of \tilde{A} and A_u from Eqs. (4.28, 4.36), since both determinants are equal to zero. This is completely the same situation as described below Eq. (4.35) arising from a specific choice of replaced column in \tilde{A} , A_u and leading to the same result, Eq. (4.36). For those interested, in *III*) we would have to replace the third column of A , Eq. (4.12) by the orthogonal complement $w_A^\dagger = (bdh, bcg, -adh, -bch)^\dagger$ to the columns of A . The resulting matrix would have non-zero determinant, thus can be inverted and results in the coin class $C_{full_2}^{(4)}$, Eq. (4.30, 4.36). Similarly in *IV*) we have to replace the second column of A .

We have shown that there exist four four-zero case *I*) – *IV*) which are governed in the not strongly trapping solution provided in Eq. (4.30). The remaining four-zero cases have to be analysed differently due to smaller rank of the matrix A , Eq. (4.12).

Four zero amplitudes and rank two

Only two four-zero cases remain for analysis,

$$i) \quad a = f = c = h = 0 \Leftrightarrow \sin \delta_1 = 0,$$

$$ii) \quad b = d = e = g = 0 \Leftrightarrow \cos \delta_1 = 0.$$

This situations correspond to even smaller rank of A , which is now two. Therefore, we cannot use result of Eq. (4.30).

Let us start with the first situation *i*). From Eq. (4.12) we see that the coin acts in the following way

$$C \begin{pmatrix} 0 \\ 0 \\ b(e) \\ 0 \end{pmatrix} = \begin{pmatrix} 0 \\ 0 \\ 0 \\ d(g) \end{pmatrix}, \quad C \begin{pmatrix} 0 \\ 0 \\ 0 \\ d(g) \end{pmatrix} = \begin{pmatrix} 0 \\ 0 \\ b(e) \\ 0 \end{pmatrix}, \quad (4.38)$$

which corresponds only to switches between $|D\rangle \rightleftharpoons |U\rangle$ coin states. There are no specific conditions on $|L\rangle, |R\rangle$ mixing. Note that elements e and g written in the brackets provide the same information as b, d and thus can be neglected or even set to zero. Nevertheless, this would lead to a six zero case that will be described afterwards. Due to Eq. (4.38) and conditions from Eq. (4.20) we have that

$$C_{UD} = \frac{d}{b} = \frac{g}{e} = \left| \frac{|b| = |d|}{|e| = |g|} \right| = e^{i\gamma} \quad \text{and} \quad C_{DU} = \frac{b}{d} = \frac{e}{g} = e^{-i\gamma},$$

which together with $C_{DD} = C_{UU} = 0$ constitutes diagonal sub-matrix C_1 of the final coin C_i . There are no other restrictions on the horizontal movements $|L\rangle, |R\rangle$ and their mixing can be driven by an arbitrary unitary matrix U similarly as in Eq. (4.6). This all leads to the coin class of the form

$$C_i = \begin{pmatrix} U & 0 \\ 0 & C_1 \end{pmatrix} = \begin{pmatrix} e^{i\alpha} \cos \delta & e^{-i\beta} \sin \delta & 0 & 0 \\ -e^{i\beta} \sin \delta & e^{-i\alpha} \cos \delta & 0 & 0 \\ 0 & 0 & 0 & e^{-i\gamma} \\ 0 & 0 & e^{i\gamma} & 0 \end{pmatrix}. \quad (4.39)$$

Indeed, this coin class describes rather one-dimensional than two-dimensional walk. There is no spreading through the vertical lattice since the particle only jumps up and immediately back.

An identical analysis can be done for the case ii). We get, instead of conditions for the vertical movements from Eq. (4.38) conditions for the horizontal movements leading to the same sub-matrix C_1 . Matrix U now mixes vertical states $|D\rangle, |U\rangle$. In total we get that

$$C_{ii} = \begin{pmatrix} C_1 & 0 \\ 0 & U \end{pmatrix}, \quad (4.40)$$

where blocks U, C_1 are the same as in Eq. (4.39). Compare the results with Eq. (4.7) derived during the proof on the support of stationary states.

Coins C_i, C_{ii} describe a two-state walk rather than a four-state walk. The left-right (up-down) movements are by the choice of the amplitudes $a, -, h$ suppressed.

Six zero amplitudes

The last situation we have to analyse is six-zero case. We look at one of these situations, since the other are analogical. For instance we might have $a = f = c = h = e = g = 0$. Then the matrix A has the same rank as in the previous subsection, it is rank two. We have already mentioned in the previous subsection that the elements e, g in the brackets appearing in Eq. (4.38) might be neglected since they do not provide any extra information. We can, without loss of generality, set them to zero. Further analysis is the same as for the case i) from the previous subsection and lead to the embedded one-dimensional coin C_i from Eq.

(4.39). We summarize all possible cases in the following diagram:

$$\left. \begin{array}{l} a = f = c = h = e = g = 0 \\ a = f = c = h = b = d = 0 \end{array} \right\} \text{lead to coin } C_{i)} \text{ from Eq. (4.39),}$$

$$\left. \begin{array}{l} b = d = e = g = a = f = 0 \\ b = d = e = g = c = h = 0 \end{array} \right\} \text{lead to coin } C_{ii)} \text{ from Eq. (4.40).}$$

We have shown that the six-zero case is analogical to the four-zero situation and the final coins are given as a direct sum of two unitary matrices. Each of these matrices control spreading on a horizontal or a vertical lattices. Moreover, one matrix contains only anti-diagonal elements and thus kills the horizontal or the vertical spreading in the case of $C_{i)}$ or $C_{ii)}$ coin. Therefore, six-zero describes rather two-state than four-state walks.

In this chapter we have classified all trapping coins for the four-state quantum walk on a two dimensional lattice. The analysis started with a proof of a restriction imposed on a support of a stationary state. Further, amplitudes of the stationary state are uniquely determined by a coin. Analysis of these amplitudes leads to their parametrization resulting in the final forms of the trapping coins. At the beginning, we had to distinguish between two basic choices for the parametrization. Both of these choices provided one coin class with all matrix elements being non-zero. Whereas one of these classes exhibited stronger version of trapping, the other one did not. Further, to complete the classification, we have analysed also all the subclasses consisting of some zero matrix elements.

Chapter 5

Limiting distribution and role of coin eigenstates

The role of the limiting distribution as approximative probability distribution becomes important when one investigates a quantum walk after infinitely many steps. If we consider t as a number of steps, the probabilities $p(x, t) = \|\psi(x, t)\|^2$ (see e.g. Eq. (1.13)) that the particle is located at position x are calculated recursively from the results for the previous steps. With increasing number of steps, this becomes a memory consuming process. Moreover, the usual oscillations in the probabilities and neighbourhood positions are for increasing number of steps less significant. The probability distribution can be then replaced by its approximation arising from the limiting density.

The expression of the limiting density function strongly depends on the coin space basis. Proper choice of the basis is accompanied by a simpler formula from which some interesting regimes can be read out. In this chapter we focus on the role of the coin space basis in order to find a suitable choice which we call suitable. Although some of the coin classes have their suitable basis formed by the eigenvectors of the coin, this fact is not a general rule. We show that the essence of the suitable basis sit is different point. Nevertheless, at least for the Wigner walks, certain connection of the suitable coin space basis to the eigenvectors of the Wigner matrices still exists.

5.1 Velocity density for the eigenvector family

Our investigation of the limiting density starts with the eigenvector family of coins $C_{def_2}^{(3)}(\rho)$, Eq. (2.17), discussed in chapter 2. This coin class were already studied from the viewpoint of the limiting distribution by T. Machida et. al. [21]. The authors calculated the group-velocity density and the trapping probability with respect to the initial coin state in the standard coin space basis $|L\rangle, |S\rangle, |R\rangle$. From the velocity density $f(v)$ it is easy to construct approximate position probability distribution for large number of steps as $\frac{1}{t}f(x/t)$. By approximate we mean that the fluctuating probabilities that are typical in the position probability distribution are smoothed out.

In [21], the eigenvector family $C_{def_2}^{(3)}(\rho)$ was modified into

$$C(\theta) = \begin{pmatrix} -\frac{1+\cos\theta}{2} & \frac{\sin\theta}{\sqrt{2}} & \frac{1-\cos\theta}{2} \\ \frac{\sin\theta}{\sqrt{2}} & \cos\theta & \frac{\sin\theta}{\sqrt{2}} \\ \frac{1-\cos\theta}{2} & \frac{\sin\theta}{\sqrt{2}} & -\frac{1+\cos\theta}{2} \end{pmatrix} \approx C_{def_2}^{(3)}(\rho). \quad (5.1)$$

For the choice

$$\cos\theta = 2\rho^2 - 1, \quad \sin\theta = 2\rho\sqrt{1-\rho^2} \quad (5.2)$$

the matrix $C(\theta)$ is exactly the eigenvector family $C_{def_2}^{(3)}(\rho)$, Eq. (2.17). In the further analysis, we will stay faithful to the parameter expressing the velocity of spreading which is ρ and the corresponding coin $C_{def_2}^{(3)}(\rho)$.

We have already mentioned that the limiting distribution was derived with respect to the initial coin state in the standard basis $|L\rangle, |S\rangle, |R\rangle$,

$$|\psi_0\rangle = |0\rangle \otimes \underbrace{(\alpha|L\rangle + \beta|S\rangle + \gamma|R\rangle)}_{|\psi_C\rangle}, \quad |\alpha|^2 + |\beta|^2 + |\gamma|^2 = 1. \quad (5.3)$$

In the limit of large number of steps $t \rightarrow \infty$, the moments of the particles re-scaled position x/t (pseudo-velocity) can be calculated as [22]

$$\lim_{t \rightarrow \infty} \left\langle \left(\frac{x}{t} \right)^r \right\rangle = \langle v^r \rangle = \int_{-\rho}^{\rho} v^r f(v) dv. \quad (5.4)$$

Here we have denoted as v the (group) velocity of the walk and $f(v)$ is the velocity density function. In the standard basis, the velocity density has the form [21]

$$\begin{aligned} f(v) &= \frac{\sqrt{1-\cos\theta}}{2\pi(1-v^2)\sqrt{1+\cos\theta-2v^2}} (d_0 + d_1v + d_2v^2) \\ &= \frac{\sqrt{1-\rho^2}}{2\pi(1-v^2)\sqrt{\rho^2-v^2}} (d_0 + d_1v + d_2v^2), \end{aligned} \quad (5.5)$$

where the range of the velocity is limited by the maximum (see Eq. (1.23)) of the group velocity, thus $v \in (-v_{max}, v_{max}) = (-\rho, \rho)$. The parameter ρ immediately gives the rate of spreading. The coefficients d_j , $j = 0, 1, 2$ crucially depend on the initial states and are equal to

$$\begin{aligned} d_0 &= |\alpha + \gamma|^2 + 2|\beta|^2, \\ d_1 &= 2 \left(-|\alpha - \beta|^2 + |\gamma - \beta|^2 - \left(2 - \frac{\sqrt{2-2\rho^2}}{\rho} \right) \operatorname{Re}((\alpha - \gamma)\bar{\beta}) \right), \\ d_2 &= |\alpha|^2 - 2|\beta|^2 + |\gamma|^2 - 2 \left(\frac{\sqrt{2-2\rho^2}}{\rho} \operatorname{Re}((\alpha - \gamma)\bar{\beta}) + \frac{2-\rho^2}{\rho^2} \operatorname{Re}(\alpha\bar{\gamma}) \right). \end{aligned} \quad (5.6)$$

Note that for the density from Eq. (5.5) we have

$$\int_{-\rho}^{\rho} f(v) dv < 1. \quad (5.7)$$

It is because the density function does not include the trapping peak at the origin with zero velocity. The supplement to one is therefore equal to the probability that the particle is trapped around the origin. In [21], the authors derived also this trapped part of the probability distribution with result

$$p_\infty(x) = \frac{1}{128(1-\rho^2)^2} \left(2(1-\rho^2)|B\nu^{|x+1}| + A\nu^{|x|}|^2 + \rho^2|B\nu^{|x+1}| + (A+B)\nu^{|x|} + A\nu^{x-1}|^2 + 2(1-\rho^2)|B\nu^{|x|} + A\nu^{|x-1}||^2 \right), \quad (5.8)$$

where

$$\begin{aligned} \nu &= -\frac{1}{\rho^2}(2-\rho^2-2\sqrt{1-\rho^2}) \\ A &= 4(1-\rho^2)\alpha + 2\rho\sqrt{2-2\rho^2}\beta \\ B &= 4(1-\rho^2)\gamma + 2\rho\sqrt{2-2\rho^2}\beta \end{aligned} \quad (5.9)$$

and

$$\sum_x p_\infty(x) = \frac{1}{8\sqrt{2}(2-2\cos\rho^2)^{3/2}} (|A|^2 + |B|^2 + 2\nu\text{Re}(A\bar{B})). \quad (5.10)$$

One can check that the sum of Eq. (5.10) and Eq. (5.7) is then normalized to unity

$$\int_{-\rho}^{\rho} f(v)dv + \sum_x p_\infty(x) = 1.$$

Both, the velocity density and the trapping probability, strongly depend on the parameters α, β, γ of the initial coin state $|\psi_C\rangle$, Eq. (5.3). This suggests that the change of the coefficients may bring some simplifications.

We suggest the idea that a proper choice of the basis coin states can lead to a simplified expression for $p_\infty(x)$ and $f(v)$ and hence allow a clear insight into the role of the coin for the propagation. One of the possibilities at hand that is often the suitable choice in quantum mechanical problems is the basis formed by the eigenvectors of the coin $C_{def_2}^{(3)}(\rho)$,

$$\begin{aligned} |u_{1,+}\rangle &= \sqrt{\frac{1-\rho^2}{2}}|L\rangle + \rho|S\rangle + \sqrt{\frac{1-\rho^2}{2}}|R\rangle = \left(\sqrt{\frac{1-\rho^2}{2}}, \rho, \sqrt{\frac{1-\rho^2}{2}} \right)^T, \\ |u_{2,-}\rangle &= \frac{\rho}{\sqrt{2}}|L\rangle - \sqrt{1-\rho^2}|S\rangle + \frac{\rho}{\sqrt{2}}|R\rangle = \left(\frac{\rho}{\sqrt{2}}, -\sqrt{1-\rho^2}, \frac{\rho}{\sqrt{2}} \right)^T, \\ |u_{3,-}\rangle &= \frac{1}{\sqrt{2}}(|L\rangle - |R\rangle) = \frac{1}{\sqrt{2}}(1, 0, -1)^T. \end{aligned} \quad (5.11)$$

Here $|u_{1,+}\rangle$ corresponds to the eigenvalue +1 of $C_{def_2}^{(3)}(\rho)$ and $|u_{2(3),-}\rangle$ correspond to the eigenvalue -1. The initial state in the new basis reads

$$|\psi_0\rangle = |0\rangle \otimes \left(g_1|u_{1,+}\rangle + g_2|u_{2,-}\rangle + g_3|u_{3,-}\rangle \right) \quad (5.12)$$

and satisfies the normalization condition

$$|g_1|^2 + |g_2|^2 + |g_3|^2 = 1.$$

Using Eq. (5.11) we find that the initial states from Eqs. (5.3) and (5.12) are connected by

$$\begin{aligned}\alpha &= \frac{1}{\sqrt{2}} \left(\sqrt{1-\rho^2} g_1 + \rho g_2 + g_3 \right), \\ \beta &= \rho g_1 - \sqrt{1-\rho^2} g_2, \\ \gamma &= \frac{1}{\sqrt{2}} \left(\sqrt{1-\rho^2} g_1 + \rho g_2 - g_3 \right).\end{aligned}\tag{5.13}$$

Note that d_1 is given by a coherent combination of the amplitudes, whereas for $d_{0,2}$ not. The substitution of Eq. (5.13) into Eq. (5.6) together with condition $|g_1|^2 + |g_2|^2 + |g_3|^2 = 1$ gives

$$\begin{aligned}d_0 &= 2(1 - |g_3|^2), \\ d_1 &= -\frac{2}{\rho}(g_2\bar{g}_3 + g_3\bar{g}_2), \\ d_2 &= \frac{2}{\rho^2}(|g_2|^2 + 2|g_3|^2 - 1).\end{aligned}\tag{5.14}$$

This change of the basis greatly simplifies the expressions for the coefficients $d_{0,1,2}$ and therefore the final expressions of the velocity density function and the trapping probability. We have

$$f(v) = \frac{\sqrt{1-\rho^2}}{\pi(1-v^2)\sqrt{\rho^2-v^2}} \left((1 - |g_3|^2) - \frac{1}{\rho}(g_2\bar{g}_3 + g_3\bar{g}_2)v + \frac{1}{\rho^2}(|g_2|^2 + 2|g_3|^2 - 1)v^2 \right)\tag{5.15}$$

in the case of the density function, Eq. (5.5) and

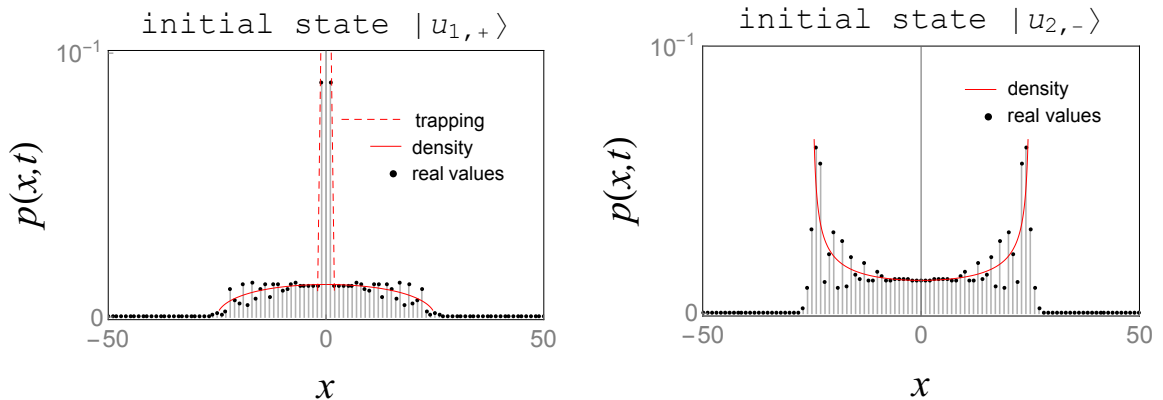
$$p_\infty(x) = \begin{cases} \frac{2-2\rho^2}{\rho^4} \nu^{2x} |g_1 + g_3|^2 & \text{for } x > 0, \\ \frac{1}{\rho^2} |\nu| (|g_1|^2 + (1-\rho^2)|g_3|^2) & \text{for } x = 0, \\ \frac{2-2\rho^2}{\rho^4} \nu^{|2x|} |g_1 - g_3|^2 & \text{for } x < 0. \end{cases}\tag{5.16}$$

for the trapping probability from Eq. (5.8). Coherent linear combination of the amplitudes appears for the position outside the origin. From these two new expressions for $f(v)$ and $p_\infty(x)$ one can unveil many interesting features that were hidden before in the complicated forms of Eqs. (5.5, 5.8). As an example we mention the choice of the initial coin state where $g_1 = \pm g_3$. In this case one half of the central peak in Eq. (5.16) corresponding to the negative or the positive positions x vanish. In Fig. (5.1), one can compare the resulting position probability distributions for several initial states. It is seen that even for smaller number of steps, the limiting density and the trapping probability $p_\infty(x)$ provide a good approximation.

The eigenvalue family is not the only option for which the coin space basis constituted by the coin eigenvectors appears to be suitable. In the following section we show how this basis affects the limiting description of the eigenvector family of coins.

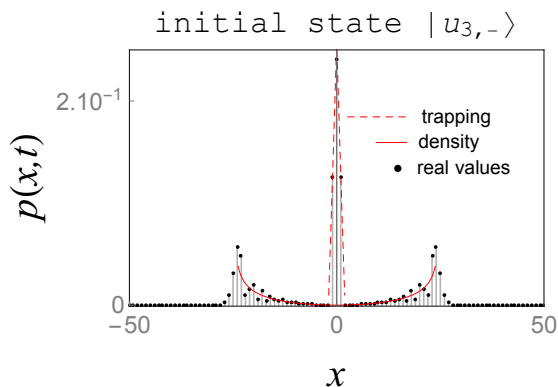
5.2 Velocity density for the eigenvalue family

A similar analysis as above can be done for the eigenvalue family $C_{def_1}^{(3)}(\varphi)$ from Eq. (2.5). For this matrix, no previous analysis was done. We start the calculations immediately in the



(a) Probability distribution for the initial state $|u_{1,+}\rangle$ from Eq. (5.11). For this choice, both travelling peaks at positions $x = \pm 25$ disappear and all travelling peaks, but the central peak is present.

(b) Probability distribution for the initial state $|u_{2,-}\rangle$ from Eq. (5.11). For this choice there exist travelling peaks, but the central peak disappears.



(c) Probability distribution for the initial state $|u_{3,-}\rangle$ from Eq. (5.11). For this choice there exist both travelling peaks as well as the trapping one.

Figure 5.1: Probability distributions for the quantum walk with $C_{def_2}^{(3)}(\rho)$ coin, Eq. (5.1). The initial states are chosen as the eigenstates of $C_{def_2}^{(3)}(\rho)$. For all figures, the parameter $\rho = \frac{1}{4}$ and the total number of steps is $t = 100$. Thus the travelling peaks are located at positions $x = \pm \rho t = \pm 25$. The red solid lines correspond to the limiting probability calculated from the group velocity density $f(v)$, Eq. (5.15), as $\frac{1}{t} f(\frac{x}{t})$. Red dashed lines depict the trapping probability from Eq. (5.16). Finally, black dots are probabilities coming from the numerical simulation of the walk. It is seen that even for relatively small number of steps, the approximations work very well.

more convenient basis. Based on the previous results, we may guess that this new basis is formed by the eigenvectors of the coin $C_{def_1}^{(3)}(\varphi)$. Let us now describe this approach in more detail. At first we remind that the eigenvalue family is given by

$$C_{def_1}^{(3)}(\varphi) = \frac{1}{6} \begin{pmatrix} -1 + e^{2i\varphi} & 2(1 + e^{2i\varphi}) & 5 - e^{2i\varphi} \\ 2(1 + e^{2i\varphi}) & 2(1 - e^{2i\varphi}) & 2(1 + e^{2i\varphi}) \\ 5 - e^{2i\varphi} & 2(1 + e^{2i\varphi}) & -1 - e^{2i\varphi} \end{pmatrix}. \quad (5.17)$$

Using the results of [16], [22] we have for the moments of the pseudo-velocity x/t

$$\left\langle \left(\frac{x}{t} \right)^r \right\rangle \xrightarrow{t \rightarrow \infty} \int_{-\pi}^{\pi} \sum_{j=1}^3 \left(\frac{i\lambda'_j(k)}{\lambda_j} \right)^r |(v_j(k), \psi_0)|^2 \frac{dk}{2\pi}, \quad (5.18)$$

where $\lambda_j(k)$ resp. $v_j(k)$ are the eigenvalues resp. the eigenvectors of the evolution operator in the Fourier representation $\tilde{U}(k) = \text{Diag}\{e^{-ik}, 1, e^{ik}\} \cdot C_{def_1}^{(3)}(\varphi)$. We have denoted first derivative of the eigenvalue with respect to the momentum k as $\lambda'_j(k)$. The eigenvalues can be written as

$$\lambda_1(k) = 1, \quad \lambda_{2,3} = e^{i(\varphi \pm \omega(k))},$$

with the momentum dependent phase

$$\omega(k) = -\arccos\left(-\frac{\cos \varphi}{3}(2 + \cos k)\right). \quad (5.19)$$

The eigenvectors corresponding to these eigenvalues read

$$v_1(k) = \sqrt{\frac{2}{5 + \cos(k)}} \begin{pmatrix} 1 \\ \frac{1}{2}(1 + e^{ik}) \\ e^{ik} \end{pmatrix}, \quad (5.20)$$

$$v_{2,3}(k) = \frac{1}{\sqrt{n_{2,3}}} \begin{pmatrix} (e^{-ik} + e^{-i(\varphi \pm \omega(k))}) \cos \varphi \\ \cos \omega(k) + e^{\pm i\omega(k)} - e^{-i(2\varphi \pm \omega(k))} + \cos k \cos \varphi \\ (e^{-ik} + e^{i(\varphi \pm \omega(k))}) \cos \varphi \end{pmatrix},$$

where the normalization factor equals to

$$n_{2,3} = \frac{4}{3} \cos^2 \varphi (9 - 4 \cos^2 \varphi \pm 2\Lambda \sin \varphi - \cos k ((4 + \cos k) \cos^2 \varphi \pm \Lambda \sin \varphi)),$$

$$\Lambda = \sqrt{9 - \cos^2 \varphi (2 + \cos k)^2}.$$

Substituting these eigenvalues and eigenvectors into Eq. (5.18) gives

$$\lim_{t \rightarrow \infty} \left\langle \left(\frac{x}{t} \right)^r \right\rangle = \langle v^r \rangle = \int_{-\pi}^{\pi} \left(\frac{d\omega}{dk} \right)^r ((-1)^r |(v_2(k), \psi_0)|^2 + |(v_3(k), \psi_0)|^2) \frac{dk}{2\pi}.$$

Note that the element of the summation corresponding to the stationary state $v_1(k)$, Eq. (5.18), disappears due to $\lambda'_1(k) = 0$. To calculate the overlaps $(v_j(k), \psi_0)$, $j = 2, 3$ we

determine the initial state in the suitable basis formed by the eigenstates of the matrix $C_{def_1}^{(3)}(\varphi)$, which are

$$\begin{aligned} |p_{1,+}\rangle &= \frac{1}{\sqrt{3}}(|L\rangle + |S\rangle + |R\rangle), \\ |p_{2,-}\rangle &= \frac{1}{\sqrt{6}}(|L\rangle - 2|S\rangle + |R\rangle), \\ |p_{3,-}\rangle &= \frac{1}{\sqrt{2}}(|L\rangle - |R\rangle), \end{aligned} \quad (5.21)$$

where

$$C_{def_1}^{(3)}(\varphi)|p_{1,+}\rangle = |p_{1,+}\rangle, \quad C_{def_1}^{(3)}(\varphi)|p_{2,-}\rangle = -|p_{2,-}\rangle, \quad C_{def_1}^{(3)}(\varphi)|p_{3,-}\rangle = -|p_{3,-}\rangle.$$

The initial coin state in the suitable basis $|\psi_C\rangle = (q_1|p_{1,+}\rangle + q_2|p_{2,-}\rangle + q_3|p_{3,-}\rangle)$ satisfying the normalization condition $|q_1|^2 + |q_2|^2 + |q_3|^2 = 1$ can be written in the standard basis as

$$|\psi_0\rangle = |0\rangle \otimes \left(\left(\frac{q_1}{\sqrt{3}} + \frac{q_2}{\sqrt{6}} + \frac{q_3}{\sqrt{2}} \right) |L\rangle + \left(\frac{q_1}{\sqrt{3}} - \sqrt{\frac{2}{3}}q_2 \right) |S\rangle + \left(\frac{q_1}{\sqrt{3}} + \frac{q_2}{\sqrt{6}} - \frac{q_3}{\sqrt{2}} \right) |R\rangle \right).$$

Now the sum of the overlaps $|(v_{2,3}(k), \psi_0)|^2$ from Eq. (??) can be divided into two cases:

r even \Rightarrow

$$|(v_2(k), \psi_0)|^2 + |(v_3(k), \psi_0)|^2 = 3|q_2|^2 + 5|q_3|^2 - 2 + \frac{12}{5 + \cos k}(1 - |q_2|^2 - 2|q_3|^2)$$

r odd \Rightarrow

$$\begin{aligned} -|(v_2(k), \psi_0)|^2 + |(v_3(k), \psi_0)|^2 &= \frac{\cos \varphi \sin k}{\Lambda}. \\ \left(-\sqrt{3}(q_2\bar{q}_3 + \bar{q}_2q_3 + i \tan \varphi(q_2\bar{q}_3 - \bar{q}_2q_3)) - i\sqrt{6} \tan \varphi \frac{2 + \cos k}{5 + \cos k}(q_1\bar{q}_3 - \bar{q}_1q_3) \right). \end{aligned} \quad (5.22)$$

Now we can perform the last step, which is change of a variable. To get a velocity density, we have to replace the momentum k in Eq. (5.22) by the group-velocity variable v . The relations used in this transformation are obtained from the dispersion relation, Eq. (5.19), from which

$$v = \frac{d\omega}{dk} = \frac{\cos \varphi \sin k}{\Lambda} = \frac{\cos \varphi \sin k}{\sqrt{9 - \cos^2 \varphi(2 + \cos k)^2}}. \quad (5.23)$$

Here ω is a phase from Eq. (5.19). Now the situation is a bit more difficult than for the $C_{def_2}^{(3)}(\rho)$ coin, since the transformation is not unique and we have to distinguish between two intervals joined by the separating point k_1 , where the transformation coincides:

$$\begin{aligned} k \in (-k_1, k_1) &\longrightarrow \cos k = \frac{2v^2 + \sqrt{1 + 3v^2 - \frac{9v^2}{\cos^2 \varphi}(1 - v^2)}}{1 - v^2}, \\ k \in (-\pi, -k_1) \cup (k_1, \pi) &\longrightarrow \cos k = \frac{2v^2 - \sqrt{1 + 3v^2 - \frac{9v^2}{\cos^2 \varphi}(1 - v^2)}}{1 - v^2}, \end{aligned}$$

with the separating point equal to

$$k_1 = \arccos \left(\frac{1}{4 \cos^2 \varphi} (9 - 5 \cos^2 \varphi - 3 \sin \varphi \sqrt{9 - \cos^2 \varphi}) \right).$$

For the sine function we obtain

$$k \in (-k_1, k_1) \longrightarrow$$

$$\sin k = \frac{v}{\cos \varphi (1 - v^2)} \sqrt{\frac{9(1 - v^2)}{\cos^2 \varphi} - 5 - 3v^2 + 4 \sqrt{1 - 9v^2 \frac{1 - v^2}{\cos^2 \varphi} + 3v^2}},$$

$$k \in (-\pi, -k_1) \cup (k_1, \pi) \longrightarrow$$

$$\sin k = \frac{v}{\cos \varphi (1 - v^2)} \sqrt{\frac{9(1 - v^2)}{\cos^2 \varphi} - 5 - 3v^2 - 4 \sqrt{1 - 9v^2 \frac{1 - v^2}{\cos^2 \varphi} + 3v^2}}.$$

We have everything necessary and can proceed with the calculation of the moments. Thus, we can summarize the results.

In the new variable v the moments read

$$\lim_{t \rightarrow \infty} \left\langle \left(\frac{x}{t} \right)^r \right\rangle = \int_{-v_{max}}^{v_{max}} v^r f(v) dv. \quad (5.24)$$

This expression is familiar from the previous case, Eq. (5.4). Nevertheless, the velocity density $f(v)$ is now much more complicated,

$$\begin{aligned} f(v) = & \frac{1}{6\pi(1 - v^2)\Theta} \left((3|q_2|^2 + 5|q_3|^3 - 2)\Upsilon_+ + (1 - |q_2|^2 - 2|q_3|^2)\Omega - \right. \\ & \left. - v\sqrt{3}(q_2\bar{q}_3 + \bar{q}_2q_3 + i(q_2\bar{q}_3 - \bar{q}_2q_3) \tan \varphi)\Upsilon_+ - iv(q_1\bar{q}_3 - \bar{q}_1q_3)\Xi \right) \end{aligned} \quad (5.25)$$

with

$$\Upsilon_{\pm} = \Phi_+ \pm \Phi_-,$$

$$\Phi_{\pm} = \sqrt{9(1 - v^2) - (5 + 3v^2) \cos^2 \varphi \pm 12\Theta \cos \varphi},$$

$$\Omega = 4 \cos \varphi \frac{(5 - 3v^2)\Upsilon_+ \cos \varphi + 3\Theta\Upsilon_-}{8 \cos^2 \varphi + 3v^2 \sin^2 \varphi},$$

$$\Xi = \frac{3\sqrt{6} \tan \varphi ((v^2 + \cos^2 \varphi)\Upsilon_+ - \Theta\Upsilon_- \cos \varphi)}{8 \cos^2 \varphi + 3v^2 \sin^2 \varphi},$$

$$\Theta = \sqrt{(v_{max}^2 - v^2) \left(v_{max}^2 - v^2 + \sin \varphi \sqrt{1 - \frac{\cos^2 \varphi}{9}} \right)}.$$

The maximal group-velocity appearing in the integral from Eq. (5.24) reads

$$v_{max} = \sqrt{\frac{3 - \cos^2 \varphi - \sin \varphi \sqrt{9 - \cos^2 \varphi}}{6}}.$$

In the previous chapter, we have derived the relations for the trapping probability. The final expression obtained for the trapping probability amplitude vector is given by

$$\psi_\infty(x) = \lim_{t \rightarrow \infty} \psi(x, t) = \frac{1}{2\pi} e^{-ixk} \int_{-\pi}^{\pi} dk (v_1(k), \psi_0) v_1(k). \quad (5.26)$$

The probability can be calculated with the help of the contour integration as shown at the end of the previous chapter. Nevertheless, this time we are lucky since we can avoid it and use previous results. One can easily check that vectors in Eq. (5.21) are equal to Eq. (5.11) with the parameter $\rho = \frac{1}{\sqrt{3}}$. This choice of ρ corresponds to the Grover matrix (1.9). The same holds for the vector $v_1(k)$ in Eq. (5.20). From this follows that the trapping probability

$$p_\infty(x) = \|\psi_\infty(x)\|^2$$

is the same as for the Grover walk, which means that it is completely independent of the parameter φ . Thus, it is sufficient to choose $\rho = \frac{1}{\sqrt{3}}$ in Eq. (5.16) and change the coefficients $g_j \rightarrow q_j$,

$$p_\infty(x) = \begin{cases} 12(5 - 2\sqrt{6})^{2x} |q_1 + q_3|^2 & \text{for } x > 0 \\ (5 - 2\sqrt{6})(3|q_1|^2 + 2|q_3|^2) & \text{for } x = 0 \\ 12(5 - 2\sqrt{6})^{|2x|} |q_1 - q_3|^2 & \text{for } x < 0 \end{cases} \quad (5.27)$$

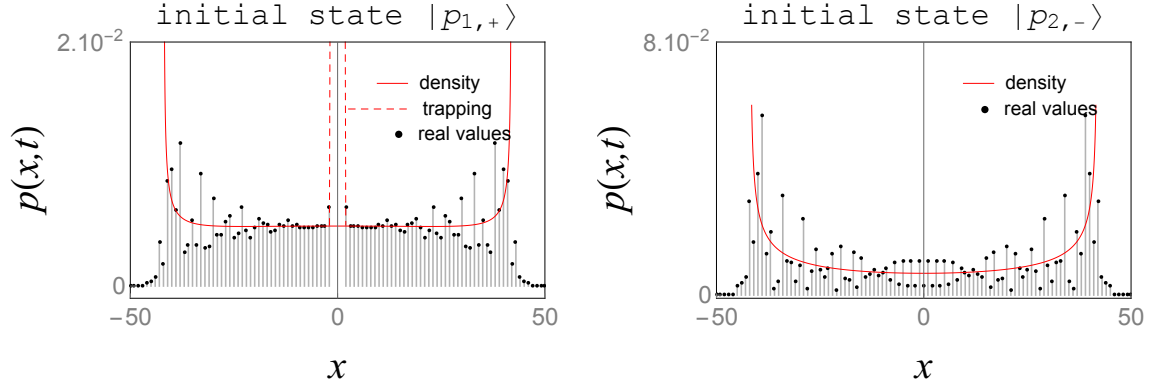
One can check that

$$\int_{-v_{max}}^{v_{max}} f(v) dv + \sum_x p_\infty(x) = 1 \quad (5.28)$$

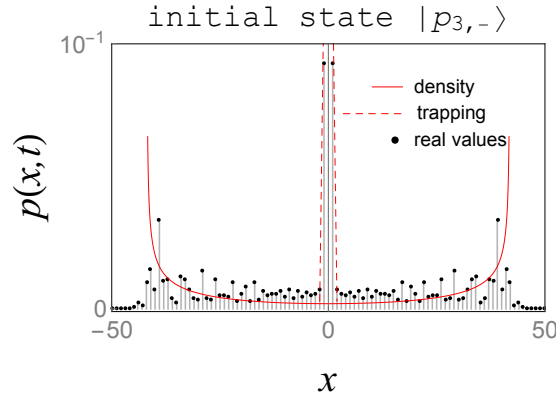
and thus the normalization of the total probability to one is satisfied.

Let us discuss some interesting regimes. For instance we see that the choice of the initial coin state $|\psi_C\rangle = |p_{2,-}\rangle$, i.e. $q_{1,3} = 0, q_2 = 1$ results in the absence of the trapping at the origin, as depicted in the Fig. (5.2b). Further, we can again cancel one half of the trapping peak with the choice $q_1 = \pm q_3$. And most importantly, although the expression of the velocity density is quite complicated in this case, the trapping probability expression is very simple. This suggest that the basis formed by the eigenvectors of the coin is a convenient choice. Behaviour of the walk is for several initial states depicted in Fig. 5.2.

One might be interested, why exactly the eigenvector basis is the suitable one and whether we can apply this construction of the new basis for other types of walks as well. The interesting point here is that one eigenvector of the coins $C_{1,2}(\rho(\varphi))$ is in both cases orthogonal to the eigenvector $v_1(k)$ corresponding to the constant eigenvalue of the evolution operator in the Fourier picture $\tilde{U}(k)$. The eigenvector $v_1(k)$ is the only one that appears in the calculation of the trapping probability amplitude Eq. (3.21). The question whether the basis formed by the eigenvector is always a good choice will be analysed more in the next section. Here we only reveal that even though the eigenvector basis is always better than the standard one, it is not necessarily the right one. Nevertheless, there is a connection of the suitable basis and the eigenvectors of the coin.



(a) Probability distribution for the initial state $|p_{1,+}\rangle$ from Eq. (5.21). For this choice of the initial state, trapping peak appears. (b) Probability distribution for the initial state $|p_{2,-}\rangle$ from Eq. (5.21). For this choice of the initial state, central peak disappears.



(c) Probability distribution for the initial state $|p_{3,-}\rangle$ from Eq. (5.21). For this choice there exist all travelling peaks as well as the trapping peak.

Figure 5.2: Probability distributions for the quantum walk with $C_{def_1}^{(3)}(\varphi)$ coin, Eq. (5.17). The initial states are eigenstates of the coin $C_{def_1}^{(3)}(\varphi)$, which form the suitable basis. Parameter φ is chosen as $\frac{\pi}{4}$ and the total number of steps is $t = 100$. The figures show only relevant region bounded by the travelling peaks. By changing the initial state we can control the dominant peaks present in the distribution. Red solid line corresponds to the group velocity density, Eq. (5.25), and red dashed line to the trapping probability, Eq. (5.27). Black dots are probabilities coming from the numerical simulation. It is seen that even for smaller number of steps, the approximative distributions work quite well.

5.3 Velocity density for the Wigner rotation matrices

This section is devoted to the model of quantum walks introduced in Sec. (1.1.2) and its limiting distribution. We will find the suitable coin space basis in which the distribution gains the simplest form and point out interesting regimes. In the previous chapter, the basis was composed of the eigenvectors of the coin. Here the situation is different and there exist a more convenient basis than the one generated by the eigenvectors. We will provide connection of the suitable basis with the shape of the probability distribution, which results in a recipe for the construction of the suitable basis also for other types of walks.

Wigner walks are defined for any dimension $2j + 1$, where half-integer j describes even state walk and integer j leads to odd number of allowed movements. T. Miyazaki et al. [23] derived a formula for calculating the velocity density for any choice of the dimension parameter j . As is known from Eq. 5.4 and [22], the moments of the particles pseudo-velocity (re-scaled position) are in the limit of large number of steps given by

$$\lim_{t \rightarrow \infty} \left\langle \left(\frac{x}{t} \right)^r \right\rangle = \langle v^r \rangle = \int v^r f^{(j)}(v) dv,$$

where $f^{(j)}(v)$ is the limiting velocity density of $2j + 1$ -dimensional walk. It was shown in [23] that its explicit form is given by

$$f^{(j)}(v) = \sum_{0 < m \leq j} f^{(j,m)}(v), \quad (5.29)$$

where the summation increases m by one and therefore the sum runs over half-integers or integers in dependence on the value of j . The total velocity density is expressed as a sum of individual densities. This indicates that the Wigner walks can be decomposed into several walks spreading through the lattice. The individual walks have different step lengths and thus different velocities as shown in Fig. (1.3). We note that the approximative position probability distribution after large number of steps t results from the limiting density as

$$p^{(j)}(x, t) \approx \frac{2}{t} f^{(j)} \left(\frac{x}{t} \right).$$

The factor of 2 follows from the fact that the Wigner walks are bipartite and thus occupy only half of the positions on a given lattice at each step.

Every density $f^{(j,m)}(v)$ reads

$$f^{(j,m)}(v) = \frac{1}{2m} \mu \left(\frac{v}{2m}, \rho \right) \mathcal{M}^{(j,m)} \left(\frac{v}{2m} \right), \quad (5.30)$$

where μ is the Konno's density function [34, 35] and

$$\mu \left(\frac{v}{2m}, \rho \right) = \frac{\sqrt{1 - \rho^2}}{\pi \left(1 - \left(\frac{v}{2m} \right)^2 \right) \sqrt{\left(\rho - \left(\frac{v}{2m} \right) \right) \left(\rho + \left(\frac{v}{2m} \right) \right)}} \mathbf{I}_{\{|v/2m| \leq |\rho|\}}. \quad (5.31)$$

The function $\mathbf{I}_{\{\bullet\}}$ is the indicator function that is equal to 1 if the condition \bullet is satisfied and 0 otherwise. The condition $|v/2m| \leq |\rho|$ arises from the fact that the velocity v cannot exceed

the maximal group velocity ρ times the length of the step $2m$, where ρ is in absolute value smaller than one (see section 1.1.2). The maximal group velocity corresponds to the velocity of the highest peaks in the probability distribution. Such peaks have the fastest propagation. The individual densities contain also weight functions $\mathcal{M}^{(j,m)}\left(\frac{v}{2m}\right)$, which are polynomials of the degree $2j$ in v .

5.3.1 Divergences of the Konno's density function

In some cases, the Konno's density function, Eq. (5.31), diverges. This occurs for instance in the case of $v = \pm 2m$. Nevertheless, this situation is not very interesting due to the fact that it can happen only for trivial walk. Indeed, let us take for example the two-state Wigner walk. Here $j = m = 1/2$ and thus the indicator function $\mathbf{I}_{|v| \leq |\rho|}$. It follows that the divergence velocity is $v = \pm 1$. One can immediately see that it means movement one step to the right (left) at each time. Such a situation may arise only with coin given by a diagonal unitary matrix that does not mix the coin states (e.g. identity matrix).

The more interesting divergence of μ appears when

$$v = \pm 2m\rho,$$

which is exactly the maximal velocity of spreading of the individual walks and also the extreme of the condition of the indicator function from Eq. (5.31). Since $\mathcal{M}^{(j,m)}\left(\frac{v}{2m}\right)$ in Eq. (5.30) is a polynomial in v , μ contains only divergences which provide the highest increment in the velocity distribution $f^{(j,m)}(v)$ from Eq. 5.30. From the velocity distribution we can easily get approximative position probability distribution. At time t it is given by $\frac{2}{t}f^{(j)}(x/t)$. Note that this approximative distribution provides a good fit only for large values of f . This allows us to formulate the statement that the fastest parts of the distribution correspond to the highest peaks in the position probability distribution and are observed at the points where the Konno's density function diverges. Although we have not mentioned the connection of some divergence to the existence of a probability peak before, the knowledge that the highest peak is the fastest is already known. In section 1.1.1, we showed it using the analogy with wave theory.

From the knowledge of the individual density functions $f^{(j,m)}(v)$, we can easily get rid of some peaks in the probability distribution by a proper choice of the initial state. To do that, we need to cancel divergences of the function μ with the help of the weight function $\mathcal{M}^{(j,m)}\left(\frac{v}{2m}\right)$. This function includes coefficients q_m of the initial coin state $|\psi_C\rangle$ in the standard basis,

$$|\psi_0\rangle = |0\rangle \otimes |\psi_C\rangle = |0\rangle \otimes \sum_{m=-j}^j q_m |m\rangle, \quad (5.32)$$

satisfying normalization condition

$$\sum_{m=-j}^j |q_m|^2 = 1.$$

We will show that the basis providing cancellations of the peaks in the probability distribution will be the suitable one with respect to the limiting density function.

5.3.2 Elimination of the parameter γ

Before turning to the construction of the suitable basis, we would like to simplify our problem as much as possible. The Wigner coins has in general three real parameters, $C_W^{(\alpha, \gamma, \rho)}$. From [23] we know that parameter α do not appear in the formulas for the weight functions $\mathcal{M}^{(j, m)}$ and therefore do not influence the velocity density $f^{(j)}(v)$, Eq. (5.29)

The parameter γ can be easily eliminated as well, since it appears only as an additional phase accompanying parameters q_m forming the initial coin state $|\psi_C\rangle$. From the distribution pattern of the phases we can read out that a rotation of the coin state basis

$$|m\rangle \rightarrow e^{im\gamma}|m\rangle$$

lead to new initial coin state in the form

$$|\psi_C^\gamma\rangle = \sum_{m=-j}^j \underbrace{e^{-im\gamma} q_m}_{\tilde{q}_m} |m\rangle.$$

Indeed, let us look at the explicit results for $j = 1/2$ that is for the two-state Wigner walk. The velocity density

$$f^{(\frac{1}{2})}(v) = \mu(v, \rho) \mathcal{M}^{(\frac{1}{2}, \frac{1}{2})} \quad (5.33)$$

has its weight function given by a polynomial

$$\mathcal{M}^{(\frac{1}{2}, \frac{1}{2})} = 1 + \mathcal{M}_1^{(\frac{1}{2}, \frac{1}{2})} v, \quad (5.34)$$

where

$$\mathcal{M}_1^{(\frac{1}{2}, \frac{1}{2})} = -|q_{1/2}|^2 + |q_{-1/2}|^2 + 2 \frac{\sqrt{1-\rho^2}}{\rho} \Re(q_{1/2} \bar{q}_{-1/2} e^{-i\gamma}). \quad (5.35)$$

The coefficients q_i , $i = \pm 1/2$ comes from Eq. (5.32). A change in the rotated basis, it is plugging

$$q_{\pm 1/2} = e^{\pm i\gamma/2} \tilde{q}_{\pm 1/2}^\gamma \quad (5.36)$$

into the function $\mathcal{M}_1^{(\frac{1}{2}, \frac{1}{2})}$ results in the desired velocity density with the only non-trivial parameter ρ .

Since we have explained and have showed on a simple example that the parameter γ can be easily cancelled, from now on we will assume that $\gamma = 0$.

5.3.3 Construction of the suitable basis

We start with the two-state walk model with $j = 1/2$. The standard basis coin states are $|-1/2\rangle$, $|1/2\rangle$, which denote the movements one step to the right and one step to the left.

From Eqs. (5.33 - 5.36) the complete velocity density in the rotated basis, which is equivalent to the standard basis (and choice $\gamma = 0$), is

$$f^{(\frac{1}{2})}(v) = \frac{\sqrt{1-\rho^2}}{\underbrace{\pi(1-v)^2\sqrt{(\rho-v)(\rho+v)}}_{\mu(v,\rho)}} \times \left(1 + \underbrace{\left(-|q_{1/2}|^2 + |q_{-1/2}|^2 + 2\frac{\sqrt{1-\rho^2}}{\rho}(q_{1/2}\bar{q}_{-1/2} + \bar{q}_{1/2}q_{-1/2}) \right)}_{\mathcal{M}_1^{(\frac{1}{2},\frac{1}{2})}} v \right). \quad (5.37)$$

Here q_m , $m = \pm 1/2$ represent the coefficients of the initial coin state, Eq. (5.32), in the standard basis. It is

$$|\psi_C\rangle = q_{1/2}|1/2\rangle + q_{-1/2}|-1/2\rangle.$$

To get rid of the divergences in the Konno's density $\mu(v, \rho)$, we have to find $q_{\pm 1/2}$ in order to satisfy the equations

$$1 + \mathcal{M}_1^{(\frac{1}{2},\frac{1}{2})} = \frac{\rho \pm v}{\rho}. \quad (5.38)$$

In other words, we have to solve the equations

$$\rho - \rho v(|q_{1/2}|^2 - |q_{-1/2}|^2) + \sqrt{1-\rho^2}(q_{1/2}\bar{q}_{-1/2} + \bar{q}_{1/2}q_{-1/2})v = \rho \pm v.$$

The solutions to these two equations

$$\begin{aligned} \rho + v : \quad & q_{1/2} = \sqrt{\frac{1-\rho}{2}}, \\ & q_{-1/2} = \sqrt{\frac{1+\rho}{2}}, \\ \rho - v : \quad & q_{1/2} = \sqrt{\frac{1+\rho}{2}}, \\ & q_{-1/2} = -\sqrt{\frac{1-\rho}{2}}, \end{aligned}$$

provide the coefficients of the initial coin state that lead to the elimination of divergences in the density $f^{(\frac{1}{2})}(v)$, Eq. (5.37). We denote the eliminating states as

$$\left. \begin{aligned} |\psi_{1/2}^+\rangle &= \sqrt{\frac{1-\rho}{2}}|1/2\rangle - \sqrt{\frac{1+\rho}{2}}|-1/2\rangle, \\ |\psi_{1/2}^-\rangle &= \sqrt{\frac{1+\rho}{2}}|1/2\rangle + \sqrt{\frac{1-\rho}{2}}|-1/2\rangle. \end{aligned} \right\} \text{Suitable basis} \quad (5.39)$$

We claim that these states form the suitable basis of the coin space. Clearly, the vectors form an orthonormal basis. Moreover, the velocity density $f^{(\frac{1}{2})}(v)$, Eq. (5.37) simplifies considerably in this new basis, which we now show.

Let us rewrite the initial state of the walk from using the new basis Eq. (5.39),

$$|\psi_C\rangle = h_{1/2}^-|\psi_{1/2}^+\rangle + h_{1/2}^+|\psi_{1/2}^-\rangle.$$

This leads to relations between coefficients of the standard basis and the suitable basis given by

$$\begin{aligned} q_{1/2} &= h_{1/2}^- \sqrt{\frac{1-\rho}{2}} + h_{1/2}^+ \sqrt{\frac{1+\rho}{2}}, \\ q_{-1/2} &= h_{1/2}^- \sqrt{\frac{1+\rho}{2}} - h_{1/2}^+ \sqrt{\frac{1-\rho}{2}}. \end{aligned} \quad (5.40)$$

Now we can plug these conversion relations into the Eq. (5.35). Let us remind that in this equation we used the fact that γ can be, without loss of generality, set to zero. The conversion of the coefficients results in a simple function

$$\mathcal{M}_1^{(\frac{1}{2}, \frac{1}{2})} = \frac{1}{\rho} (1 - 2|h_{1/2}^+|^2). \quad (5.41)$$

When we plug this relation into the velocity density function, Eq. (5.37), we get a much simpler formula

$$f^{(\frac{1}{2})}(v) = \frac{\sqrt{1-\rho^2} (\rho + (1 - 2|h_{1/2}^+|^2)v)}{\rho\pi(1-v)^2 \sqrt{(\rho-v)(\rho+v)}}.$$

It is also immediately seen that the choice $h_{1/2}^+$ means that the initial coin state $|\psi_C\rangle$ in the suitable state $|\psi_{1/2}^+\rangle$ from Eq. (5.39), cancels the divergence of the $|\psi_{1/2}^+\rangle$ for $v \rightarrow \rho$,

$$f^{(\frac{1}{2})}(v) \Big|_{|\psi_C\rangle=|\psi_{1/2}^+\rangle} = \frac{\sqrt{1-\rho^2} \sqrt{\rho-v}}{\rho\pi(1-v)^2 \sqrt{\rho+v}}.$$

Therefore, the right travelling peak in the position probability distribution is not observed for this choice. The same situation for the left travelling probability peak and divergence $v \rightarrow -\rho$ occurs when $h_{1/2}^+ = 0$, i.e. $|\psi_C\rangle = |\psi_{1/2}^-\rangle$. These situations are illustrated in Fig. (5.3)

5.3.4 Relation of the suitable basis to the eigensystem of the Wigner matrix

For higher dimensional Wigner walks, calculation of the right choice of the coefficients q_m , Eq. (5.32) leading to the cancellation of the divergences in Eq. (5.30) becomes difficult. Therefore it is worth to find an easier way to construct the suitable basis. Motivated by the results for the Grover walk from the previous sections, where the suitable basis was given by the eigenvectors of the Grover matrix, we might assume similar connection here.

Indeed, we can use coin eigenvectors for the suitable basis construction. The eigenvectors of

$$C_W^{(\frac{1}{2})} = \begin{pmatrix} \rho & -\sqrt{1-\rho^2} \\ \sqrt{1-\rho^2} & \rho \end{pmatrix}$$

read

$$\begin{aligned} |\varphi_1^+\rangle &= \frac{1}{\sqrt{2}} (|1/2\rangle - i| -1/2\rangle), \\ |\varphi_1^-\rangle &= \frac{1}{\sqrt{2}} (|1/2\rangle + i| -1/2\rangle) \end{aligned} \quad (5.42)$$

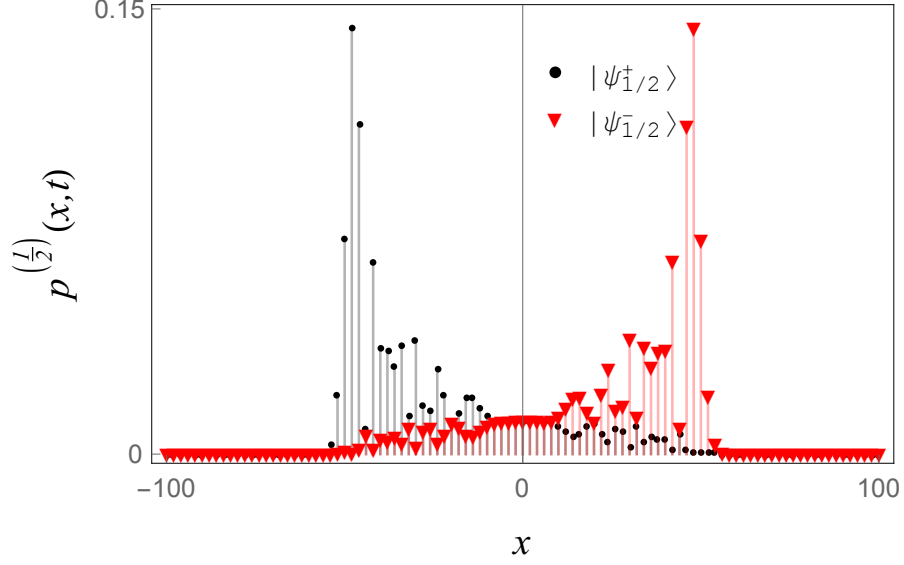


Figure 5.3: Position probability distribution for the two-state Wigner walk after $t = 100$. The initial states are the suitable states $|\psi_{1/2}^\pm\rangle = |\chi_{1/2}^\mp\rangle$ from Eq. (5.39). It is seen that the suitable state as the initial coin state eliminates one of the probability peaks.

and satisfy the eigenvalue equations

$$C_W^{(\frac{1}{2})}|\varphi_1^+\rangle = e^{i\varphi_1}|\varphi_1^+\rangle, \quad C^{(\frac{1}{2})}|\varphi_1^-\rangle = e^{-i\varphi_1}|\varphi_1^-\rangle. \quad (5.43)$$

The phase factor is equal to

$$\varphi_1 = \arccos \rho.$$

The eigenvectors from Eq. (5.42) are clearly different than the suitable basis, Eq. (5.39). Nevertheless, if we take a simple combination of the eigenvectors, Eq. (5.42), and the corresponding eigenvalues in the form

$$\begin{aligned} |\chi_{1/2}^-\rangle &= \frac{1}{\sqrt{2}} \left(e^{-i\frac{\varphi_1}{2}} |\varphi_1^+\rangle - e^{i\frac{\varphi_1}{2}} |\varphi_1^-\rangle \right), \\ |\chi_{1/2}^+\rangle &= \frac{i}{\sqrt{2}} \left(e^{-i\frac{\varphi_1}{2}} |\varphi_1^+\rangle + e^{i\frac{\varphi_1}{2}} |\varphi_1^-\rangle \right) \end{aligned} \quad (5.44)$$

and rewrite it using the standard coin space basis $|\pm 1/2\rangle$ we get that

$$\begin{aligned} |\chi_{1/2}^-\rangle &= \sqrt{\frac{1+\rho}{2}} |1/2\rangle - \sqrt{\frac{1-\rho}{2}} |-1/2\rangle, \\ |\chi_{1/2}^+\rangle &= \sqrt{\frac{1-\rho}{2}} |1/2\rangle + \sqrt{\frac{1+\rho}{2}} |-1/2\rangle. \end{aligned} \quad (5.45)$$

Comparison of Eq. (5.39) with the suitable states from Eq. (5.45) shows that

$$|\chi_{1/2}^\pm\rangle = |\psi_{1/2}^\mp\rangle.$$

We got a suggestion for a new approach for the construction of the suitable basis that can be easily followed also in the case of higher-dimensional Wigner walks. In higher dimensions, we always find $\lfloor (2j+1)/2 \rfloor$ pairs of the coin eigenstates $|\varphi_i^\pm\rangle$, $i = 1, \dots, \lfloor (2j+1)/2 \rfloor$ corresponding to the eigenvalues $e^{\pm i\varphi_i}$ (see Eqs. (5.42, 5.43)). For the odd-state walk we have one more eigenstate $|\varphi_0\rangle$ orthogonal to all the vectors $|\varphi_i^\pm\rangle$.

We can conclude that states $|\chi_{1/2}^\pm\rangle$ from Eq. (5.45) given by the linear combination of the eigenstates $|\varphi_1^\pm\rangle$ from Eq. (5.42) with the help of the corresponding eigenvalues from Eq. (5.43) constitute the suitable basis of the coin space and the Hilbert space can be rewritten as

$$\mathcal{H}_C = \text{Span}\{|\chi_{1/2}^+\rangle, |\chi_{1/2}^-\rangle\}. \quad (5.46)$$

5.3.5 Three-state Wigner walk, $j=1$

In this section we analyse the Wigner walk where $j = 1$ (the three-state Wigner walk). The allowed movements here are, according to the step operator from Eq. (1.25) two steps to the right and left or stay at the actual position. Thus, only even sites are occupied at any time, odd sites are always empty. This only affects the limiting distribution by an additional factor of two,

$$p^{(1)}(x, t) \approx \frac{2}{t} f^{(1)}\left(\frac{x}{t}\right).$$

The standard basis of the coin space is denoted as $|-1\rangle$, $|0\rangle$, $|1\rangle$ and the relevant coin $C_W^{(1)}$ is given by the matrix elements Eq. (1.24) with non-relevant parameters α, γ set to zero. It is

$$C_W^{(1)} = \begin{pmatrix} \rho^2 & -\sqrt{2}\rho\sqrt{1-\rho^2} & 1-\rho^2 \\ \sqrt{2}\rho\sqrt{1-\rho^2} & -1+2\rho^2 & -\sqrt{2}\rho\sqrt{1-\rho^2} \\ 1-\rho^2 & \sqrt{2}\rho\sqrt{1-\rho^2} & \rho^2 \end{pmatrix}. \quad (5.47)$$

This matrix is very similar to the modified Grover coin introduced in subsection 2.2.1 and analysed in more detail from the viewpoint of the limiting distribution in [21, III] and section 5.1. Compared to the modified Grover coin, only two elements have different signs here. Therefore, it is not surprising that these two three-state walk models give the same results as will be checked later.

Following Eq. (5.32) we have for the initial state in the standard basis

$$|\psi_C\rangle = q_{-1}|-1\rangle + q_0|0\rangle + q_1|1\rangle. \quad (5.48)$$

The results of [23] say that in the standard coin space basis, the velocity density reads

$$f^{(1)}(v) = \frac{1}{2}\mu\left(\frac{v}{2}, \rho\right) \mathcal{M}^{(1,1)}\left(\frac{v}{2}\right), \quad (5.49)$$

where $\mathcal{M}^{(1,1)}(v)$ can be expressed as a polynomial in v ,

$$\mathcal{M}^{(1,1)}(v) = \mathcal{M}_0^{(1,1)} + \mathcal{M}_1^{(1,1)}v + \mathcal{M}_2^{(1,1)}v^2.$$

Note that for the two-state Wigner walk the degree of this polynomial was only one. The individual members of the weight function $\mathcal{M}^{(1,1)}(v)$ are given by

$$\begin{aligned}
\mathcal{M}_0^{(1,1)} &= \frac{1}{2} (|q_1|^2 + 2|q_0|^2 + |q_{-1}|^2 - q_1\bar{q}_{-1} - \bar{q}_1q_{-1}), \\
\mathcal{M}_1^{(1,1)} &= -|q_1|^2 + |q_{-1}|^2 + \\
&\quad + \frac{\sqrt{1-\rho^2}}{\sqrt{2}\rho} (q_1\bar{q}_0 + \bar{q}_1q_0 + q_0\bar{q}_{-1} + \bar{q}_0q_{-1}), \\
\mathcal{M}_2^{(1,1)} &= \frac{1}{2} (|q_1|^2 - 2|q_0|^2 + |q_{-1}|^2) - \\
&\quad - \frac{\sqrt{1-\rho^2}}{\sqrt{2}\rho} (q_1\bar{q}_0 + \bar{q}_1q_0 - q_0\bar{q}_{-1} - \bar{q}_0q_{-1}) + \\
&\quad + \frac{2-\rho^2}{2\rho^2} (q_1\bar{q}_{-1} + \bar{q}_1q_{-1}). \tag{5.50}
\end{aligned}$$

Let us note that the suitable basis of the coin space can be constructed similarly as in previous subsection, Eq. (5.44), by a linear combination of the eigenstates of the coin $C_W^{(1)}$. In the three-state case, we need one more suitable vector $|\varphi_0\rangle$ which will complete the orthonormal basis. The eigenvectors of the three-dimensional Wigner coin $C_W^{(1)}$, Eq. (5.47), read

$$\begin{aligned}
|\varphi_0\rangle &= \frac{1}{\sqrt{2}}(|1\rangle + |-1\rangle), \\
|\varphi_1^-\rangle &= \frac{1}{2}(-i|1\rangle + \sqrt{2}|0\rangle + i|-1\rangle), \\
|\varphi_1^+\rangle &= \frac{1}{2}(i|1\rangle + \sqrt{2}|0\rangle - i|-1\rangle)
\end{aligned}$$

and satisfy the eigenvalue equations

$$\begin{aligned}
C_W^{(1)}|\varphi_0\rangle &= |\varphi_0\rangle, \\
C_W^{(1)}|\varphi_1^-\rangle &= e^{-i\varphi_1}|\varphi_1^-\rangle, \\
C_W^{(1)}|\varphi_1^+\rangle &= e^{i\varphi_1}|\varphi_1^+\rangle,
\end{aligned}$$

with the phase factor

$$\varphi_1 = \arccos(2\rho^2 - 1).$$

Two elements of the suitable basis are given by a linear combination of the eigenvectors having the eigenvalues with the same phase, i.e. states $|\varphi_1^\pm\rangle$. We need one more state to complete the new orthonormal basis. Since $|\varphi_0\rangle, |\varphi_1^-\rangle, |\varphi_1^+\rangle$ are orthogonal, $|\varphi_0\rangle$ will be orthogonal to any linear combination of $|\varphi_1^\pm\rangle$ and therefore, directly $|\varphi_0\rangle$ can be chosen as the third element of the new basis.

Thus the suitable basis of the coin space

$$\mathcal{H}_C = \text{Span}\{|\chi_0\rangle, |\chi_1^+\rangle, |\chi_1^-\rangle\} \tag{5.51}$$

is formed by the states

$$\begin{aligned} |\chi_0\rangle &= |\varphi_0\rangle, \\ |\chi_1^+\rangle &= \frac{1}{\sqrt{2}} \left(e^{-i\frac{\varphi}{2}} |\varphi_1^+\rangle + e^{i\frac{\varphi}{2}} |\varphi_1^-\rangle \right), \\ |\chi_1^-\rangle &= \frac{i}{\sqrt{2}} \left(e^{-i\frac{\varphi}{2}} |\varphi_1^+\rangle - e^{i\frac{\varphi}{2}} |\varphi_1^-\rangle \right). \end{aligned}$$

These states can be rewritten in the standard basis as

$$\begin{aligned} |\chi_0\rangle &= \frac{1}{\sqrt{2}} (|1\rangle + |-1\rangle), \\ |\chi_1^+\rangle &= \sqrt{\frac{1-\rho^2}{2}} |1\rangle + \rho |0\rangle - \sqrt{\frac{1-\rho^2}{2}} |-1\rangle, \\ |\chi_1^-\rangle &= \frac{\rho}{\sqrt{2}} |1\rangle - \sqrt{1-\rho^2} |0\rangle - \frac{\rho}{\sqrt{2}} |-1\rangle, \end{aligned}$$

and the initial coin state in the new basis reads

$$|\psi_C\rangle = h_0 |\chi_0\rangle + h_1^+ |\chi_1^+\rangle + h_1^- |\chi_1^-\rangle. \quad (5.52)$$

The new basis allows us to find relations between the initial state in the standard and the suitable basis, Eqs. (5.48, 5.52). These relations can be expressed through the initial state coefficients as

$$\begin{aligned} q_1 &= \frac{1}{\sqrt{2}} h_0 + h_1^+ \sqrt{\frac{1-\rho^2}{2}} + h_1^- \frac{\rho}{2}, \\ q_0 &= h_1^+ \rho - h_1^- \sqrt{1-\rho^2}, \\ q_{-1} &= \frac{1}{\sqrt{2}} h_0 - h_1^+ \sqrt{\frac{1-\rho^2}{2}} - h_1^- \frac{\rho}{2}. \end{aligned}$$

Once these relations are inserted into Eq. (5.50) the weight elements gain the following simple form

$$\begin{aligned} \mathcal{M}_0^{(1,1)} &= |h^+|^2 + |h^-|^2, \\ \mathcal{M}_1^{(1,1)} &= -\frac{1}{\rho} (h_0 \bar{h}^- + \bar{h}_0 h^-), \\ \mathcal{M}_2^{(1,1)} &= \frac{1}{\rho^2} (|h_0|^2 - |h^+|^2). \end{aligned}$$

Now we can check that the basis we have chosen, Eq. (5.51) is really suitable. We do that by comparing the elements $\mathcal{M}_{0,1,2}^{(1,1)}$ with the results for the eigenvalue family derived in section 5.1. Indeed, Eq. (5.53) and the results for $d_{0,1,2}$ of the modified Grover coin, Eq. (5.14) are the same. To see it we have to ignore the factor two in $d_{0,1,2}$ since for the Wigner walk it is a part of the Konno's density $\mu(\frac{v}{2}, \rho)$, Eq. (5.49). We also have to employ the normalization condition $|h_0|^2 + |h_1^+|^2 + |h_1^-|^2 = 1$ and the correspondence $h_0 \rightarrow g_3$, $h_1^- \rightarrow g_2$.

As for the Grover and the modified Grover walk, the velocity density does not fully describe the total probability distribution. Three-state quantum walk with Wigner coin exhibits

trapping at the vicinity of the origin as well as the modified Grover walk (its eigenvector deformation). The process of calculation of the trapping is described in [III] and subsection 5.1. It is not surprising that even for the trapping probability we get the same results as for the eigenvector deformation of the Grover walk. The only difference here is that the odd sides of the lattice are empty. Therefore

$$p_\infty(2x) = \begin{cases} \nu^{2|x|} \frac{2(1-\rho^2)}{\rho^4} |h_0 - h_1^+|^2, & x < 0, \\ \frac{\nu}{\rho^2} ((1-\rho^2)|h_0|^2 + |h_1^+|^2), & x = 0, \\ \nu^{2x} \frac{2(1-\rho^2)}{\rho^4} |h_0 + h_1^+|^2, & x > 0, \end{cases} \quad (5.53)$$

where we have denoted

$$\nu = \frac{2 - \rho^2 - 2\sqrt{1 - \rho^2}}{\rho^2}.$$

It is seen that the choices $h_0 = \pm h_1^+$ set the trapping probability either for positive or for negative positions of x to zero. This situation is depicted in Fig. (5.6). It follows that such a property can be used for another simplification of the trapping probability from Eq. (5.53). We emphasize that here we are talking only about further simplification of the trapping probability and not of the limiting density, for which the suitable basis is clear.

The initial state ignoring left half of the trapping peak is of the form

$$|\psi_C\rangle = |\lambda_1^+\rangle = \frac{1}{\sqrt{2}} (|\chi_0\rangle + |\chi_1^+\rangle).$$

Similarly, the state

$$|\psi_C\rangle = |\lambda_1^-\rangle = \frac{1}{\sqrt{2}} (|\chi_0\rangle - |\chi_1^+\rangle)$$

shows trapping only for negative positions of x . Moreover, states $|\lambda^+\rangle, |\lambda^-\rangle$ are orthogonal. Therefore we are allowed to use them as a basis in the subspace of the coin space affecting trapping and decompose the initial coin state as

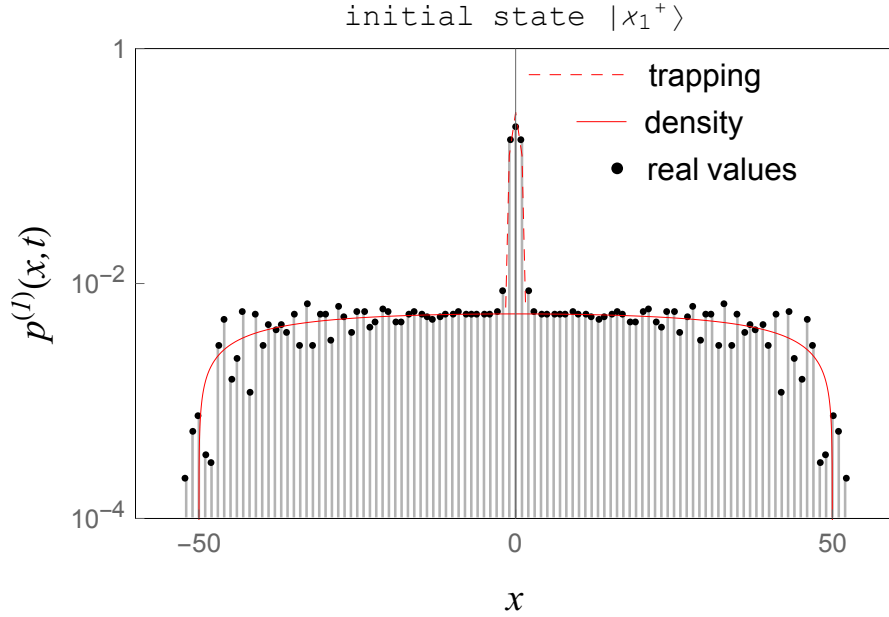
$$|\psi_C\rangle = l_1^+ |\lambda_1^+\rangle + l_1^- |\lambda_1^-\rangle + h_1^- |\chi_1^-\rangle.$$

Here $|\chi_1^-\rangle$ completes the orthonormal basis. We find that the trapping probability turns into

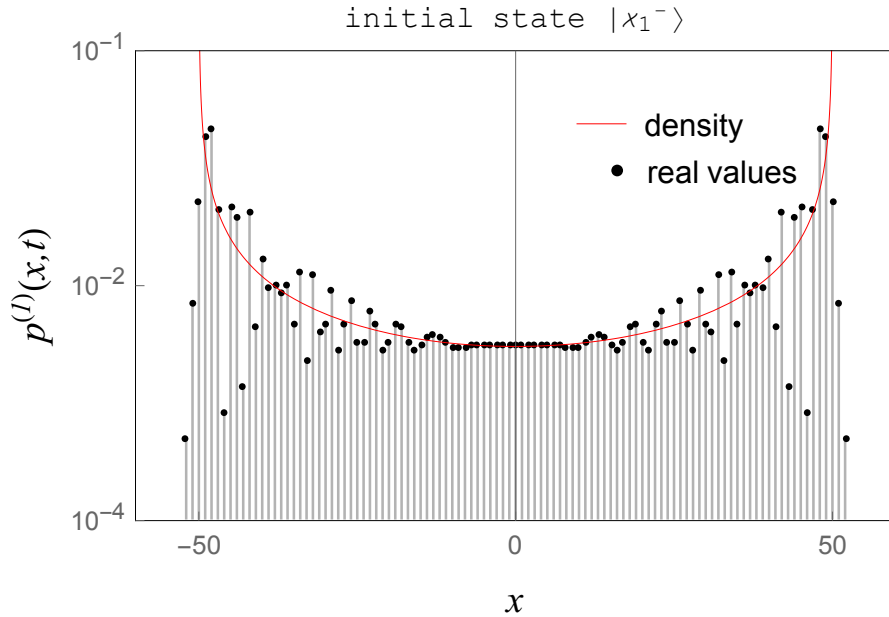
$$p_\infty(2x) = \begin{cases} Q^{2|x|} \frac{2(1-\rho^2)}{\rho^4} |l_1^-|^2, & x < 0, \\ \frac{Q}{\rho^2} \left(|l_1^+|^2 + |l_1^-|^2 - \frac{1}{2\rho^2} |l_1^+ + l_1^-|^2 \right), & x = 0, \\ Q^{2x} \frac{2(1-\rho^2)}{\rho^4} |l_1^+|^2, & x > 0. \end{cases}$$

This additional change of the basis affecting trapping will become more interesting for models with larger values of j .

Note that the suitable basis does not have the same effect on the probability distribution as for the two-state walk with suitable states eliminating left or right probability peak. For

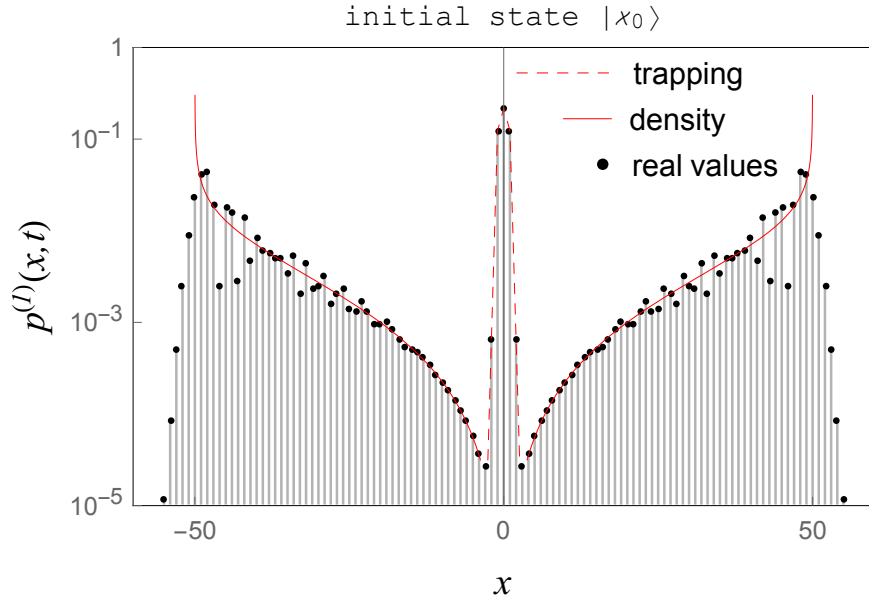


(a) For this initial state, both travelling peaks disappear, but trapping is observed.

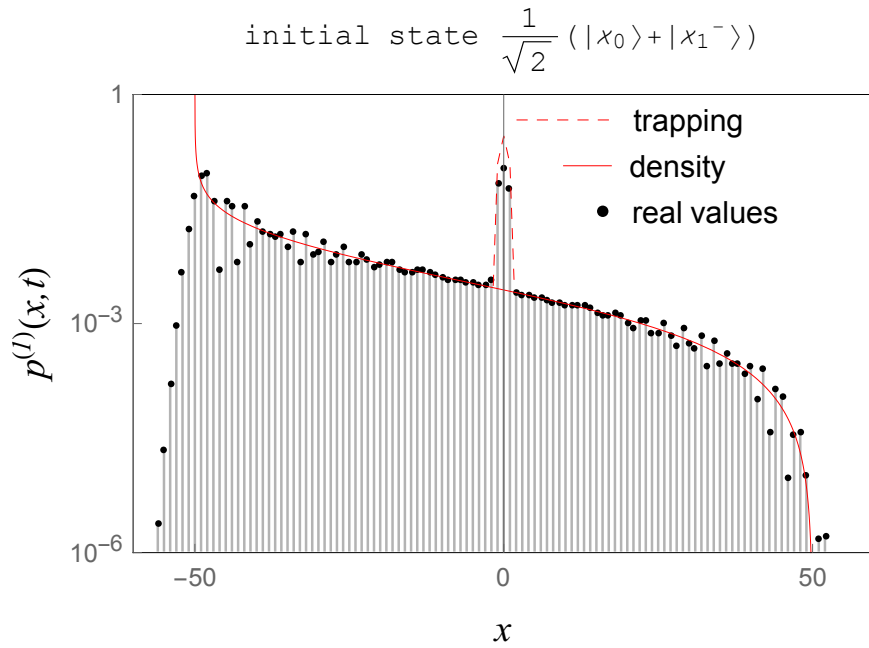


(b) Here we see the opposite situation to the previous figure. For this initial state, trapping is not observed and both travelling peaks are present.

Figure 5.4: Spreading of the three-state Wigner walk after $t = 100$ steps. The initial coin state was chosen as the suitable states $|\chi_1^\pm\rangle$ and the coin parameter is $\rho = 0.5$. This initial state eliminates both travelling peaks or the trapping peak. Red solid line is the approximative distribution arising from the limiting density, red dashed line trapping probability and black dots probabilities coming from simulation of the time evolution. Due to significant difference in heights of the trapping and the travelling peaks, we use a logarithmic scale on the y -axis.



(a) For this suitable state as the initial state of the walk, all the peaks are present.



(b) Simple linear combination of the suitable states gives an initial state which eliminates only one travelling peak.

Figure 5.5: Spreading of the three-state Wigner walk after $t = 100$ steps. The initial coin state was chosen as the suitable state $|\chi_0\rangle$ and a combination of the suitable states $\frac{1}{\sqrt{2}}(|\chi_0\rangle + |\chi_1^-\rangle)$. Coin parameter is $\rho = 0.5$. The initial states eliminate none of the travelling peaks or one travelling peak, which is similar to the two-state Wigner walk with the initial state equals the suitable state. Red solid line is the approximative distribution arising from the limiting density, red dashed line trapping probability and black dots probabilities coming from simulation of the time evolution. Due to significant difference in heights of the trapping and the travelling peaks, we use a logarithmic scale on the y -axis.

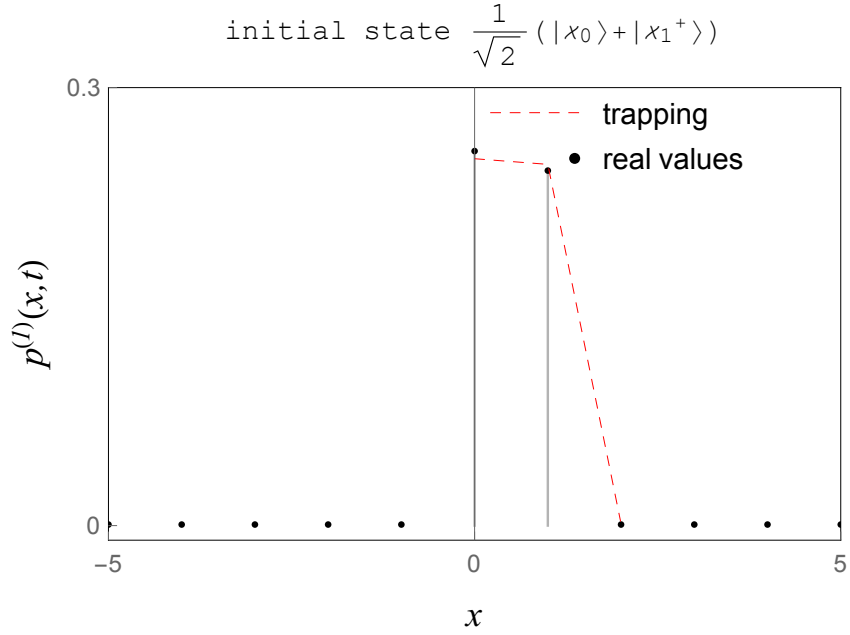


Figure 5.6: Detail of the trapping peak after $t = 500$ steps and for the coin parameter $\rho = 0.5$. The initial coin state $\frac{1}{\sqrt{2}}(|\chi_0\rangle + |\chi_1^+\rangle)$ eliminates half of the trapping peak. Red dashed line corresponds to the limiting trapping probability and black dots are exact probabilities for a given number of steps. We can see that the trapping probability fits quite well.

the three-state Wigner walk, the position probability distributions with the suitable initial states are depicted in the Figs. (5.4a-5.5a). It is seen that the initial state $|\psi_C\rangle = |\chi_1^-\rangle$ eliminates the central non-moving peak. Next, the state $|\chi_1^+\rangle$ eliminates both left and right travelling peaks and preserves the presence of the central trapping peak. The last state $|\chi_0\rangle$ was chosen as an orthogonal complement to states $|\chi_1^\pm\rangle$ and maintains all three position probability peaks. Nevertheless, it is not difficult to find a new basis whose two constituting states eliminate either the left or the right probability peak similarly to the two-state walk. These states are

$$\begin{aligned}
 |\eta^+\rangle &= \frac{1}{\sqrt{2}}(|\chi_0\rangle + |\chi_1^-\rangle) \\
 |\eta^-\rangle &= \frac{1}{\sqrt{2}}(|\chi_0\rangle - |\chi_1^-\rangle).
 \end{aligned}$$

The orthogonal complement to these states is the suitable state $|\chi_1^+\rangle$, which eliminates both travelling peaks. The basis $\{|\eta^+\rangle, |\eta^-\rangle, |\chi_1^+\rangle\}$ brings the initial coin state into the form

$$|\psi_C\rangle = n^+|\eta^+\rangle + n^-|\eta^-\rangle + h^+|\chi_1^+\rangle$$

and therefore

$$\begin{aligned}\mathcal{M}_0^{(1,1)} &= 1 + |h^+|^2 + \frac{1}{2}(n^+\overline{n^-} + n^+\overline{n^-}), \\ \mathcal{M}_1^{(1,1)} &= -\frac{1}{\rho}(|n^+|^2 - |n^-|^2), \\ \mathcal{M}_2^{(1,1)} &= \frac{1}{\rho^2}(1 - \frac{3}{2}|h^+|^2 - \frac{1}{2}(n^+\overline{n^-} + n^+\overline{n^-})).\end{aligned}$$

From the comparison with the results in the suitable basis, Eq. (5.44), we see that now we have a more complicated result. Even through the suitable basis influence the probability distribution in a different way than we expected from the two-state walk, it is truly the convenient choice. Nevertheless, basis $\{|\eta^+\rangle, |\eta^-\rangle, |\chi_1^+\rangle\}$ is still more convenient choice than the standard basis $\{|-1\rangle, |0\rangle, |1\rangle\}$.

5.3.6 Higher dimensions

We summarize the results for the four and five-state Wigner walks. In appendix A.3 we provide result also for the six-state Wigner walk. We use the construction of the new basis described in the previous subsection. Some technical details are omitted and one can find them in the appendix. It was shown that we have to distinguish between even and odd state walks during the construction of the suitable basis.

Four-state walk

The choice of $j = 3/2$ leads to a four-state walk. Since the allowed movements are three steps to the left (right) and one step to the left (right), the walk jumps between even and odd positions on the lattice. The coin states in the standard basis read

$$|-3/2\rangle, |-1/2\rangle, |1/2\rangle, |3/2\rangle.$$

The initial state in the standard basis is given by

$$|\psi_C\rangle = q_{3/2}|3/2\rangle + q_{1/2}|1/2\rangle + q_{-1/2}|-1/2\rangle + q_{-3/2}|-3/2\rangle$$

and satisfies the normalization condition

$$\sum_{j=-3/2}^{3/2} |q_j|^2 = 1.$$

The four-dimensional Wigner coin whose matrix elements are given by Eq. (1.24) has the form

$$C_W^{(\frac{3}{2})} = \begin{pmatrix} \rho^3 & -\sqrt{3}\rho^2\sqrt{1-\rho^2} & \sqrt{3}\rho(1-\rho^2) & -(1-\rho^2)^{\frac{3}{2}} \\ \sqrt{3}\rho^2\sqrt{1-\rho^2} & \rho(3\rho^2-2) & (1-3\rho^2)\sqrt{1-\rho^2} & \sqrt{3}\rho(1-\rho^2) \\ \sqrt{3}\rho(1-\rho^2) & -\sqrt{1-\rho^2}(1-3\rho^2) & \rho(3\rho^2-2) & -\sqrt{3}\rho^2\sqrt{1-\rho^2} \\ (1-\rho^2)^{\frac{3}{2}} & \sqrt{3}\rho(1-\rho^2) & \sqrt{3}\rho^2\sqrt{1-\rho^2} & \rho^3 \end{pmatrix}$$

and parameter ρ corresponding to the velocity of spreading ranges from zero to one. To construct the suitable basis we need the eigenvectors of $C_W^{(\frac{3}{2})}$ that are

$$\begin{aligned} |\varphi_1^+\rangle &= \frac{1}{\sqrt{8}}(\sqrt{3}|3/2\rangle - i|1/2\rangle + |-1/2\rangle - i\sqrt{3}|-3/2\rangle), \\ |\varphi_1^-\rangle &= \frac{1}{\sqrt{8}}(\sqrt{3}|3/2\rangle + i|1/2\rangle + |-1/2\rangle + i\sqrt{3}|-3/2\rangle), \\ |\varphi_2^+\rangle &= \frac{1}{\sqrt{8}}(|3/2\rangle + i\sqrt{3}|1/2\rangle - \sqrt{3}|-1/2\rangle - i|-3/2\rangle), \\ |\varphi_2^-\rangle &= \frac{1}{\sqrt{8}}(|3/2\rangle - i\sqrt{3}|1/2\rangle - \sqrt{3}|-1/2\rangle + i|-3/2\rangle). \end{aligned}$$

The corresponding eigenvalue equations read

$$\begin{aligned} C_W^{(\frac{3}{2})}|\varphi_1^-\rangle &= e^{-i\varphi_1}|\varphi_1^-\rangle, & C_W^{(\frac{3}{2})}|\varphi_1^+\rangle &= e^{i\varphi_1}|\varphi_1^+\rangle, \\ C_W^{(\frac{3}{2})}|\varphi_2^-\rangle &= e^{-i\varphi_2}|\varphi_2^-\rangle, & C_W^{(\frac{3}{2})}|\varphi_2^+\rangle &= e^{i\varphi_2}|\varphi_2^+\rangle, \end{aligned}$$

where the phases are given by

$$\begin{aligned} \varphi_1 &= \arccos \rho, \\ \varphi_2 &= \begin{cases} \arccos(\rho(4\rho^2 - 3)), & 0 < \rho \leq \frac{1}{2}, \\ 2\pi - \arccos(\rho(4\rho^2 - 3)), & \frac{1}{2} < \rho \leq 1. \end{cases} \end{aligned}$$

In the construction of the suitable basis we mix only the eigenvectors corresponding to the same phase factor φ_1 or φ_2 . It means that we assume the suitable basis in the form

$$\begin{aligned} |\chi_1^+\rangle &= \frac{1}{\sqrt{2}}(e^{-i\frac{\varphi_1}{2}}|\psi_1^+\rangle + e^{i\frac{\varphi_1}{2}}|\psi_1^-\rangle), \\ |\chi_1^-\rangle &= \frac{i}{\sqrt{2}}(e^{-i\frac{\varphi_1}{2}}|\psi_1^+\rangle - e^{i\frac{\varphi_1}{2}}|\psi_1^-\rangle), \\ |\chi_2^+\rangle &= \frac{1}{\sqrt{2}}(e^{-i\frac{\varphi_2}{2}}|\psi_2^+\rangle + e^{i\frac{\varphi_2}{2}}|\psi_2^-\rangle), \\ |\chi_2^-\rangle &= \frac{i}{\sqrt{2}}(e^{-i\frac{\varphi_2}{2}}|\psi_2^+\rangle - e^{i\frac{\varphi_2}{2}}|\psi_2^-\rangle) \end{aligned} \quad (5.54)$$

and the initial coin state is expressed in this basis as

$$|\psi_C\rangle = h_1^+|\chi_1^+\rangle + h_1^-|\chi_1^-\rangle + h_2^+|\chi_2^+\rangle + h_2^-|\chi_2^-\rangle.$$

One can rewrite this initial state in the standard basis and obtain transformation relation between the standard coefficients q_n , $n = -3/2, \dots, 3/2$ and the suitable coefficients $h_{1,2}^\pm$. One can find these relations in appendix A.1.

The total velocity density is a sum of two densities, as stated for example in Eq. (5.29). Therefore,

$$f^{(\frac{3}{2})}(v) = f^{(\frac{3}{2}, \frac{1}{2})}(v) + f^{(\frac{3}{2}, \frac{3}{2})}(v),$$

with

$$\begin{aligned} f^{(\frac{3}{2}, \frac{1}{2})}(v) &= \mu(v, \rho) \mathcal{M}^{(\frac{3}{2}, \frac{1}{2})}(v), \\ f^{(\frac{3}{2}, \frac{3}{2})}(v) &= \frac{1}{3} \mu\left(\frac{v}{3}, \rho\right) \mathcal{M}^{(\frac{3}{2}, \frac{3}{2})}\left(\frac{v}{3}\right). \end{aligned} \quad (5.55)$$

Each of these densities has two divergent points and thus the position probability distribution exhibits maximally four probability peaks corresponding to the divergences of the Konno's density functions $\mu(v, \rho), \mu\left(\frac{v}{3}, \rho\right)$.

For $m = \frac{1}{2}$, the weight function from Eq. (5.55) is equal to

$$\mathcal{M}^{(\frac{3}{2}, \frac{1}{2})}(v) = \mathcal{M}_0^{(\frac{3}{2}, \frac{1}{2})} + \mathcal{M}_1^{(\frac{3}{2}, \frac{1}{2})}v + \mathcal{M}_2^{(\frac{3}{2}, \frac{1}{2})}v^2 + \mathcal{M}_3^{(\frac{3}{2}, \frac{1}{2})}v^3,$$

which can be expressed in the new suitable basis with the help of the transformation relations from Eq. (A.1) and results from [23] as

$$\begin{aligned} \mathcal{M}_0^{(\frac{3}{2}, \frac{1}{2})} &= |h_1^+|^2 + |h_1^-|^2, \\ \mathcal{M}_1^{(\frac{3}{2}, \frac{1}{2})} &= -\frac{1}{\rho} \left[2(|h_1^+|^2 - |h_1^-|^2) + \frac{\sqrt{3}}{2}(h_1^+ \overline{h_2^+} + \overline{h_1^+} h_2^+ - h_1^- \overline{h_2^-} - \overline{h_1^-} h_2^-) \right], \\ \mathcal{M}_2^{(\frac{3}{2}, \frac{1}{2})} &= -\frac{\sqrt{3}}{4\rho^2} \left[\sqrt{3}(|h_1^+|^2 + |h_1^-|^2 - |h_2^+|^2 - |h_2^-|^2) - (h_1^+ \overline{h_2^+} + \overline{h_1^+} h_2^+ + h_1^- \overline{h_2^-} + \overline{h_1^-} h_2^-) \right], \\ \mathcal{M}_3^{(\frac{3}{2}, \frac{1}{2})} &= \frac{3}{4\rho^3} \left[(3|h_1^+|^2 - 3|h_1^-|^2 + |h_2^+|^2 - |h_2^-|^2) + \sqrt{3}(h_1^+ \overline{h_2^+} + \overline{h_1^+} h_2^+ - h_1^- \overline{h_2^-} - \overline{h_1^-} h_2^-) \right]. \end{aligned}$$

Similarly, the second weight function from Eq. (5.55) for $m = \frac{3}{2}$ is determined as

$$\mathcal{M}^{(\frac{3}{2}, \frac{3}{2})}(v) = \mathcal{M}_0^{(\frac{3}{2}, \frac{3}{2})} + \mathcal{M}_1^{(\frac{3}{2}, \frac{3}{2})}v + \mathcal{M}_2^{(\frac{3}{2}, \frac{3}{2})}v^2 + \mathcal{M}_3^{(\frac{3}{2}, \frac{3}{2})}v^3.$$

Here

$$\begin{aligned} \mathcal{M}_0^{(\frac{3}{2}, \frac{3}{2})} &= |h_2^+|^2 + |h_2^-|^2, \\ \mathcal{M}_1^{(\frac{3}{2}, \frac{3}{2})} &= \frac{\sqrt{3}}{2\rho} (h_1^+ \overline{h_2^+} + \overline{h_1^+} h_2^+ - h_1^- \overline{h_2^-} - \overline{h_1^-} h_2^-), \\ \mathcal{M}_2^{(\frac{3}{2}, \frac{3}{2})} &= \frac{\sqrt{3}}{4\rho^2} \left[\sqrt{3}(|h_1^+|^2 + |h_1^-|^2 - |h_2^+|^2 - |h_2^-|^2) - (h_1^+ \overline{h_2^+} + \overline{h_1^+} h_2^+ + h_1^- \overline{h_2^-} + \overline{h_1^-} h_2^-) \right], \\ \mathcal{M}_3^{(\frac{3}{2}, \frac{3}{2})} &= -\frac{1}{4\rho^3} \left[(3|h_1^+|^2 - 3|h_1^-|^2 + |h_2^+|^2 - |h_2^-|^2) + \sqrt{3}(h_1^+ \overline{h_2^+} + \overline{h_1^+} h_2^+ - h_1^- \overline{h_2^-} - \overline{h_1^-} h_2^-) \right]. \end{aligned}$$

The behaviour of the four-state Wigner walk together with its limiting distribution is depicted in Figs. (5.7 - 5.10) for several choices of the initial coin state.

Five-state walk

For $j = 2$ we have a five-state walk model, which spreads through the lattice performing four and two steps to the left and right. Therefore, the walk occupies only even positions on the lattice. Since the dimension of the walk is odd, the particle has also a possibility to stay at

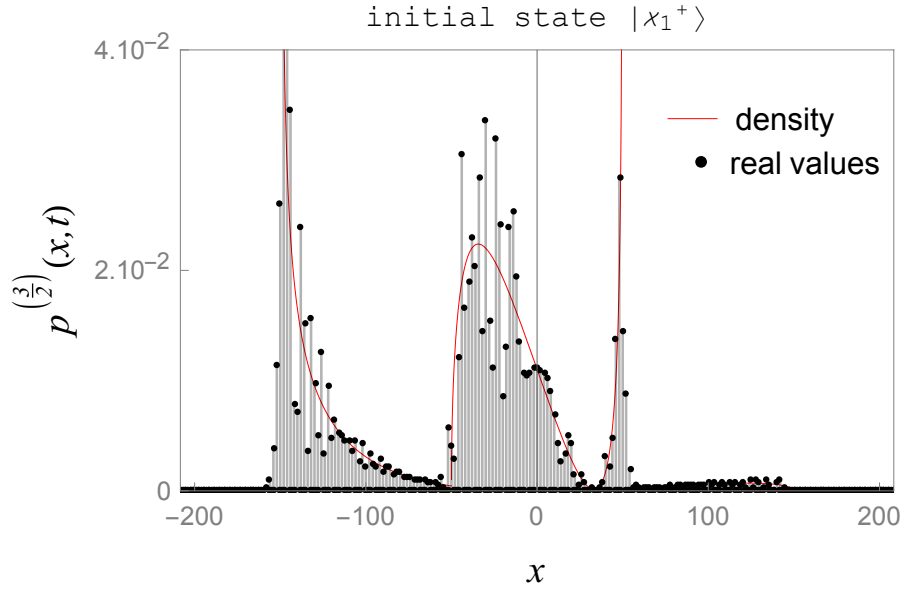


Figure 5.7: Position probability distribution of the four-state Wigner walk on a line. The initial state is the suitable state $|\chi_1^+\rangle$, Eq. (5.54) and the total number of steps $t = 100$. It is seen that in the limit of large number of steps, two probability peaks will be neglected.

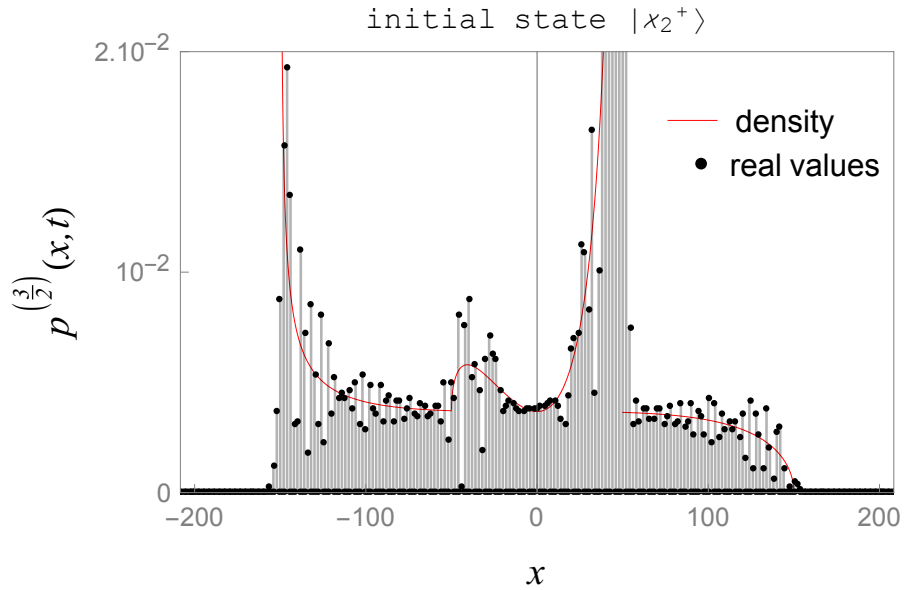


Figure 5.8: Position probability distribution of the four-state Wigner walk on a line. The initial state is the suitable state $|\chi_2^+\rangle$, Eq. (5.54) and the total number of steps $t = 100$. It is seen that in the limit of large number of steps, two of four probability peaks will be neglected.

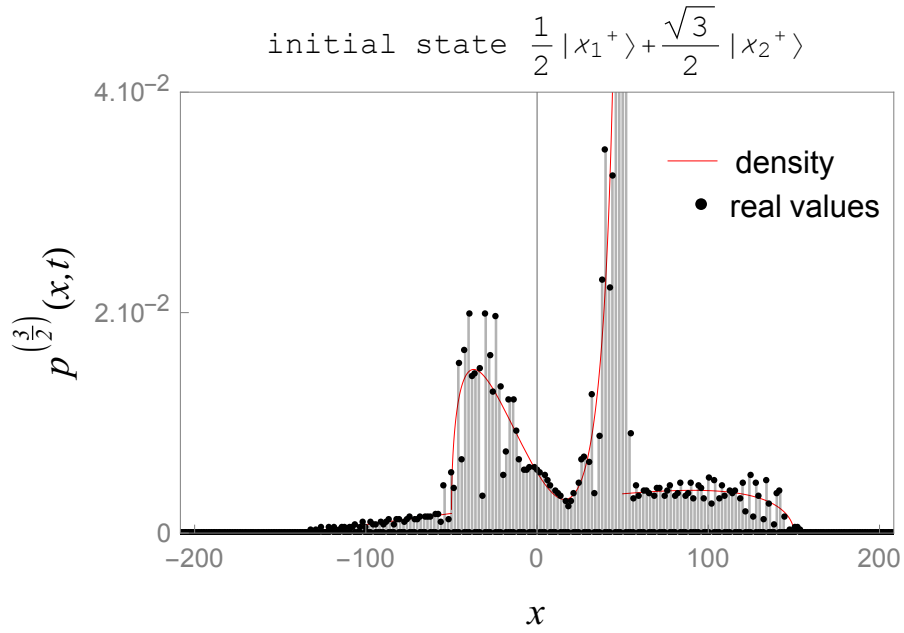


Figure 5.9: Position probability distribution of the four-state Wigner walk on a line. The initial state is a linear combination of the suitable states $|\chi_1^+\rangle, |\chi_2^+\rangle$, Eq. (5.54) and the total number of steps $t = 100$. It is seen that in the limit of large number of steps, both faster peaks vanish.

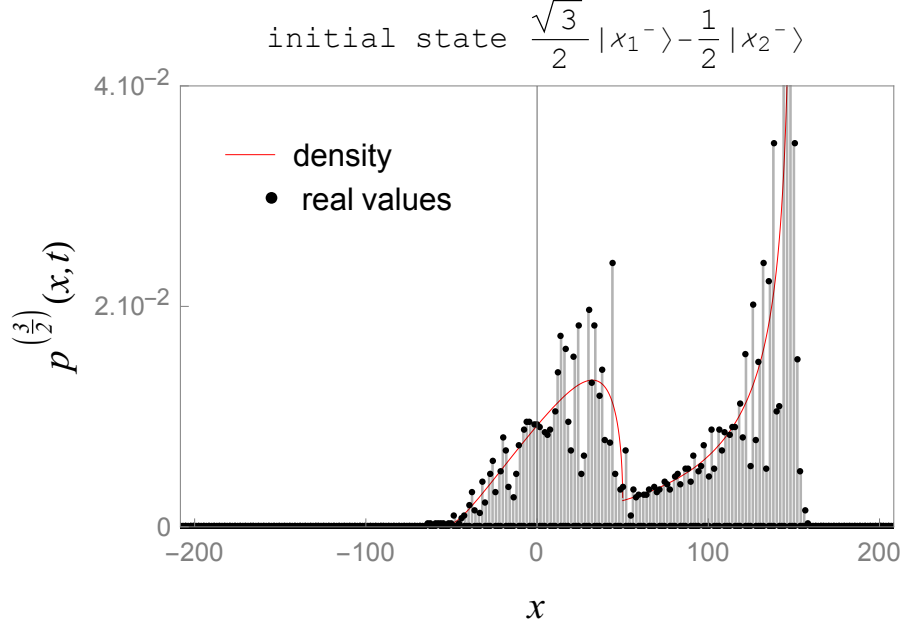


Figure 5.10: Position probability distribution of the four-state Wigner walk on a line. The initial state is a linear combination of the suitable states $|\chi_1^-\rangle, |\chi_2^-\rangle$, Eq. (5.54) and the total number of steps $t = 100$. It is seen that in the limit of large number of steps, both slower peaks vanish.

the actual position as depicted in the Fig. (1.3). The coin space is spanned by the standard basis states

$$\mathcal{H}_C = \text{Span}\{|-2\rangle, |-1\rangle, |0\rangle, |1\rangle, |2\rangle\},$$

and the initial coin state is in the standard basis given by

$$|\psi_C\rangle = q_{-2}|-2\rangle + q_{-1}|-1\rangle + q_0|0\rangle + q_1|1\rangle + q_2|2\rangle.$$

We remind that five-state Wigner walk on a line exhibits trapping at the vicinity of the origin.

The matrix representation of the coin operator is given by a five-dimensional Wigner matrix with matrix elements formulated in Eq. (1.24),

$$C_W^{(2)} = \begin{pmatrix} \rho^4 & -2\sqrt{\mathcal{R}}\rho^3 & \sqrt{6}\mathcal{R}\rho^2 & -2\mathcal{R}^{3/2}\rho & \mathcal{R}^2 \\ 2\sqrt{\mathcal{R}}\rho^3 & \rho^2(4\rho^2 - 3) & \sqrt{6}\sqrt{\mathcal{R}}\rho(1 - 2\rho^2) & -\mathcal{R}(1 - 4\rho^2) & -2\mathcal{R}^{3/2}\rho \\ \sqrt{6}\mathcal{R}\rho^2 & \sqrt{6}\sqrt{\mathcal{R}}\rho(2\rho^2 - 1) & 6\rho^4 - 6\rho^2 + 1 & \sqrt{6}\sqrt{\mathcal{R}}\rho(1 - 2\rho^2) & \sqrt{6}\mathcal{R}\rho^2 \\ 2\mathcal{R}^{3/2}\rho & -\mathcal{R}(1 - 4\rho^2) & \sqrt{6}\sqrt{\mathcal{R}}\rho(2\rho^2 - 1) & \rho^2(4\rho^2 - 3) & -2\sqrt{\mathcal{R}}\rho^3 \\ \mathcal{R}^2 & 2\mathcal{R}^{3/2}\rho & \sqrt{6}\mathcal{R}\rho^2 & 2\sqrt{\mathcal{R}}\rho^3 & \rho^4 \end{pmatrix}$$

and

$$\mathcal{R} = 1 - \rho^2.$$

Its eigenstates can be written as

$$\begin{aligned} |\varphi_0\rangle &= \sqrt{\frac{3}{8}}|2\rangle + \frac{1}{2}|0\rangle + \sqrt{\frac{3}{8}}|-2\rangle, \\ |\varphi_1^+\rangle &= \frac{1}{2}(i|2\rangle + |1\rangle + |-1\rangle - i|-2\rangle), \\ |\varphi_1^-\rangle &= \frac{1}{2}(-i|2\rangle + |1\rangle + |-1\rangle + i|-2\rangle), \\ |\varphi_2^+\rangle &= \frac{1}{4}(|2\rangle + 2i|1\rangle - \sqrt{6}|0\rangle - 2i|-1\rangle + |-2\rangle), \\ |\varphi_2^-\rangle &= \frac{1}{4}(|2\rangle - 2i|1\rangle - \sqrt{6}|0\rangle + 2i|-1\rangle + |-2\rangle) \end{aligned} \quad (5.56)$$

and satisfy the eigenvalue equations of the form

$$\begin{aligned} C_W^{(2)}|\varphi_0\rangle &= |\varphi_0\rangle, \\ C_W^{(2)}|\varphi_1^\pm\rangle &= e^{\pm i\varphi_1}|\varphi_1^\pm\rangle, \\ C_W^{(2)}|\varphi_2^\pm\rangle &= e^{\pm i\varphi_2}|\varphi_2^\pm\rangle. \end{aligned}$$

For the phases of the eigenvalues we have the following expressions

$$\begin{aligned} \varphi_1 &= \arccos(2\rho^2 - 1), \\ \varphi_2 &= \begin{cases} \arccos(8\rho^4 - 8\rho^2 + 1), & 0 < \rho \leq \frac{1}{\sqrt{2}}, \\ 2\pi - \arccos(8\rho^4 - 8\rho^2 + 1), & \frac{1}{\sqrt{2}} < \rho < 1. \end{cases} \end{aligned} \quad (5.57)$$

Similarly as in the case where index $j = 1$, for the construction of the suitable basis, we combine only the eigenvectors with the complex conjugate eigenvalues, i.e. with the same eigenvalue phase factor φ_1 or φ_2 . These combinations provide us four suitable vectors. The last vector of the new basis is given directly by the eigenstate of the coin $C_W^{(2)}$ with real eigenvalue, which is the vector $|\psi_0\rangle$. Hence we get the suitable basis in the form

$$\begin{aligned}
|\chi_0\rangle &= |\varphi_0\rangle, \\
|\chi_1^+\rangle &= \frac{1}{\sqrt{2}} \left(e^{-i\frac{\varphi_1}{2}} |\varphi_1^+\rangle + e^{i\frac{\varphi_1}{2}} |\varphi_1^-\rangle \right), \\
|\chi_1^-\rangle &= \frac{i}{\sqrt{2}} \left(e^{-i\frac{\varphi_1}{2}} |\varphi_1^+\rangle - e^{i\frac{\varphi_1}{2}} |\varphi_1^-\rangle \right), \\
|\chi_2^+\rangle &= \frac{1}{\sqrt{2}} \left(e^{-i\frac{\varphi_2}{2}} |\varphi_2^+\rangle + e^{i\frac{\varphi_2}{2}} |\varphi_2^-\rangle \right), \\
|\chi_2^-\rangle &= \frac{i}{\sqrt{2}} \left(e^{-i\frac{\varphi_2}{2}} |\varphi_2^+\rangle - e^{i\frac{\varphi_2}{2}} |\varphi_2^-\rangle \right).
\end{aligned} \tag{5.58}$$

It allows us to decompose the initial state as

$$|\psi_C\rangle = h_0|\chi_0\rangle + h_1^+|\chi_1^+\rangle + h_1^-|\chi_1^-\rangle + h_2^+|\chi_2^+\rangle + h_2^-|\chi_2^-\rangle.$$

From this initial state expressed in the standard basis follow relations allowing us to rewrite all previous results into the new basis. The relations can be found in appendix A.2.

The total density $f^{(2)}(v)$ is a sum of two densities for the walk with $m = 1$ and the walk with $m = 2$. Therefore

$$f^{(2)}(v) = f^{(2,1)}(v) + f^{(2,2)}(v),$$

where

$$\begin{aligned}
f^{(2,1)}(v) &= \frac{1}{2}\mu\left(\frac{v}{2}\right)\mathcal{M}^{(2,1)}\left(\frac{v}{2}\right), \\
f^{(2,2)}(v) &= \frac{1}{4}\mu\left(\frac{v}{4}\right)\mathcal{M}^{(2,2)}\left(\frac{v}{4}\right).
\end{aligned}$$

The first weight functions can be expressed in the powers of the velocity v as

$$\mathcal{M}^{(2,1)}(v) = \mathcal{M}_0^{(2,1)} + \mathcal{M}_1^{(2,1)}v + \mathcal{M}_2^{(2,1)}v^2 + \mathcal{M}_3^{(2,1)}v^3 + \mathcal{M}_4^{(2,1)}v^4,$$

The particular elements with respect to the standard coin space basis can be found in [23] and, using the relations from Eq. (A.2) read

$$\begin{aligned}
\mathcal{M}_0^{(2,1)} &= |h_1^+|^2 + |h_1^-|^2, \\
\mathcal{M}_1^{(2,1)} &= \frac{1}{\rho} \left[h_1^+ \overline{h_2^-} + \overline{h_1^+} h_2^- + h_2^+ \overline{h_1^-} + \overline{h_2^+} h_1^- + \sqrt{3}(h_0 \overline{h_1^-} + \overline{h_0} h_1^-) \right], \\
\mathcal{M}_2^{(2,1)} &= \frac{1}{\rho^2} \left[3|h_0|^2 - 4|h_1^+|^2 - |h_1^-|^2 + |h_2^+|^2 + |h_2^-|^2 + \sqrt{3}(h_0 \overline{h_2^+} + \overline{h_0} h_2^+) \right], \\
\mathcal{M}_3^{(2,1)} &= -\frac{1}{\rho^3} \left[2(h_1^+ \overline{h_2^-} + \overline{h_1^+} h_2^-) + h_2^+ \overline{h_1^-} + \overline{h_2^+} h_1^- + \sqrt{3}(h_0 \overline{h_1^-} + \overline{h_0} h_1^-) \right], \\
\mathcal{M}_4^{(2,1)} &= -\frac{1}{\rho^4} \left[3|h_0|^2 - 4|h_1^+|^2 + |h_2^+|^2 + \sqrt{3}(h_0 \overline{h_2^+} + \overline{h_0} h_2^+) \right].
\end{aligned}$$

For the second weight function we have

$$\mathcal{M}^{(2,2)}(v) = \mathcal{M}_0^{(2,2)} + \mathcal{M}_1^{(2,2)}v + \mathcal{M}_2^{(2,2)}v^2 + \mathcal{M}_3^{(2,2)}v^3 + \mathcal{M}_4^{(2,2)}v^4,$$

with the individual elements expressed in the suitable basis as

$$\begin{aligned} \mathcal{M}_0^{(2,2)} &= |h_2^+|^2 + |h_2^-|^2, \\ \mathcal{M}_1^{(2,2)} &= -\frac{1}{\rho} \left[h_1^+ \bar{h}_2^- + \bar{h}_1^+ h_2^- + h_1^- \bar{h}_2^+ + \bar{h}_1^- h_2^+ \right], \\ \mathcal{M}_2^{(2,2)} &= \frac{1}{\rho^2} \left[|h_1^+|^2 + |h_1^-|^2 - |h_2^+|^2 - |h_2^-|^2 - \frac{\sqrt{3}}{2} (h_0 \bar{h}_2^+ + \bar{h}_0 h_2^+) \right], \\ \mathcal{M}_3^{(2,2)} &= \frac{1}{2\rho^3} \left[2(h_1^+ \bar{h}_2^- + \bar{h}_1^+ h_2^-) + (h_1^- \bar{h}_2^+ + \bar{h}_1^- h_2^+) + \sqrt{3} (h_0 \bar{h}_1^- + \bar{h}_0 h_1^-) \right], \\ \mathcal{M}_4^{(2,2)} &= \frac{1}{4\rho^4} \left[(3|h_0|^2 - 4|h_1^+|^2 + |h_2^+|^2) + \sqrt{3} (h_0 \bar{h}_2^+ + \bar{h}_0 h_2^+) \right]. \end{aligned}$$

Note that especially the zero-order part $\mathcal{M}_0^{(2,2)}$ depends only on the probabilities of being in the eigenstates corresponding to the eigenvalue phase factor φ_2 , Eq. (5.57). On the other hand, $\mathcal{M}_0^{(2,1)}$ depends only on the probabilities to be in the eigenstates corresponding to the phase factor φ_1 . It is not possible to see similar correspondence for higher order parts.

Let us note that the weight function $\mathcal{M}^{(2,1)}(v)$ describing the inner walk can be set to zero quite easily. Indeed, for the initial coin state

$$|\psi_C\rangle = \frac{1}{2}|\chi_0\rangle - \frac{\sqrt{3}}{2}|\chi_2^+\rangle,$$

all terms $\mathcal{M}_i^{(2,1)}$, $i = 1, \dots, 4$ vanish. Hence, for this initial state the moments of the quantum walk are determined by a single density which reads

$$f^{(2,2)}(v) = \frac{3\sqrt{1-\rho^2}}{16\pi \left(1 - \left(\frac{v}{4}\right)^2\right) \sqrt{\left(\rho - \frac{v}{4}\right) \left(\rho + \frac{v}{4}\right)}}.$$

Here we have demonstrated the power of the initial state which has completely eliminated one of two densities.

The calculation of the trapping probability described in section 5.1 results in

$$p_\infty^{(2)}(2x) = \begin{cases} Q^{2x} 3 \frac{1-\rho^2}{2\rho^4} (|l_0 + f(x)l^+|^2 + |l^+|^2), & x > 0, \\ 9 \frac{1-\rho^2}{4\rho^4} Q^2 (|l^+|^2 + |l^-|^2) + \frac{3}{8} Q^2 |l^+ + l^-|^2 + \frac{2-\rho^2-\sqrt{1-\rho^2}}{4\rho^2} Q |l_0|^2 - \\ \quad - \sqrt{6} \frac{2-r^2+\frac{1}{2}\sqrt{1-r^2}}{8r^2} Q^2 \left((l^+ + l^-) \bar{l}_0 + (\bar{l}^+ + \bar{l}^-) l_0 \right), & x = 0, \\ Q^{2|x|} 3 \frac{1-\rho^2}{2\rho^4} (|l_0 + f(x)l^-|^2 + |l^-|^2), & x < 0. \end{cases} \quad (5.59)$$

Here Q is the same as for the three-state Wigner walk, i.e.

$$Q = \frac{2 - \rho^2 - 2\sqrt{1 - \rho^2}}{\rho^2}$$

and

$$f(x) = \frac{\sqrt{6}}{\rho^2} \left(\rho^2 - 2 + 2|x|\sqrt{1 - \rho^2} \right).$$

Moreover, the coefficients l_0, l^\pm can be expressed by the amplitudes of the initial state in the suitable basis as

$$\begin{aligned} l_0 &= 1/2h_0 - \frac{\sqrt{3}}{2}h_2^+, \\ l^+ &= \sqrt{\frac{3}{8}}h_0 + \frac{1}{\sqrt{2}}h_1^+ + \frac{1}{\sqrt{8}}h_2^+, \\ l^- &= \sqrt{\frac{3}{8}}h_0 - \frac{1}{\sqrt{2}}h_1^+ + \frac{1}{\sqrt{8}}h_2^+. \end{aligned}$$

Figs. (5.11-5.16) depict the trapping probability together with the limiting distribution and the real probabilities calculated for a given number of steps. We have chosen the initial states as the suitable basis states.

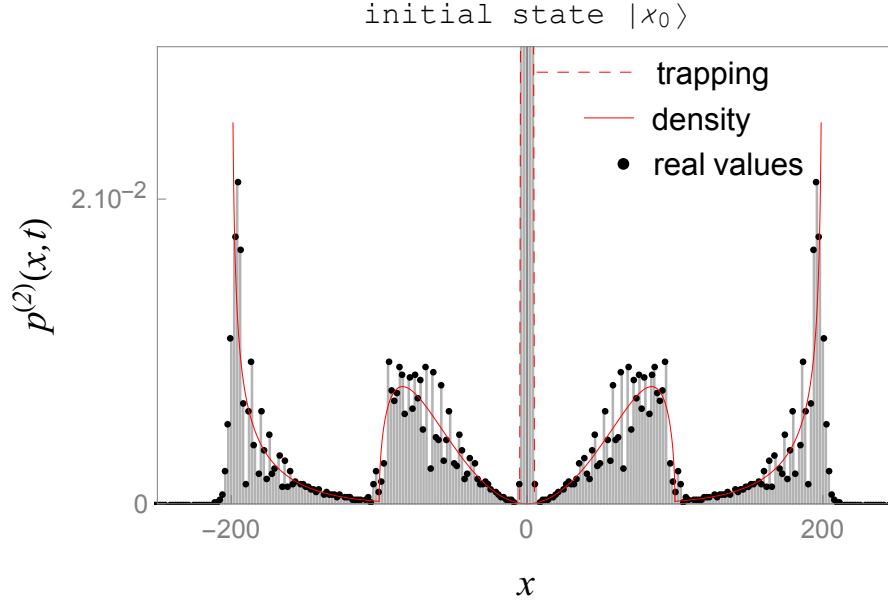


Figure 5.11: Position probability distribution of the five-state Wigner walk on a line. The initial state is the suitable state $|\chi_0\rangle$ from Eq. (5.56) and the total number of steps $t = 100$. It is seen that in the limit of large number of steps, all the peaks are present.

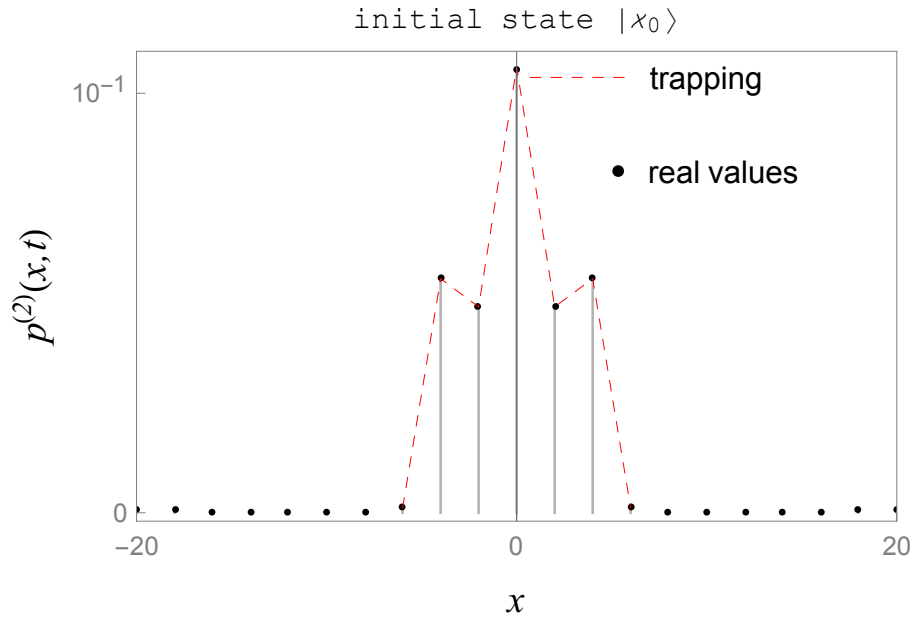


Figure 5.12: Detail of the trapping peak of the five-state Wigner walk on a line. The initial state is the suitable state $|\chi_0\rangle$ from Eq. (5.56) and the total number of steps $t = 500$. It is seen that the probabilities are not monotonically decreasing.

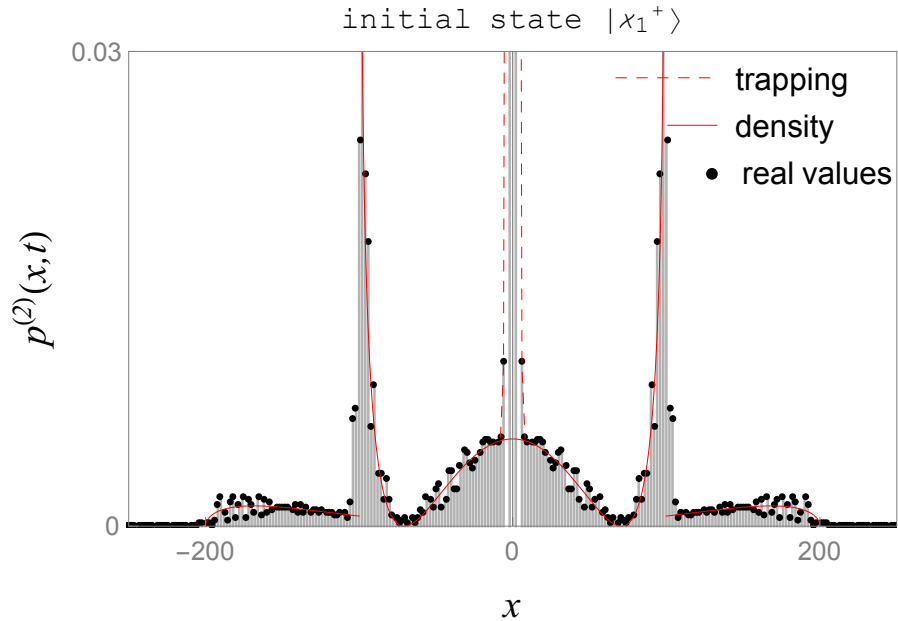


Figure 5.13: Position probability distribution of the five-state Wigner walk on a line. The initial state is the suitable state $|\chi_1^+\rangle$ from Eq. (5.56) and the total number of steps $t = 100$. It is seen that in the limit of large number of steps, the fastest peaks vanish.

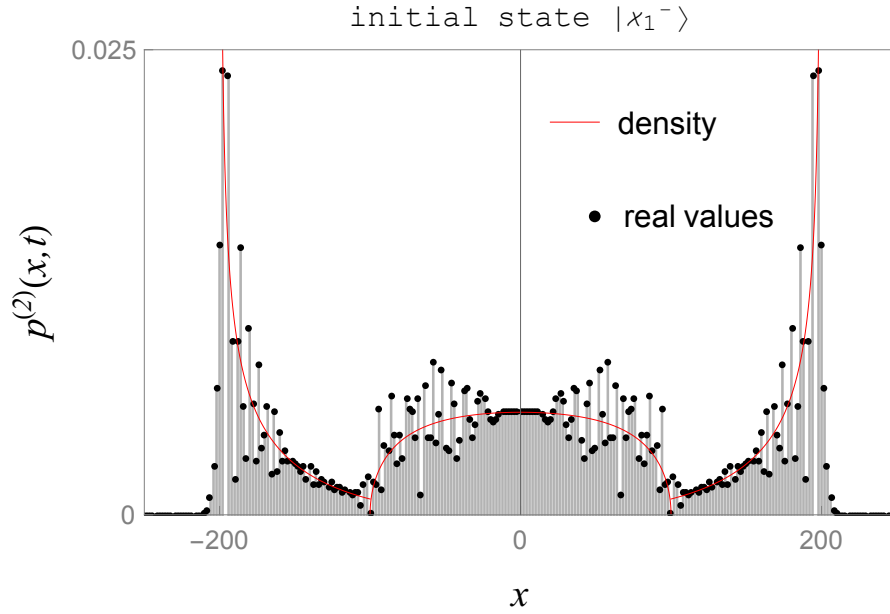


Figure 5.14: Position probability distribution of the five-state Wigner walk on a line. The initial state is the suitable state $|\chi_1^-\rangle$ from Eq. (5.56) and the total number of steps $t = 100$. It is seen that in the limit of large number of steps, the slower peaks as well as the trapping peak vanish.

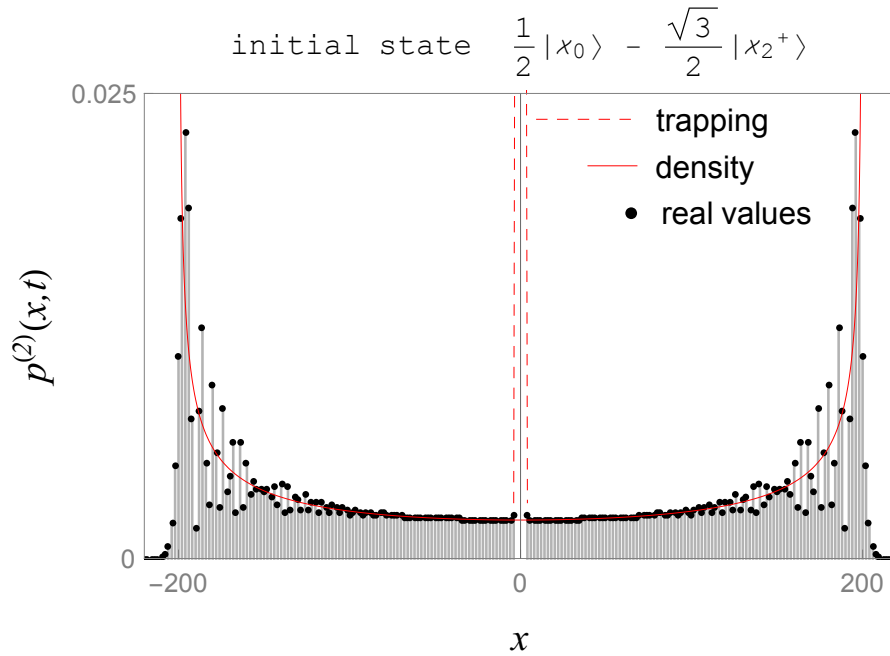


Figure 5.15: Position probability distribution of the five-state Wigner walk on a line. The initial state is a linear combination of the suitable states $|\chi_0\rangle, |\chi_2^+\rangle$ from Eq. (5.56) and the total number of steps $t = 100$. It is seen that in the limit of large number of steps, the slower peaks vanish. It is due to zero density $f^{(3/2,1/2)}(v)$.

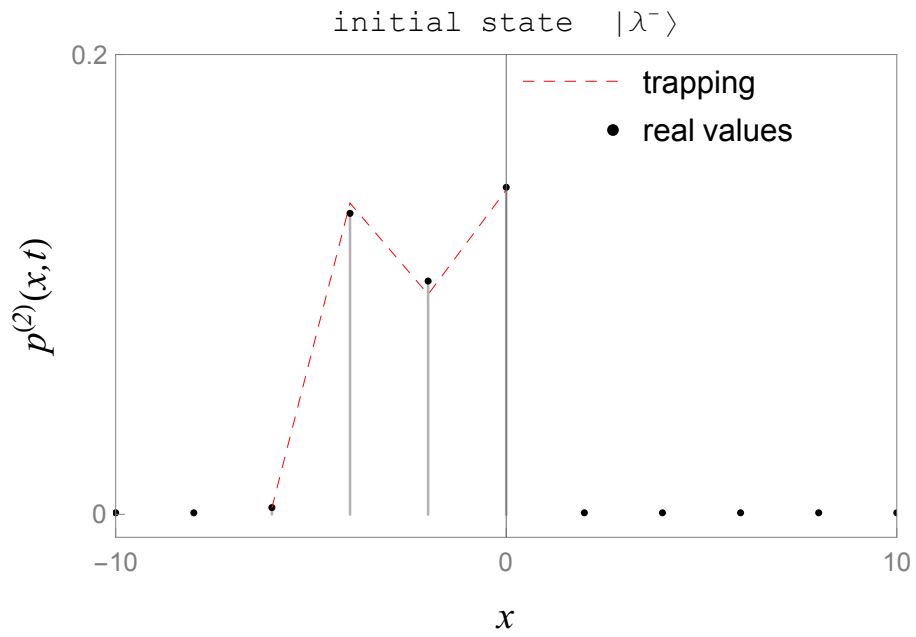


Figure 5.16: Detail of the trapping peak for the initial coin state $|\lambda^-\rangle = \sqrt{\frac{3}{8}}|\chi_0\rangle - \frac{1}{\sqrt{2}}|\chi_1^+\rangle + \frac{1}{\sqrt{8}}|\chi_2^+\rangle$. For this particular choice, the right half of the peak vanishes. Moreover, the rest of the peak is not decreasing. The total number of steps is 500.

Appendices

Appendix A

Remarks on Wigner walks

A.1 Four-state Wigner walk

During the derivation of the weight function in the suitable basis in subsection 5.3.6, we have skipped several technical steps. For those interested, here we provide relations that are necessary for turning the results from [23] into the suitable basis.

In terms of the standard basis, the new compiled in Eq. (5.54) reads

$$\begin{aligned}
|\chi_1^+\rangle &= \frac{\sqrt{3}}{2\sqrt{2}}\sqrt{1+\rho}|3/2\rangle - \frac{\sqrt{1-\rho}}{2\sqrt{2}}|1/2\rangle + \frac{\sqrt{1+\rho}}{2\sqrt{2}}|-1/2\rangle - \frac{\sqrt{3}}{2\sqrt{2}}\sqrt{1-\rho}|-3/2\rangle, \\
|\chi_1^-\rangle &= \frac{\sqrt{3}}{2\sqrt{2}}\sqrt{1-\rho}|3/2\rangle + \frac{\sqrt{1+\rho}}{2\sqrt{2}}|1/2\rangle + \frac{\sqrt{1-\rho}}{2\sqrt{2}}|-1/2\rangle + \frac{\sqrt{3}}{2\sqrt{2}}\sqrt{1+\rho}|-3/2\rangle, \\
|\chi_2^+\rangle &= \frac{(1-2\rho)\sqrt{1+\rho}}{2\sqrt{2}}|3/2\rangle + \frac{\sqrt{3}(1+2\rho)\sqrt{1-\rho}}{2\sqrt{2}}|1/2\rangle - \\
&\quad - \frac{\sqrt{3}(1-2\rho)\sqrt{1+\rho}}{2\sqrt{2}}|-1/2\rangle - \frac{(1+2\rho)\sqrt{1-\rho}}{2\sqrt{2}}|-3/2\rangle, \\
|\chi_2^-\rangle &= \frac{(1+2\rho)\sqrt{1-\rho}}{2\sqrt{2}}|3/2\rangle - \frac{\sqrt{3}(1-2\rho)\sqrt{1+\rho}}{2\sqrt{2}}|1/2\rangle - \\
&\quad - \frac{\sqrt{3}(1+2\rho)\sqrt{1-\rho}}{2\sqrt{2}}|-1/2\rangle + \frac{(1-2\rho)\sqrt{1+\rho}}{2\sqrt{2}}|-3/2\rangle.
\end{aligned}$$

The expressions provide us the transformation relations between the coefficients in the standard and the suitable basis as

$$\begin{aligned}
q_{3/2} &= h_1^+ \frac{\sqrt{3}}{2\sqrt{2}}\sqrt{1+\rho} + h_1^- \frac{\sqrt{3}}{2\sqrt{2}}\sqrt{1-\rho} + h_2^+ \frac{(1-2\rho)\sqrt{1+\rho}}{2\sqrt{2}} + h_2^- \frac{(1+2\rho)\sqrt{1-\rho}}{2\sqrt{2}}, \\
q_{-3/2} &= h_1^+ \frac{-\sqrt{3}}{2\sqrt{2}}\sqrt{1-\rho} + h_1^- \frac{\sqrt{3}}{2\sqrt{2}}\sqrt{1+\rho} - h_2^+ \frac{(1+2\rho)\sqrt{1-\rho}}{2\sqrt{2}} + h_2^- \frac{(1-2\rho)\sqrt{1+\rho}}{2\sqrt{2}}, \\
q_{1/2} &= -h_1^+ \frac{\sqrt{1-\rho}}{2\sqrt{2}} + h_1^- \frac{\sqrt{1+\rho}}{2\sqrt{2}} + h_2^+ \frac{\sqrt{3}(1+2\rho)\sqrt{1-\rho}}{2\sqrt{2}} - h_2^- \frac{\sqrt{3}(1-2\rho)\sqrt{1+\rho}}{2\sqrt{2}}, \\
q_{-1/2} &= h_1^+ \frac{\sqrt{1+\rho}}{2\sqrt{2}} + h_1^- \frac{\sqrt{1-\rho}}{2\sqrt{2}} - h_2^+ \frac{\sqrt{3}(1-2\rho)\sqrt{1+\rho}}{2\sqrt{2}} - h_2^- \frac{\sqrt{3}(1+2\rho)\sqrt{1-\rho}}{2\sqrt{2}}.
\end{aligned} \tag{A.1}$$

These relations are now applied to the results from [23] and lead to the final weights $\mathcal{M}_i^{(\frac{3}{2}, \frac{1}{2})}$ and $\mathcal{M}_i^{(\frac{3}{2}, \frac{3}{2})}$ with $i = 0, 1, 2, 3$ stated in subsection 5.3.6.

A.2 Five-state Wigner walk

In subsection 5.3.6 we have referred to this appendix consisting of the relations leading to the transition between the standard and the suitable basis of the coin space.

Using the Eq. (5.56), the suitable basis can be expressed in terms of the standard coin space basis as

$$\begin{aligned}
|\chi_0\rangle &= \sqrt{\frac{3}{8}}|2\rangle + \frac{1}{2}|0\rangle + \sqrt{\frac{3}{8}}|-2\rangle, \\
|\chi_1^+\rangle &= \sqrt{\frac{1-\rho^2}{2}}|2\rangle + \frac{\rho}{\sqrt{2}}|1\rangle + \frac{\rho}{\sqrt{2}}|-1\rangle - \sqrt{\frac{1-\rho^2}{2}}|-2\rangle, \\
|\chi_1^-\rangle &= -\frac{\rho}{\sqrt{2}}|2\rangle + \sqrt{\frac{1-\rho^2}{2}}|1\rangle + \sqrt{\frac{1-\rho^2}{2}}|-1\rangle + \frac{\rho}{\sqrt{2}}|-2\rangle, \\
|\chi_2^+\rangle &= \frac{1-2\rho^2}{2\sqrt{2}}|2\rangle + \rho\sqrt{2-2\rho^2}|1\rangle - \frac{\sqrt{3}}{2}(1-2\rho^2)|0\rangle - \rho\sqrt{2-2\rho^2}|-1\rangle + \\
&\quad + \frac{1-2\rho^2}{2\sqrt{2}}|-2\rangle, \\
|\chi_2^-\rangle &= \rho\sqrt{\frac{1-\rho^2}{2}}|2\rangle - \frac{1-2\rho^2}{\sqrt{2}}|1\rangle - \rho\sqrt{3-3\rho^2}|0\rangle + \frac{1-2\rho^2}{\sqrt{2}}|-1\rangle + \\
&\quad + \rho\sqrt{\frac{1-\rho^2}{2}}|-2\rangle.
\end{aligned}$$

Let us remind that the initial coin state can be expressed in the standard and the suitable basis as

$$|\psi_C\rangle = h_0|\chi_0\rangle + h_1^+|\chi_1^+\rangle + h_1^-|\chi_1^-\rangle + h_2^+|\chi_2^+\rangle + h_2^-|\chi_2^-\rangle = q_{-2}|-2\rangle + q_{-1}|-1\rangle + q_0|0\rangle + q_1|1\rangle + q_2|2\rangle.$$

These facts lead to the transformation relations from the standard coin space basis coefficients q_i , $i = -2, \dots, 2$ to the new coefficients h_0, h_1^\pm, h_2^\pm which are

$$\begin{aligned}
q_2 &= \sqrt{\frac{3}{8}}h_0 + \sqrt{\frac{1-\rho^2}{2}}h_1^+ - \frac{\rho}{\sqrt{2}}h_1^- + \frac{1-2\rho^2}{2\sqrt{2}}h_2^+ + \rho\sqrt{\frac{1-\rho^2}{2}}h_2^-, \\
q_1 &= \frac{\rho}{\sqrt{2}}h_1^+ + \sqrt{\frac{1-\rho^2}{2}}h_1^- + \rho\sqrt{2-2\rho^2}h_2^+ - \frac{1-2\rho^2}{\sqrt{2}}h_2^-, \\
q_0 &= \frac{1}{2}h_0 - \rho\sqrt{3-3\rho^2}h_2^-, \\
q_{-1} &= \frac{\rho}{\sqrt{2}}h_1^+ + \sqrt{\frac{1-\rho^2}{2}}h_1^- - \rho\sqrt{2-2\rho^2}h_2^+ + \frac{1-2\rho^2}{\sqrt{2}}h_2^-, \\
q_{-2} &= \sqrt{\frac{3}{8}}h_0 - \sqrt{\frac{1-\rho^2}{2}}h_1^+ + \frac{\rho}{\sqrt{2}}h_1^- + \frac{1-2\rho^2}{2\sqrt{2}}h_2^+ + \rho\sqrt{\frac{1-\rho^2}{2}}h_2^-. \tag{A.2}
\end{aligned}$$

Final weights are then obtained from these equations and the results for the five-state Wigner walks with respect to the standard coin space basis from [23].

A.3 Six-state Wigner walk

We would like to illustrate how the suitable basis affect even more complicated walk, namely the six-state Wigner walk. This part is presented in the appendix, since we deal only with the analysis of the behaviour based on the previous results and we do not provide any new insight into the problem. Nevertheless, we find the results depicted especially in the figures interesting. The suitable basis brings the desired simplifications here as well. Despite the fact that the resulting formulas are even in the simplifying basis very complicated, they are reachable.

The six-state Wigner walks occurs for $j = 5/2$. Performed movements are one, three and five steps to the left and right, which lead to the standard coin space basis

$$\mathcal{H}_C = \text{Span}\{|-5/2\rangle, |-3/2\rangle, |-1/2\rangle, |1/2\rangle, |3/2\rangle, |5/2\rangle\}$$

and the standard initial coin state of the form

$$|\psi_C\rangle = q_{-5/2}|-5/2\rangle + q_{-3/2}|-3/2\rangle + q_{-1/2}|-1/2\rangle + q_{1/2}|1/2\rangle + q_{3/2}|3/2\rangle + q_{5/2}|5/2\rangle.$$

The walk is driven by quite a complicated coin with its matrix elements given by Eq. (1.24),

$$C_W^{(\frac{5}{2})} = \begin{pmatrix} \rho^5 & -\sqrt{5}\mathcal{R}\rho^4 & \sqrt{10}\mathcal{R}\rho^3 & -\sqrt{10}\mathcal{R}^{3/2}\rho^2 & \sqrt{5}\mathcal{R}^2\rho & -\mathcal{R}^{5/2} \\ \sqrt{5}\mathcal{R}\rho^4 & \mathcal{W}\rho^3 & \sqrt{2}\mathcal{R}\mathcal{V}\rho^2 & \sqrt{2}\mathcal{U}\rho & \mathcal{R}^{3/2}\mathcal{X} & \sqrt{5}\mathcal{R}^2\rho \\ \sqrt{10}\mathcal{R}\rho^3 & -\sqrt{2}\mathcal{R}\mathcal{V}\rho^2 & \mathcal{T}\rho & -\sqrt{\mathcal{R}}\mathcal{S} & \sqrt{2}\mathcal{U}\rho & -\sqrt{10}\mathcal{R}^{3/2}\rho^2 \\ \sqrt{10}\mathcal{R}^{3/2}\rho^2 & \sqrt{2}\mathcal{U}\rho & \sqrt{\mathcal{R}}\mathcal{S} & \mathcal{T}\rho & \sqrt{2}\mathcal{R}\mathcal{V}\rho^2 & \sqrt{10}\mathcal{R}\rho^3 \\ \sqrt{5}\mathcal{R}^2\rho & -\mathcal{R}^{3/2}\mathcal{X} & \sqrt{2}\mathcal{U}\rho & -\sqrt{2}\mathcal{R}\mathcal{V}\rho^2 & \mathcal{W}\rho^3 & -\sqrt{5}\mathcal{R}\rho^4 \\ \mathcal{R}^{5/2} & \sqrt{5}\mathcal{R}^2\rho & \sqrt{10}\mathcal{R}^{3/2}\rho^2 & \sqrt{10}\mathcal{R}\rho^3 & \sqrt{5}\mathcal{R}\rho^4 & \rho^5 \end{pmatrix}. \quad (\text{A.3})$$

Here

$$\begin{aligned} \mathcal{R} &= 1 - \rho^2, \\ \mathcal{S} &= 1 - 8\rho^2 + 10\rho^4, \\ \mathcal{T} &= 3 - 12\rho^2 + 10\rho^4, \\ \mathcal{U} &= -2 + 7\rho^2 - 5\rho^4, \\ \mathcal{V} &= 3 - 5\rho^2, \\ \mathcal{W} &= -4 + 5\rho^2, \\ \mathcal{X} &= 1 - 5\rho^2. \end{aligned}$$

The eigenstates of the coin $C_W^{(\frac{5}{2})}$ are

$$\begin{aligned} |\varphi_1^\pm\rangle &= \frac{1}{4} \left(\pm i\sqrt{5}|-5/2\rangle + |-3/2\rangle \pm i\sqrt{2}|-1/2\rangle + \sqrt{2}|1/2\rangle \pm i|+3/2\rangle + \sqrt{5}|5/2\rangle \right), \\ |\varphi_2^\pm\rangle &= \frac{1}{4\sqrt{2}} \left(\pm i\sqrt{5}|-5/2\rangle - 3|-3/2\rangle \mp i\sqrt{2}|-1/2\rangle - \sqrt{2}|1/2\rangle \mp 3i|3/2\rangle + \sqrt{5}|5/2\rangle \right), \\ |\varphi_3^\pm\rangle &= \frac{1}{4\sqrt{2}} \left(\pm i, \sqrt{5}|-5/2\rangle \mp i|-3/2\rangle + \sqrt{10}|-1/2\rangle - \sqrt{10}|1/2\rangle \pm i\sqrt{5}|3/2\rangle + |5/2\rangle \right), \end{aligned}$$

satisfying the eigenvalue equation

$$C_W^{(\frac{5}{2})} |\varphi_{1,2,3}^\pm\rangle = e^{\pm i\varphi_{1,2,3}} |\varphi_{1,2,3}^\pm\rangle. \quad (\text{A.4})$$

The phases are

$$\begin{aligned} \varphi_1 &= \arccos(\rho), \\ \varphi_2 &= \begin{cases} \arccos(\rho(4\rho^2 - 3)), & 0 < \rho \leq \frac{1}{2} \\ 2\pi - \arccos(\rho(4\rho^2 - 3)), & \frac{1}{2} < \rho \leq 1, \end{cases} \\ \varphi_3 &= \begin{cases} 2\pi + \arccos(\rho(5 - 20\rho^2 + 16\rho^4)), & 0 < \rho \leq \frac{1}{4}(-1 + \sqrt{5}), \\ 2\pi - \arccos(\rho(5 - 20\rho^2 + 16\rho^4)), & \frac{1}{4}(-1 + \sqrt{5}) < \rho \leq \frac{1}{4}(1 + \sqrt{5}), \\ \arccos(\rho(5 - 20\rho^2 + 16\rho^4)), & \frac{1}{4}(1 + \sqrt{5}) < \rho \leq 1. \end{cases} \end{aligned}$$

Thus, the suitable basis is then given by

$$\begin{aligned} |\chi_1^+\rangle &= \frac{1}{\sqrt{2}} \left(e^{-i\frac{\varphi_1}{2}} |\varphi_1^+\rangle + e^{i\frac{\varphi_1}{2}} |\varphi_1^-\rangle \right) \\ |\chi_1^-\rangle &= \frac{i}{\sqrt{2}} \left(e^{-i\frac{\varphi_1}{2}} |\varphi_1^+\rangle - e^{i\frac{\varphi_1}{2}} |\varphi_1^-\rangle \right) \\ |\chi_2^+\rangle &= \frac{1}{\sqrt{2}} \left(e^{-i\frac{\varphi_2}{2}} |\varphi_2^+\rangle + e^{i\frac{\varphi_2}{2}} |\varphi_2^-\rangle \right) \\ |\chi_2^-\rangle &= \frac{i}{\sqrt{2}} \left(e^{-i\frac{\varphi_2}{2}} |\varphi_2^+\rangle - e^{i\frac{\varphi_2}{2}} |\varphi_2^-\rangle \right) \\ |\chi_3^+\rangle &= \frac{1}{\sqrt{2}} \left(e^{-i\frac{\varphi_3}{2}} |\varphi_3^+\rangle + e^{i\frac{\varphi_3}{2}} |\varphi_3^-\rangle \right) \\ |\chi_3^-\rangle &= \frac{i}{\sqrt{2}} \left(e^{-i\frac{\varphi_3}{2}} |\varphi_3^+\rangle - e^{i\frac{\varphi_3}{2}} |\varphi_3^-\rangle \right). \end{aligned} \quad (\text{A.5})$$

We can now express the initial coin state in the new basis as

$$|\psi_C\rangle = h_1^+ |\chi_1^+\rangle + h_1^- |\chi_1^-\rangle + h_2^+ |\chi_2^+\rangle + h_2^- |\chi_2^-\rangle + h_3^+ |\chi_3^+\rangle + h_3^- |\chi_3^-\rangle$$

In the case of the five-state walk, the total velocity density is the sum of three individual densities for inner, middle and outer walk

$$f^{(\frac{5}{2})}(v) = f^{(\frac{5}{2}, \frac{1}{2})}(v) + f^{(\frac{5}{2}, \frac{3}{2})}(v) + f^{(\frac{5}{2}, \frac{5}{2})}(v).$$

Every density can be expressed by Konno's density function μ and weight function \mathcal{M} as

$$f^{(\frac{5}{2}, m)}(v) = \frac{1}{2m} \mu\left(\frac{v}{2m}, \rho\right) \mathcal{M}^{(\frac{5}{2}, m)}\left(\frac{v}{2m}\right), \quad m = \frac{1}{2}, \frac{3}{2}, \frac{5}{2}. \quad (\text{A.6})$$

The weight function is given by a polynomial in $v/2m$ up to the power five, i.e.

$$\mathcal{M}^{(\frac{5}{2}, m)}\left(\frac{v}{2m}\right) = \sum_{i=0}^5 \mathcal{M}_i^{(\frac{5}{2}, m)} \left(\frac{v}{2m}\right)^i.$$

The exact formulas for the elements of the weight function can be found in [23]. Then we only have to use the transformation relations between the standard and the suitable basis, it is between the coefficients q_i , $i = -5/2, \dots, 5/2$ and h_j^\pm , $j = 1, 2, 3$. The conversion relations are given by

$$\begin{aligned}
q_{5/2} &= \frac{1}{4} \left(h_3^+ \sin\left(\frac{\varphi_3}{2}\right) - h_3^- \cos\left(\frac{\varphi_3}{2}\right) + \sqrt{5} \left(h_2^+ \sin\left(\frac{\varphi_2}{2}\right) + -h_2^- \cos\left(\frac{\varphi_2}{2}\right) + \right. \\
&\quad \left. + \sqrt{2} \left(h_1^+ \sin\left(\frac{\varphi_1}{2}\right) - h_1^- \cos\left(\frac{\varphi_1}{2}\right) \right) \right), \\
q_{3/2} &= \frac{1}{4} \left(\sqrt{2} h_1^- \sin\left(\frac{\varphi_1}{2}\right) - 3h_2^- \sin\left(\frac{\varphi_2}{2}\right) + \sqrt{5} h_3^- \sin\left(\frac{\varphi_3}{2}\right) + \sqrt{2} h_1^+ \cos\left(\frac{\varphi_1}{2}\right) - \right. \\
&\quad \left. - 3h_2^+ \cos\left(\frac{\varphi_2}{2}\right) + \sqrt{5} h_3^+ \cos\left(\frac{\varphi_3}{2}\right) \right), \\
q_{1/2} &= \frac{1}{4} \left(2h_1^+ \sin\left(\frac{\varphi_1}{2}\right) - 2h_1^- \cos\left(\frac{\varphi_1}{2}\right) + \sqrt{2} \left(-h_2^+ \sin\left(\frac{\varphi_2}{2}\right) + h_2^- \cos\left(\frac{\varphi_2}{2}\right) + \right. \\
&\quad \left. + \sqrt{5} \left(h_3^- \cos\left(\frac{\varphi_3}{2}\right) - h_3^+ \sin\left(\frac{\varphi_3}{2}\right) \right) \right), \\
q_{-1/2} &= \frac{1}{4} \left(2h_1^- \sin\left(\frac{\varphi_1}{2}\right) + 2h_1^+ \cos\left(\frac{\varphi_1}{2}\right) - \sqrt{2} \left(h_2^- \sin\left(\frac{\varphi_2}{2}\right) + h_2^+ \cos\left(\frac{\varphi_2}{2}\right) + \right. \\
&\quad \left. + \sqrt{5} \left(h_3^- \sin\left(\frac{\varphi_3}{2}\right) + h_3^+ \cos\left(\frac{\varphi_3}{2}\right) \right) \right), \\
q_{-3/2} &= \frac{1}{4} \left(\sqrt{2} h_1^+ \sin\left(\frac{\varphi_1}{2}\right) - 3h_2^+ \sin\left(\frac{\varphi_2}{2}\right) + \sqrt{5} h_3^+ \sin\left(\frac{\varphi_3}{2}\right) - \sqrt{2} h_1^- \cos\left(\frac{\varphi_1}{2}\right) \right. \\
&\quad \left. + 3h_2^- \cos\left(\frac{\varphi_2}{2}\right) - \sqrt{5} h_3^- \cos\left(\frac{\varphi_3}{2}\right) \right), \\
q_{-5/2} &= \frac{1}{4} \left(h_3^- \sin\left(\frac{\varphi_3}{2}\right) + h_3^+ \cos\left(\frac{\varphi_3}{2}\right) + \sqrt{5} \left(h_2^- \sin\left(\frac{\varphi_2}{2}\right) + h_2^+ \cos\left(\frac{\varphi_2}{2}\right) + \right. \\
&\quad \left. + \sqrt{2} \left(h_1^- \sin\left(\frac{\varphi_1}{2}\right) + h_1^+ \cos\left(\frac{\varphi_1}{2}\right) \right) \right).
\end{aligned}$$

Once we have the suitable basis and the transformation relations, we can express the weights in the new basis. Let us start with the most inner walk, it is $m = 1/2$. The corresponding weight is given by

$$\mathcal{M}^{(\frac{5}{2}, \frac{1}{2})}(v) = \mathcal{M}_0^{(\frac{5}{2}, \frac{1}{2})} + \mathcal{M}_1^{(\frac{5}{2}, \frac{1}{2})} v + \mathcal{M}_2^{(\frac{5}{2}, \frac{1}{2})} v^2 + \mathcal{M}_3^{(\frac{5}{2}, \frac{1}{2})} v^3 + \mathcal{M}_4^{(\frac{5}{2}, \frac{1}{2})} v^4 + \mathcal{M}_5^{(\frac{5}{2}, \frac{1}{2})} v^5.$$

In the suitable basis, the coefficients in the polynomial are significantly simplified. We start with absolute term which read

$$\mathcal{M}_0^{(\frac{5}{2}, \frac{1}{2})} = |h_1^+|^2 + |h_1^-|^2.$$

Following terms are given by

$$\mathcal{M}_1^{(\frac{5}{2}, \frac{1}{2})} = \frac{1}{\rho} \left(3(|h_1^+|^2 - |h_1^-|^2) + \sqrt{2}(h_1^- \bar{h}_2^- + h_2^- \bar{h}_1^- - h_1^+ \bar{h}_2^+ - h_2^+ \bar{h}_1^+) \right),$$

$$\begin{aligned}
\mathcal{M}_2^{(\frac{5}{2}, \frac{1}{2})} &= -\frac{1}{4\rho^2} \left(8(|h_1^+|^2 + |h_1^-|^2 - |h_2^+|^2 - |h_2^-|^2) - \right. \\
&\quad \left. - 3\sqrt{2}(h_1^- \bar{h}_2^- + h_2^- \bar{h}_1^- + h_1^+ \bar{h}_2^+ + h_2^+ \bar{h}_1^+) + \sqrt{10}(h_1^- \bar{h}_3^- + h_3^- \bar{h}_1^- + h_1^+ \bar{h}_3^+ + h_3^+ \bar{h}_1^+) \right),
\end{aligned}$$

$$\begin{aligned}\mathcal{M}_3^{(\frac{5}{2}, \frac{1}{2})} &= \frac{1}{2\rho^3} (16(|h_1^-|^2 - |h_1^+|^2) + 8(|h_2^-|^2 - |h_2^+|^2) + \\ &\quad + \sqrt{10}(h_1^- \bar{h}_3^- + h_3^- \bar{h}_1^- - h_1^+ \bar{h}_3^+ - h_3^+ \bar{h}_1^+) + \sqrt{5}(h_2^- \bar{h}_3^- + h_3^- \bar{h}_2^- - h_2^+ \bar{h}_3^+ - h_3^+ \bar{h}_2^+)) ,\end{aligned}$$

$$\begin{aligned}\mathcal{M}_4^{(\frac{5}{2}, \frac{1}{2})} &= \frac{1}{8\rho^4} (10(|h_1^-|^2 + |h_1^+|^2) - 15(|h_2^-|^2 + |h_2^+|^2) + 5(|h_3^-|^2 + |h_3^+|^2) - \\ &\quad - 5\sqrt{2}(h_1^- \bar{h}_2^- + h_2^- \bar{h}_1^- + h_1^+ \bar{h}_2^+ + h_2^+ \bar{h}_1^+) + 3\sqrt{10}(h_1^- \bar{h}_3^- + h_3^- \bar{h}_1^- + h_1^+ \bar{h}_3^+ + h_3^+ \bar{h}_1^+) + \\ &\quad + \sqrt{5}(h_2^- \bar{h}_3^- + h_3^- \bar{h}_2^- + h_2^+ \bar{h}_3^+ - h_3^+ \bar{h}_2^+)) ,\end{aligned}$$

$$\begin{aligned}\mathcal{M}_5^{(\frac{5}{2}, \frac{1}{2})} &= -\frac{5}{8\rho^5} (10(|h_1^-|^2 - |h_1^+|^2) + 5(|h_2^-|^2 - |h_2^+|^2) + |h_3^-|^2 - |h_3^+|^2 + \\ &\quad + 5\sqrt{2}(h_1^- \bar{h}_2^- + h_2^- \bar{h}_1^- - h_1^+ \bar{h}_2^+ - h_2^+ \bar{h}_1^+) + \sqrt{5}(h_2^- \bar{h}_3^- + h_3^- \bar{h}_2^- - h_2^+ \bar{h}_3^+ + h_3^+ \bar{h}_2^+) + \\ &\quad + \sqrt{10}(h_1^- \bar{h}_3^- + h_3^- \bar{h}_1^- - h_1^+ \bar{h}_3^+ - h_3^+ \bar{h}_1^+)) .\end{aligned}$$

The second density for the middle walk with $m = 3/2$ read

$$\begin{aligned}\mathcal{M}^{(\frac{5}{2}, \frac{3}{2})} \left(\frac{v}{3}\right) &= \mathcal{M}_0^{(\frac{5}{2}, \frac{3}{2})} + \mathcal{M}_1^{(\frac{5}{2}, \frac{3}{2})} \frac{v}{3} + \mathcal{M}_2^{(\frac{5}{2}, \frac{3}{2})} \left(\frac{v}{3}\right)^2 + \\ &\quad + \mathcal{M}_3^{(\frac{5}{2}, \frac{3}{2})} \left(\frac{v}{3}\right)^3 + \mathcal{M}_4^{(\frac{5}{2}, \frac{3}{2})} \left(\frac{v}{3}\right)^4 + \mathcal{M}_5^{(\frac{5}{2}, \frac{3}{2})} \left(\frac{v}{3}\right)^5 .\end{aligned}$$

The individual elements are in the suitable basis given by

$$\mathcal{M}_0^{(\frac{5}{2}, \frac{3}{2})} = |h_2^-|^2 + |h_2^+|^2 ,$$

$$\begin{aligned}\mathcal{M}_1^{(\frac{5}{2}, \frac{3}{2})} &= \frac{1}{3\rho} \left(\sqrt{2}(h_1^- \bar{h}_2^- + h_2^- \bar{h}_1^- - h_1^+ \bar{h}_2^+ - h_2^+ \bar{h}_1^+) + \right. \\ &\quad \left. + \frac{\sqrt{5}}{2}(h_2^- \bar{h}_3^- + h_3^- \bar{h}_2^- - h_2^+ \bar{h}_3^+ - h_3^+ \bar{h}_2^+) \right) ,\end{aligned}$$

$$\begin{aligned}\mathcal{M}_2^{(\frac{5}{2}, \frac{3}{2})} &= \frac{1}{4\rho^2} (8(|h_1^-|^2 + |h_1^+|^2) - 13(|h_2^-|^2 + |h_2^+|^2) + 5(|h_3^-|^2 + |h_3^+|^2) - \\ &\quad - 3\sqrt{2}(h_1^- \bar{h}_2^- + h_2^- \bar{h}_1^- + h_1^+ \bar{h}_2^+ + h_2^+ \bar{h}_1^+) + \\ &\quad + 2\sqrt{10}(h_1^- \bar{h}_3^- + h_3^- \bar{h}_1^- + h_1^+ \bar{h}_3^+ + h_3^+ \bar{h}_1^+)) ,\end{aligned}$$

$$\begin{aligned}\mathcal{M}_3^{(\frac{5}{2}, \frac{3}{2})} &= \frac{1}{8\rho^3} (24(|h_1^+|^2 - |h_1^-|^2) + 8(|h_2^+|^2 - |h_1^-|^2) - \\ &\quad - 19\sqrt{2}(h_1^- \bar{h}_2^- + h_2^- \bar{h}_1^- - h_1^+ \bar{h}_2^+ - h_2^+ \bar{h}_1^+) - 3\sqrt{10}(h_1^- \bar{h}_3^- + h_3^- \bar{h}_1^- + h_1^+ \bar{h}_3^+ + h_3^+ \bar{h}_1^+) - \\ &\quad - 8\sqrt{5}(h_2^- \bar{h}_3^- + h_3^- \bar{h}_2^- - h_2^+ \bar{h}_3^+ + h_3^+ \bar{h}_2^+)) ,\end{aligned}$$

$$\begin{aligned} \mathcal{M}_4^{(\frac{5}{2}, \frac{3}{2})} = & -\frac{1}{16\rho^4} (10(|h_1^+|^2 + |h_1^-|^2) - 15(|h_2^+|^2 + |h_2^-|^2) + 5(|h_3^+|^2 + |h_3^-|^2) - \\ & -5\sqrt{2}(h_1^- \bar{h}_2^- + h_2^- \bar{h}_1^- + h_1^+ \bar{h}_2^+ + h_2^+ \bar{h}_1^+) + 3\sqrt{10}(h_1^- \bar{h}_3^- + h_3^- \bar{h}_1^- + h_1^+ \bar{h}_3^+ + h_3^+ \bar{h}_1^+) + \\ & + \sqrt{5}(h_2^- \bar{h}_3^- + h_3^- \bar{h}_2^- + h_2^+ \bar{h}_3^+ + h_3^+ \bar{h}_2^+)), \end{aligned}$$

$$\begin{aligned} \mathcal{M}_5^{(\frac{5}{2}, \frac{3}{2})} = & -\frac{5}{16\rho^5} (10(|h_1^-|^2 - |h_1^+|^2) + 5(|h_2^-|^2 - |h_2^+|^2) + (|h_3^-|^2 - |h_3^+|^2) + \\ & +5\sqrt{2}(h_1^- \bar{h}_2^- + h_2^- \bar{h}_1^- - h_1^+ \bar{h}_2^+ + h_2^+ \bar{h}_1^+) + \sqrt{10}(h_1^- \bar{h}_3^- + h_3^- \bar{h}_1^- - h_1^+ \bar{h}_3^+ + h_3^+ \bar{h}_1^+) + \\ & + \sqrt{5}(h_2^- \bar{h}_3^- + h_3^- \bar{h}_2^- - h_2^+ \bar{h}_3^+ + h_3^+ \bar{h}_2^+)). \end{aligned}$$

Finally, the last density for the outer walk read

$$\begin{aligned} \mathcal{M}^{(\frac{5}{2}, \frac{5}{2})} \left(\frac{v}{5} \right) = & \mathcal{M}_0^{(\frac{5}{2}, \frac{5}{2})} + \mathcal{M}_1^{(\frac{5}{2}, \frac{5}{2})} \frac{v}{5} + \mathcal{M}_2^{(\frac{5}{2}, \frac{5}{2})} \left(\frac{v}{5} \right)^2 + \\ & + \mathcal{M}_3^{(\frac{5}{2}, \frac{5}{2})} \left(\frac{v}{5} \right)^3 + \mathcal{M}_4^{(\frac{5}{2}, \frac{5}{2})} \left(\frac{v}{5} \right)^4 + \mathcal{M}_5^{(\frac{5}{2}, \frac{5}{2})} \left(\frac{v}{5} \right)^5 \end{aligned}$$

and its elements are given by

$$\mathcal{M}_0^{(\frac{5}{2}, \frac{5}{2})} = |h_3^-|^2 + |h_3^+|^2,$$

$$\mathcal{M}_1^{(\frac{5}{2}, \frac{5}{2})} = -\frac{\sqrt{5}}{2\rho} (h_2^- \bar{h}_3^- + h_3^- \bar{h}_2^- - h_2^+ \bar{h}_3^+ - h_3^+ \bar{h}_2^+),$$

$$\begin{aligned} \mathcal{M}_2^{(\frac{5}{2}, \frac{5}{2})} = & \frac{1}{\sqrt{4\rho^2}} (5(|h_2^-|^2 + |h_2^+|^2 - |h_3^-|^2 - |h_3^+|^2) - \\ & - \sqrt{10}(h_1^- \bar{h}_3^- + h_3^- \bar{h}_1^- + h_1^+ \bar{h}_3^+ + h_3^+ \bar{h}_1^+)), \end{aligned}$$

$$\begin{aligned} \mathcal{M}_3^{(\frac{5}{2}, \frac{5}{2})} = & \frac{1}{8\rho^3} \left(5\sqrt{2}(h_1^- \bar{h}_2^- + h_2^- \bar{h}_1^- - h_1^+ \bar{h}_2^+ - h_2^+ \bar{h}_1^+) + \right. \\ & + \sqrt{10}(h_1^- \bar{h}_3^- + h_3^- \bar{h}_1^- - h_1^+ \bar{h}_3^+ - h_3^+ \bar{h}_1^+) + \\ & \left. + 4\sqrt{5}(h_2^- \bar{h}_3^- + h_3^- \bar{h}_2^- - h_2^+ \bar{h}_3^+ - h_3^+ \bar{h}_2^+) \right), \end{aligned}$$

$$\begin{aligned} \mathcal{M}_4^{(\frac{5}{2}, \frac{5}{2})} = & \frac{1}{16\rho^4} (10(|h_1^-|^2 + |h_1^+|^2) - 15(|h_2^-|^2 + |h_2^+|^2) + 5(|h_3^-|^2 + |h_3^+|^2) - \\ & -5\sqrt{2}(h_1^- \bar{h}_2^- + h_2^- \bar{h}_1^- + h_1^+ \bar{h}_2^+ + h_2^+ \bar{h}_1^+) + 3\sqrt{10}(h_1^- \bar{h}_3^- + h_3^- \bar{h}_1^- + h_1^+ \bar{h}_3^+ + h_3^+ \bar{h}_1^+) + \\ & + \sqrt{5}(h_2^- \bar{h}_3^- + h_3^- \bar{h}_2^- + h_2^+ \bar{h}_3^+ + h_3^+ \bar{h}_2^+)), \end{aligned}$$

$$\begin{aligned} \mathcal{M}_5^{(\frac{5}{2}, \frac{5}{2})} = & -\frac{1}{16\rho^5} (10(|h_1^-|^2 - |h_1^+|^2) + 5(|h_2^-|^2 - |h_2^+|^2) + |h_3^-|^2 - |h_3^+|^2 + \\ & +5\sqrt{2}(h_1^- \bar{h}_2^- + h_2^- \bar{h}_1^- - h_1^+ \bar{h}_2^+ - h_2^+ \bar{h}_1^+) + \sqrt{10}(h_1^- \bar{h}_3^- + h_3^- \bar{h}_1^- - h_1^+ \bar{h}_3^+ - h_3^+ \bar{h}_1^+) + \\ & + \sqrt{5}(h_2^- \bar{h}_3^- + h_3^- \bar{h}_2^- - h_2^+ \bar{h}_3^+ - h_3^+ \bar{h}_2^+)). \end{aligned}$$

We illustrate the results graphically on several figures for several choices of the initial state, Figs. (A.1 - A.3).

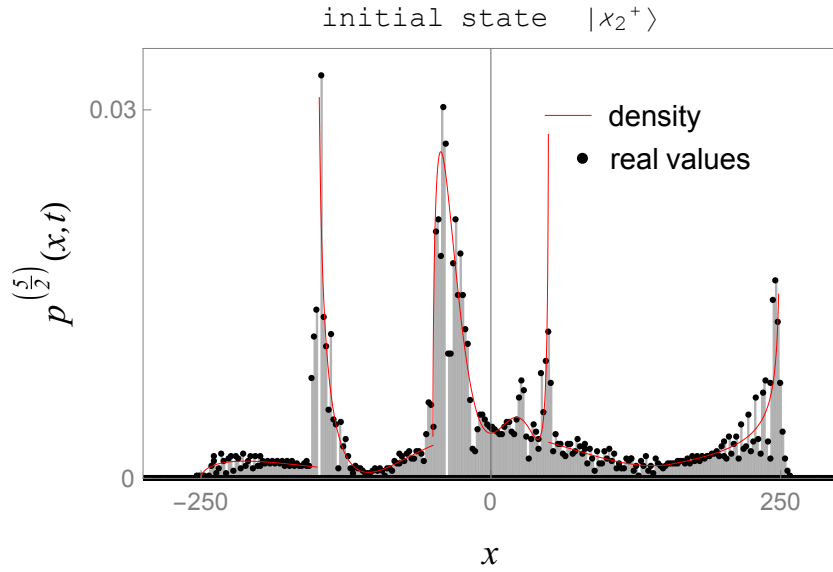


Figure A.1: Position probability distribution for the six-state Wigner walk. The initial coin state is the suitable state $|\chi_2^+\rangle$ from Eq. (A.5), the total number of steps $t = 100$ and parameter $\rho = 1/2$. Red solid line is the limiting density $\frac{1}{t}f^{(5/2)}(x/t)$, Eq. (A.6). It is seen that only three probability peaks are present since the suitable initial state eliminates one divergence for each density from $f^{(5/2)}(x/t)$.

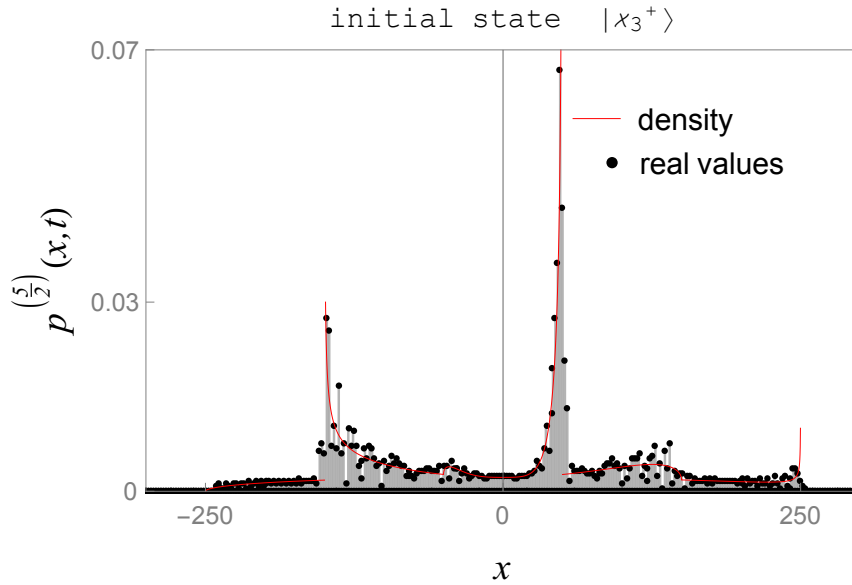


Figure A.2: Position probability distribution for the six-state Wigner walk. The initial coin state is the suitable state $|\chi_3^+\rangle$ from Eq. (A.5), the total number of steps $t = 100$ and parameter $\rho = 1/2$. Red solid line is the limiting density $\frac{1}{t}f^{(5/2)}(x/t)$, Eq. (A.6). It is seen that only three probability peaks are present since the suitable initial state eliminates one divergence for each density from $f^{(5/2)}(x/t)$.

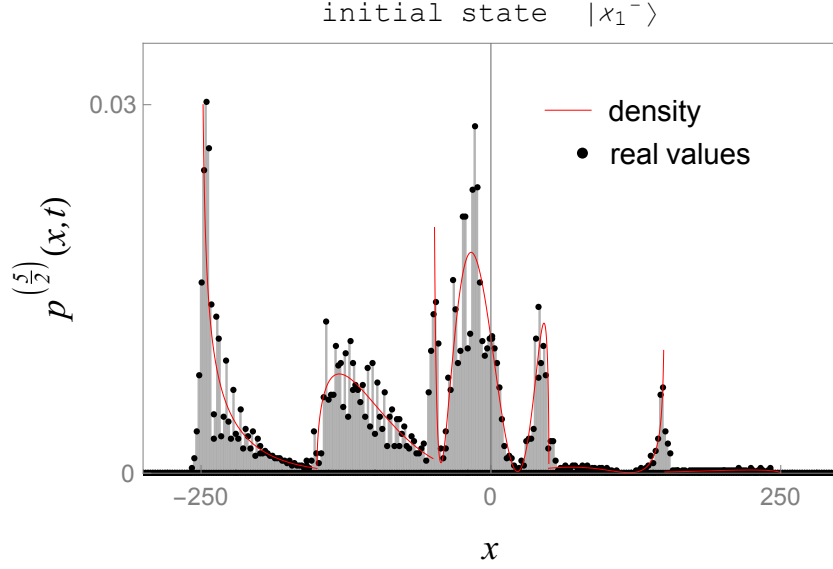


Figure A.3: Position probability distribution for the six-state Wigner walk. The initial coin state is the suitable state $|\chi_1^-\rangle$ from Eq. (A.5), the total number of steps $t = 100$ and parameter $\rho = 1/2$. Red solid line is the limiting density $\frac{1}{t}f^{(5/2)}(x/t)$, Eq. (A.6). It is seen that only three probability peaks are present since the suitable initial state eliminates one divergence for each density from $f^{(5/2)}(x/t)$. It is seen that after one hundred steps, the real values (black dots) located closely on the left hand side from the origin exceed the slowest left probability peak, respectively its real values. Of course, this situation disappears with higher number of steps. Nevertheless, we find the situation of an additional probability hill quite interesting, since there was nothing similar in the lower dimension. The only hills in the limiting density (red solid line) appeared for probability peaks that were destroyed by a choice of the initial state, i.e. cancelled divergence in the Konno's density function. Similar but smaller hill near the origin of the lattice and at position that does not correspond to a probability peak is observed also for the walk with initial $|\chi_2^+\rangle$ state, Fig. (A.1).

Conclusions and outlook

The entire thesis is devoted to the analysis of trapping as an interesting and promising property certain quantum walks exhibit. Whereas the travelling peaks decreases with increasing number of steps, the central trapping peaks still holds a large amount of probability around the origin of the lattice. We have limited ourselves only to discrete-time and translationally invariant quantum walks, where some of the properties can be studied by the wave theory methods. After the introductory part describing basic concepts and tools used for analysis of the walks, we have investigated trapping walks in more detail and provided several new result. We have mostly focused on classification of the coins responsible for trapping and on the limiting approximation of the position probability distribution, control of probability peaks and role of the free parameters. The following paragraphs summarize the main results of the individual chapters.

The introductory chapter one is followed by constructions of specific trapping one-parameter families of coins in chapter two. The approach is based on a connection of some trivial matrices that share the eigenvalues or the eigenvectors with the well-known Grover matrix, for which the trapping was found. Addition of a parameter into the eigenvectors or the eigenvalues of the trivial matrix led to continuous transitions (one-parameter families) between the trivial and the Grover matrix, whereas the trapping was preserved for all choices of the new parameter. These ideas hidden in the structure of the new coin classes result in the names eigenvalue and eigenvector family. We started with a three-state walk on a line and showed that extensions to higher dimensional walks are possible without significant increase of the difficulty of the construction. Furthermore, following chapters had often referred to these new coin classes as a starting point or due to comparison of the results.

We have revealed that instead of isolated coins, there exist whole families of coins exhibiting trapping. This fact naturally leads to the question of completeness, which was studied in chapter three. From the approach presented in the previous chapter that resulted in two one-parameter families, a conclusion regarding the completeness could not be obtained as a simple consequence of the way of construction starting from a special choice of a known trapping coin. Therefore, in chapter three we began with a general matrix and found conditions trapping matrix for three-state quantum walk on a line has to satisfy. These conditions were imposed to a general unitary matrix in a special form, given as a product of three matrices, where one of these matrices is a quark-mixing matrix known from standard model. The remaining two are simple diagonal matrices. As a result we found two classes of coins with

five and six real parameters and showed that most of these parameters can be ignored, since only two or three parameters influence the spreading of the walk and the trapping. Moreover, these classes are generalizations of the eigenvalue and the eigenvector family derived in chapter two. The choice of the general coin containing the mixing matrix was the key point in the classification due to its convenient form. Different coins together with the conditions on trapping led to more complicated equations for which the analytical solution could not be revealed with certainty that it is complete. As a consequence, application of this method to higher dimensional walk is not suitable as we have showed on a special example at the beginning of chapter four. Let us emphasize that for the three-state quantum walk on a line, the described approach provided a classification of the trapping coins and the completeness of the classification followed, without any doubts, from the presented construction starting with the most general coin in a convenient form.

As the method successful for the full classification for the 3D walk is not suitable for higher dimension, in chapter four we developed a completely new approach that was applied on a four-state quantum walk on a two-dimensional lattice. Since the trapping walks are quantum walks with non-empty point spectrum, there exist a stationary state as an eigenstate corresponding to this constant eigenvalue. It can be shown that this stationary state is localized on maximally 2×2 support of the lattice. This restriction allowed us to begin the analysis with the most general stationary state and thus guaranteed completeness of the classification. Further restrictions on the amplitudes determining the stationary state stem from the action of the coin a step operator on the stationary state and the fact that coin has to be unitary. This all together determined an existence of two possible situations. The first one could be solved only by inverting a matrix composed of the amplitudes of the stationary state. This case gave us not only a trapping, but a strongly trapping coin class. The second case corresponded to the situation where this simple inversion could not be done due to determinant equal to zero. We altered the matrix to satisfy the requirements on the non-zero determinant and got a coin class which is trapping but not strongly trapping. We analysed also all trivial cases to provide a full classification of the trapping coins for the four-state quantum walk on a 2D lattice.

At the end of the thesis, we looked at the limiting distribution for several types of quantum walks. The limiting distribution is approximative probability distribution that is very useful when one considers large number of steps. We showed that it is not always convenient to express this distribution in the standard coin space basis. Although the standard basis is simple, it might provide quite complicated and physically non-transparent results. Therefore, we propose a different basis in which the limiting density gains the simplest form. First we provided suitable basis and resulting distribution for eigenvalue and eigenvector families of coins. In these cases, the suitable basis was given directly by the eigenvectors of the coins. We assumed that the eigenvector basis is always suitable, since it is a natural basis in many quantum mechanical problems. In the case of the Wigner walks studied in the last section of this fifth chapter, we found out that the idea behind the suitable basis has to be different. Three-state Wigner walk is analogical in spreading to quantum walk with eigenvector family

of coins. Nevertheless, in the case of three-state Wigner walk, the eigenvalue basis provided different and more difficult density function. This led us to idea that the suitable basis is composed of the initial coin states, for which a peak in the position probability distribution disappears. We showed that this basis gave the same results as the eigenvector basis for the eigenvector family of coins. Moreover, we found a connection of the suitable basis to the coin's eigenvectors and thus provided simple recipe for construction of this basis even for higher dimensional Wigner walks. The proposed suitable basis is not only helpful in the simplification of the limiting distribution function, it also reveals some interesting properties that can be observed for a special choice of the initial state. The decrease of the trapping peak is not purely exponential. The trapping probability may even increase for certain positions. Simple combinations of a suitable basis state as the initial states of the walk breaks a symmetry of the trapping peak with respect to the origin of the lattice in a very special way. It leads to cancellation of the left or the right half of the peak.

Trapping is a rare feature certain quantum walks exhibit. This effect is closely related to the choice of the coin and the initial state. It is not a property of an isolated coin, there exist whole trapping classes. We focused on two basic facts. It is what types of coins results in a trapping walk and how these coins and the corresponding initial states affects trapping. We presented results in this direction that can be further developed. We outline the possible direction in the following comments. We provided a classification of trapping coins for several types of walk, i.e. three-state quantum walk on a line and four-state quantum walk on a two-dimensional lattice. Compared to the analysis of the three-state walk, the approach used for the four state walk is more straightforward and thus of high potential in application for a different type of walks, probably even in higher dimension. The amount of information we could get only from basic properties of the coin was very surprising and promising. This greatly simplified the whole process of classification which was then, compared to the less-dimensional three-state walk, easier to implement. The question of stability under percolations is also interesting, especially for the strong trapping coin class. Furthermore, figures showing spectrum of the walks are similar to that appearing in topological phases studies. We showed that classification of the trapping coin for the three-state quantum walk on a line results in two non-trivial classes of coins. Each of these classes comprised eigenvalue or eigenvector family of coins that were found by a modification of the Grover walk. Similar situation can be found for the four-state walk on a 2D lattice. In this case we can even construct (up to phases) the final non-trivial classes by a modification of the four-state Grover walk similarly as in chapter two. Nevertheless, it is not enough to deform only the eigenvalues or the eigenvectors of the Grover coin and we have to deform both eigenvalues and eigenvectors. The difference between the final two classes sits in the number of eigenvalues that are deformed. Suitable bases introduced in the last chapter control the existence of the peaks in the position probability distribution. The provided simplifications this suitable bases provide are significant. Suitable basis also affect a subject of this theses, which is trapping, in a striking way. We especially mean cancellation of one half of the trapping peak and the fact, the the peak might not be purely decreasing. Of course, these

interesting behaviours of the trapping peaks exist also in the standard basis description. Nevertheless, the expressions are enormously complicated and thus this properties cannot be decoded. On the other hand, suitable basis brings these features almost for free. This all is obviously connected to simplifications of descriptions even for more complicated types of walks, which might be subject of further studies as well.

References

- [1] K. Pearson (1905), *Nature*, 72, 294.
- [2] Y. Aharonov, L. Davidovich and Z. N. Zagury (1993), *Phys. Rev. A*, 48, 1687.
- [3] D. Meyer (1996), *J. Stat. Phys.*, 85, 551.
- [4] E. Fahri and S. Gutmann (1998), *Phys. Rev. A*, 58, 915.
- [5] N. Shenvi, J. Kempe and K. B. Whaley (2003), *Phys. Rev. A*, 67, 052307.
- [6] M. Santha (2008), 5th TAMC, LNCS 4978, 31.
- [7] O. Mülken and A. Blumen (2011), *Phys. Rep.* 502, 37.
- [8] M. Mohseni, P. Rebentrost, S. Lloyd and A. Aspuru-Guzik (2008), *J. Chem. Phys.*, 129, 174106
- [9] A. M. Childs (2009), *Phys. Rev. Lett.*, 102, 180501.
- [10] M. Karski, L. Förster, J. Choi, A. Steffen, W. Alt, D. Meschede and A. Widera (2009), *Science*, 325, 174.
- [11] H. Schmitz, R. Matjeschk, Ch. Schneider, J. Glueckert, M. Enderlein, T. Huber and T. Schaetz (2009), *Phys. Rev. Lett.* 103, 090504.
- [12] F. Zähringer, G. Kirchmair, R. Gerritsma, E. Solano, R. Blatt and C. F. Roos (2010), *Phys. Rev. Lett.* 104, 100503.
- [13] A. Schreiber, K. N. Cassemiro, V. Potoček, A. Gábris, P. J. Mosley, E. Andersson, I. Jex and Ch. Silberhorn (2010), *Phys. Rev. Lett.* 104, 050502
- [14] A. Schreiber, A. Gábris, P. P. Rohde, K. Laiho, M. Štefaňák, V. Potoček, C. Hamilton, I. Jex and Ch. Silberhorn (2012), *Science* 336, 55.
- [15] R. Wong (2001), *Classics in Applied Mathematics*, 34, SIAM.
- [16] N. Inui, N. Konno and E. Segawa (2005), *Phys. Rev. E*, 72, 056112.
- [17] N. Inui and N. Konno (2005), *Physica A*, 353, 133.
- [18] B. Kollár, M. Štefaňák, T. Kiss, I. Jex (2010), *Phys. Rev. A*, 82, 012303.

- [19] N. Inui, Y. Konishi and N. Konno (2004), Phys. Rev. A, 69, 052323.
- [20] C. Jarlskog (2005), J. Math. Phys., 46, 103508.
- [21] T. Machida, arXiv:1401.1522.
- [22] G. Grimmett, S. Janson and P. F. Scudo (2004), Phys. Rev. E, 69, 026119.
- [23] T. Miyazaki, M. Katori and N. Konno (2007), Phys. Rev. A, 76, 012332.
- [24] A.M. Childs (2010), Commun. Math. Phys., 294, 581.
- [25] A. Ambainis, E. Bach, A. Nayak, A. Vishwanath, J. Watrous (2001), in Proceedings of the 33th STOC (ACM Press, New York), p. 60.
- [26] A. Nayak, A. Vishwanath (2000), arXiv:quant-ph/0010117.
- [27] A. Messiah, Quantum mechanics, vol. II, (North Holland, Amsterdam, 1962).
- [28] E. P. Wigner, Group Theory and Its Application to the Quantum Mechanics of Atomic Spectra, (Academic Press, New York, 1959).
- [29] B. Kollár, T. Kiss and I. Jex (2015), Phys. Rev. A, 91, 022308.
- [30] I. Bezděková (2012), *Quantum walks as a wave phenomenon*, Master's Thesis, Czech Technical University in Prague.
- [31] K. Watabe, N. Kobayashi, M. Katori and N. Konno (2008), Phys. Rev. A, 77, 062331
- [32] K. Nakamura et. al (2010), J. phzs. G, 37, 75021.
- [33] G. Auberson, A. Martin and G. Mennessier (1991), Comm. Math. Phys, 140, 523.
- [34] N. Konno (2002), Quantum Inf. Process. 1, 345.
- [35] N. Konno (2005), J. Math. Soc. Jpn, 57, 1179.

List of publications

Publications related to the thesis

- [I] M. Štefaňák, I. Bezděková and I. Jex (2012), *Eur. Phys. J. D*, 66, 142.
- [II] M. Štefaňák, I. Bezděková, I. Jex and S. M. Barnett, *Quant. Inf. Comput.*, 13& 14, 1213.
- [III] M. Štefaňák, I. Bezděková, I. Jex (2014), *Phys. Rev. A*, 90, 012342.
- [IV] I. Bezděková, M. Štefaňák, I. Jex (2015), *Phys. Rev. A*, 92, 022347.

Other publications

- [V] W.P. Schleich, I. Bezděková, M.B. Kim, P.C. Abbott, H. Maier, H. Montgomery and J.W. Neuberger, Equivalent formulations of the Riemann Hypothesis based on lines of constant phase, *Acta Arithmetica* (submitted February 2017).